

**PERFORMANCE OF  
ALKALI ACTIVATED CONCRETE  
MIXES WITH STEEL SLAG AS COARSE  
AGGREGATE FOR RIGID PAVEMENTS**

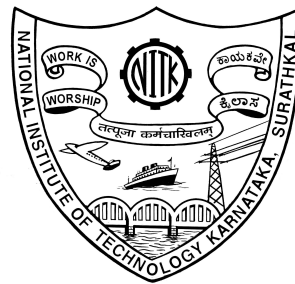
Thesis

Submitted in partial fulfilment of the requirements for the degree  
of

**DOCTOR OF PHILOSOPHY**

by

**NITENDRA PALANKAR**



**DEPARTMENT OF CIVIL ENGINEERING  
NATIONAL INSTITUTE OF TECHNOLOGY KARNATAKA  
SURATHKAL-575025**

**JULY 2016**

# DECLARATION

*By the Ph.D Scholar*

I hereby *declare* that the thesis entitled “**Performance of Alkali Activated Concrete Mixes with Steel Slag as Coarse Aggregate for Rigid pavements**” which is being submitted to the **National Institute of Technology Karnataka, Surathkal** in partial fulfilment of the requirements for the award of the Degree of **Doctor of Philosophy in Civil Engineering**, is a *bonafide report of the research work carried out by me*. The material contained in this thesis has not been submitted to any University or Institution for the award of any degree.

**(NITENDRA PALANKAR)**

Register No. **121172CV12F03**,  
Department of Civil Engineering

Place: NITK-Surathkal

Date: 04-07-2016

## CERTIFICATE

This is to *certify* that the thesis entitled “**Performance of Alkali Activated Concrete Mixes with Steel Slag as Coarse Aggregate for Rigid pavements**” submitted by **Mr. NITENDRA PALANKAR** (Register Number: **121172CV12F03**) as the record of the research work carried out by him, is *accepted as the thesis submission* in partial fulfilment of the requirements for the award of degree of **Doctor of Philosophy**.

**Dr. A.U. Ravi Shankar**  
**Research Guide**  
(Signature with date and seal)

**Chairman - DRPC**  
(Signature with date and seal)

*DEDICATED*  
*TO*  
*MY PARENTS,*  
*FAMILY MEMBERS, FRIENDS*  
*AND*  
*TEACHERS*

## **ACKNOWLEDGEMENT**

I would like to express my sincere gratitude to my research supervisor Prof. A.U Ravi Shankar for his motivation and invaluable guidance throughout my research work. I am grateful to him for his keen interest in the preparation of this thesis. It has been my pleasure to work with him.

I acknowledge my sincere thanks to Prof. Vijay Desai, Dept. of Mechanical Engineering and Prof.M.C. Narasimhan, Dept. of Civil Engineering for being the members of Research Progress Assessment Committee and giving valuable suggestions and the encouragement provided at various stages of this work.

I wish to thank Director NITK Surathkal, Mr. Swapan Bhattacharya; Prof. KattaVenkataramana, former Head of the Civil Engineering Department and Prof. Lokesh K N, Head of the Civil Engineering for their support and encouragement throughout my stay atthe NITK campus.

I appreciate the co-operation and help rendered by the staff of laboratories and the office of the Civil Engineering Department. My special thanks to Mr.Ramanath, Mr. Shashikant, Mr. Vishwanth and Mr.Dheeraj for their help in completing my experimental work. I extend my sincere thanks to the office staff Mrs. Vagdevi, Mrs. Vijay Laxmi and Mr .Monaappa for their support at various stages of this work

I also like to extend my gratitude to all the teaching faculty and supporting staff of the Civil Engineering Department, for their encouragement, help and support provided during the research work.

I am also thankful to Mr. Subramanya, JSW Iron and Steel Bellary, Karnataka for providing steel slag. My special thanks to my friends in JSW Iron and Steel Bellary, Karnataka Mr. Sagar Muchandikar and Mr. Abhishek for their efforts and support extended procuring the steel slag.

I am fortunate to have my friends, Mr. Mithun B M, Mr. Sanjeev Gadad, whose contributions and encouragements have taken me this far. I am very much thankful to all my friends and fellow research scholars of this institute for their continuous encouragement and suggestions during the

course of my research work. The informal support and encouragement of my friends has been indispensable.

I am especially grateful to my father Sri. Nagesh Palankar and mother Smt. Jaya Palankar, who provided me the best available education and encouraged in all my endeavors. They have always been a source of inspiration for me.

Finally, I am grateful to everybody who helped and encouraged me during this research work.

NITK Surathkal

NITENDRA PALANKAR

Date: 04-07-2016

## ABSTRACT

Improved road connectivity is very essential for any countries progress. Well designed and constructed concrete pavements have been identified component for the development of a sustainable highway infrastructure. The higher demand for concrete roads and other construction purposes has resulted in the increased production of Ordinary Portland Cement (OPC), which is one of the basic constituents required for concrete production. However, the production of OPC is associated with emissions of large amounts of CO<sub>2</sub>, with the cement industry accounting for about 5-8% of worldwide CO<sub>2</sub> emissions. In addition to CO<sub>2</sub> emissions, the production of OPC requires considerable amounts of natural raw materials and energy. The present research community is focused on the development of alternative binders, with the aim of minimization of production of OPC. Alkali Activated Binders (AABs) such as Alkali Activated Slag (AAS), Alkali Activated Slag Fly Ash (AASF), Geopolymers, etc. can be considered as potential alternatives to OPC. Steel slag, an industrial by-product obtained from manufacture of steel can be identified as an alternative to natural aggregates for concrete production, since there is a possibility of acute shortage of natural aggregates for concrete in future.

The present study is conducted to evaluate the performance of steel slag as coarse aggregates in Alkali Activated Slag Concrete (AASC) and Alkali Activated Slag Fly Ash Concrete (AASFC) by replacing natural granite aggregates. AASC and AASFC mixes are designed to attain a minimum strength of M40 grade and compared with conventional OPC concrete mix of similar grade. AASC mixes are prepared with 100% GGBFS as sole binder, while AASFC mixes are prepared by mixing GGBFS and FA in different proportions, i.e. 75:25, 50:50 and 25:75. Preliminary tests are carried out to identify the optimal activator modulus and dosage of alkaline activators for each of the AASC and AASFC mixes. Steel slag as coarse aggregates are incorporated in the AASC and AASFC mixes by replacing the natural coarse aggregates by volume replacement method at different levels of replacement, i.e. 0%, 25%, 50%, 75% and 100%. The fresh and hardened properties such as workability, compressive strength, split tensile strength,

flexural strength, and modulus of elasticity of different concretes are evaluated as per standard test procedures. The durability of concrete mixes, in terms of resistance to sulphuric acid, magnesium sulphate, water absorption and Volume of Permeable Voids (VPV) are investigated. Flexural fatigue performance of various concrete mixes is evaluated by carrying out repeated load tests on beam specimens using repeated load testing equipment. The fatigue life data obtained are represented and analyzed using S-N curves to establish fatigue equations. Probabilistic analysis of fatigue data is carried out using two parameter Weibull distribution method. Further, the goodness-of-fit test is done to ascertain the statistical relevance of the fatigue data using Weibull distribution model. Survival probability analysis to predict the fatigue lives of concrete mixes with required probability of failure is carried out. The impact of the properties of AASC and AASFC mixes on the rigid concrete design is analyzed by carrying out standard pavement design. The ecological and economical benefits of AASC and AASFC mixes in comparison with conventional OPC concrete are analyzed and discussed.

The results indicated that incorporation of steel slag in AASC and AASFC mixes resulted in slight reduction in mechanical strength. Reduction in number of cycles for fatigue failure was observed in AASC and AASFC mixes containing steel slag as compared to granite aggregates. Two parameter Weibull distribution was used for statistical analysis of fatigue data and it was observed that the fatigue data of concrete mixes can be approximately modelled using Weibull distribution. The inclusion of steel slag aggregates slightly reduced the durability performance of AASC and AAFM mixes. The higher water absorption and subsequent VPV increase, with inclusion of steel slag in both AASC and AASFC mixes, due to higher water absorption of steel slag as compared to normal aggregates. Alkali activated concrete mixes with natural aggregates exhibited better resistance to sulphuric acid and magnesium sulphate environments as compared to OPCC, which may be attributed to properties/structure of binders. The acid and sulphate resistance of alkali activated concrete mixes decreased with replacement of natural aggregates with steel slag. The Embodied Energy (EE), Embodied Carbon Dioxide Emission (ECO<sub>2e</sub>) and cost of alkali activated concrete with natural aggregates are found



to be quite lower as compared to OPCC. Incorporation of steel slag in alkali activated concrete mixes led to further reduction in EE,  $ECO_{2e}$  and cost as compared to OPCC. Steel slag aggregates reported acceptable performance in AASC and AASFC mixes for its use in pavement quality concrete.

**Keywords:** Alkali activated concrete mixes; Steel slag aggregates; Mechanical properties; Durability; Fatigue behaviour; Eco-friendly concrete.

<b>No.</b>	<b>CONTENTS</b>	<b>Page No.</b>
	Title	
	Declaration	
	Certificate	
	Acknowledgement	
	Abstract	
	Contents	
	List of Figures	
	List of Tables	
	Nomenclature	
<b>1</b>	<b>INTRODUCTION</b>	
	1.0 GENERAL	1
	1.1 RIGID PAVEMENTS	2
	1.2 RIGID PAVEMENTS - IN INDIAN CONTEXT	3
	1.3 CONCRETE	4
	1.4 ALKALI ACTIVATED BINDERS (AAB)	6
	1.5 STEEL SLAG	8
	1.6 NEED AND SIGNIFICANCE OF PRESENT INVESTIGATION	9
	1.7 OBJECTIVES OF THE PRESENT RESEARCH WORK	11
	1.8 SCOPE OF WORK	12
	1.9 ORGANIZATION OF THESIS	13
<b>2</b>	<b>LITERATURE REVIEW</b>	
	2.0 GENERAL	15
	2.1 HISTORICAL DEVELOPMENT OF ALKALI ACTIVATED	17

	<b>BINDERS</b>	
2.2	<b>ACTIVATION MECHANISMS OF ALKALI ACTIVATED BINDERS</b>	19
2.2.1	Alkali Activation of Slag Systems	19
2.2.2	Activation of Geopolymer Systems	20
2.2.3	Alkali Activated Slag-Fly Ash	21
2.3	<b>SOURCE MATERIALS AND ALKALINE ACTIVATORS</b>	22
2.3.1	Fly Ash (FA)	22
2.3.2	Ground Granulated Blast Furnace Slag (GGBFS)	23
2.3.3	Influence of Type, Dosage and Modulus of Alkaline Activators	24
2.4	<b>PROPERTIES OF ALKALI ACTIVATED BINDERS</b>	27
2.4.1	Mechanical Properties of Alkali Activated Slag	27
2.4.2	Curing Regime	29
2.4.3	Mechanical Properties of Alkali Activated Slag-Fly Ash	30
2.4.4	Effect of Fly Ash on the Workability Properties of Alkali Activated Slag-Fly Ash	31
2.5	<b>DURABILITY PROPERTIES OF ALKALI ACTIVATED BINDERS</b>	32
2.6	<b>FATIGUE CHARACTERISTICS OF CONCRETE PAVEMENTS</b>	34
2.6.1	S-N Curves and Probabilistic Approach	36
2.7	<b>STEEL SLAG</b>	38
2.7.1	Physical and Chemical Composition of Steel Slag Aggregates	39
2.7.2	Acceptability of Steel Slag Aggregates	40
2.7.3	Previous Studies on Steel Slag Aggregates in Concrete	42
2.8	<b>SUMMARY</b>	43

<b>3</b>	<b>MATERIALS AND METHODS</b>	
3.0	GENERAL	45
3.1	INGREDIENT MATERIALS	45
3.1.1	Cement	45
3.1.2	Ground Granulated Blast-Furnace Slag (GGBFS)	46
3.1.3	Fly Ash (FA)	47
3.1.4	Fine Aggregates	48
3.1.5	Coarse Aggregates	48
3.1.6	Steel Slag Aggregates	48
3.1.6.1	<i>Weathering of steel slag aggregates</i>	50
3.1.7	Water	53
3.1.8	Super-plasticizer	54
3.1.9	Alkaline Activators	54
3.2	PRELIMINARY STUDIES ON ALKALI ACTIVATED CONCRETE MIXES	55
3.3	MIX DESIGN	60
3.4	MIXING, PLACING, COMPACTION AND CURING OF CONCRETE MIXES	63
3.5	TESTING OF CONCRETE MIXES	64
3.5.1	Workability of Fresh Concrete	64
3.5.2	Mechanical and Durability Properties of Hardened Concrete Mixes	64
3.5.2.1	<i>Acid Attack</i>	64
3.5.2.2	<i>Sulphate Attack</i>	65
3.5.2.3	<i>Flexural Fatigue Testing</i>	65
3.5.2.4	<i>Accelerated Fatigue Testing Equipment</i>	66
3.6	SUMMARY	68
<b>4</b>	<b>MECHANICAL PROPERTIES OF CONCRETE MIXES</b>	

4.0	INTRODUCTION	71
4.1	WORKABILITY AND UNIT WEIGHT	71
4.2	COMPRESSIVE STRENGTH OF CONCRETE MIXES	72
4.3	STATIC FLEXURAL STRENGTH OF CONCRETE MIXES	74
4.4	SPLIT TENSILE STRENGTH OF CONCRETE MIXES	77
4.5	MODULUS OF ELASTICITY OF CONCRETE MIXES	80
4.6	SUMMARY	83
<b>5</b>	<b>DURABILITY OF CONCRETE MIXES</b>	
5.0	INTRODUCTION	85
5.1	WATER ABSORPTION AND VPV	85
5.2	SULPHURIC ACID ATTACK	87
	5.2.1 Visual Inspection of Samples to Acid Solution	91
5.3	MAGNESIUM SULPHATE ATTACK	94
5.4	SUMMARY	97
<b>6</b>	<b>FATIGUE PERFORMANCE OF CONCRETE MIXES</b>	
6.0	INTRODUCTION	99
6.1	S-N CURVE	99
6.2	PROBABILISTIC ANALYSIS OF FATIGUE DATA	100
	6.2.1 Graphical Method	101
6.3	FATIGUE LIFE OF CONCRETE MIXES	102
6.4	PROBABILISTIC ANALYSIS OF FATIGUE DATA OF CONCRETE MIXES	109
6.5	ESTIMATION OF WEIBULL DISTRIBUTION PARAMETERS USING GRAPHICAL METHOD	109
6.6	GOODNESS-OF-FIT TEST FOR FATIGUE DATA	112
6.7	SURVIVAL PROBABILITY AND S-N RELATIONSHIP	114
6.8	SUMMARY	115

<b>7</b>	<b>ANALYSIS AND DESIGN OF RIGID PAVEMENTS</b>	
7.0	INTRODUCTION	117
7.1	ECOLOGICAL AND ECONOMICAL ANALYSIS OF CONCRETE MIXES	117
7.2	PAVEMENT ANALYSIS AND DESIGN	118
7.3	RESULTS AND DISCUSSIONS	119
	7.3.1 Ecological and Economical Analysis of Concrete Mixes	119
	7.3.2 Pavement analysis and design	121
7.4	SUMMARY	124
<b>8</b>	<b>CONCLUSIONS</b>	127
8.1	RECOMMENDATIONS	132
8.2	SCOPE FOR FUTURE STUDY	132
	<b>REFERENCES</b>	133
	APPENDIX I	148
	APPENDIX II	151
	APPENDIX III	154
	APPENDIX IV	160
	APPENDIX V	163
	<b>LIST OF PUBLICATIONS</b>	170
	<b>BIO DATA</b>	171

## LIST OF FIGURES

<b>No.</b>	<b>Title</b>	<b>Page No.</b>
2.1	Reaction mechanism of alkali activated slag	20
2.2	Mechanism of gel formations in alkali activated fly ash binder	21
2.3	Moduli of sodium silicate solution Vs 28-day strength for different types of GGBFS	26
2.4	A typical S-N curve	37
3.1	Images showing steel slag aggregates before and after weathering process	53
3.2	Compressive strength v/s activator modulus for AASC mix (100:0)	56
3.3	Compressive strength v/s activator modulus for AASFC mix (75:25)	57
3.4	Compressive strength v/s activator modulus for AASFC mix (50:50)	57
3.5	Compressive strength v/s activator modulus for AASFC mix (25:50)	58
3.6	Immersion of cubes in plastic containers for durability tests	65
3.7	Repeated load testing set up	68
4.1	Flexural strength of AASC mix (100:0) at different ages	76
4.2	Flexural strength of AASFC mix (75:25) at different ages	76
4.3	Flexural strength of AASFC mix (50:50) at different ages	77
4.4	Flexural strength of AASFC mix (25:75) at different ages	77
4.5	28-day Split tensile strength of the AASC mix (100:0)	78
4.6	28-day Split tensile strength of the AASFC mix (75:25)	79
4.7	28-day Split tensile strength of the AASFC mix (50:50)	79
4.8	28-day Split tensile strength of the AASFC mix (25:75)	80
4.9	28-day Modulus of elasticity of the AASC mix (100:0)	81
4.10	28-day Modulus of elasticity of the AASFC mix (75:25)	82
4.11	28- day Modulus of elasticity of the AASFC mix (50:50)	82
4.12	28-day Modulus of elasticity of the AASFC mix (25:75)	83
5.1	Strength loss of AASC mixes (100:0) in pH=1 sulphuric acid	87

5.2	Strength loss of AASFC mixes (75:25) in pH=1 sulphuric acid	88
5.3	Strength loss of AASFC mixes (50:50) in pH=1 sulphuric acid	88
5.4	Strength loss of AASFC mixes (25:75) in pH=1 sulphuric acid	89
5.5	Concrete specimen after immersion in sulphuric acid solution for 120 days	92
5.6	Deterioration of steel slag aggregates	93
5.7	Strength loss of AASC mix (100:0) in magnesium sulphate solution	94
5.8	Strength loss of AASFC mix (75:25) in magnesium sulphate solution	94
5.9	Strength loss of AASFC mix (50:50) in magnesium sulphate solution	95
5.10	Strength loss of AASFC mix (25:75) in magnesium sulphate solution	95
6.1	S-N curve for AASC (100:0) with/without steel slag aggregates	107
6.2	Graphical analysis of fatigue data for 4-A-100 at stress ratio of 0.70	110
6.3	Predicted fatigue lives corresponding to different survival probabilities for various concrete mixes	115
7.1	Stress Vs Modulus of Subgrade Reaction for pavement thickness of 200 mm for contraction joint spacing of 4.5 m.	122
7.2	Variation of total stress for different pavement thickness for zone 1	123
A.3.1	S-N curve for AASFC (75:25) mix with/without steel slag aggregates	154
A.3.2	S-N curve for AASFC (50:50) mix with/without steel slag aggregates	155
A.3.3	S-N curve for AASFC (25:75) mix with/without steel slag aggregates	156
A.3.4	Predicted fatigue lives at different survival probabilities for AASFC (75:25) mix	157
A.3.5	Predicted fatigue lives at different survival probabilities for AASFC (50:50) mix	158
A.3.6	Predicted fatigue lives at different survival probabilities for AASFC (25:75) mix	159



## LIST OF TABLES

<b>No.</b>	<b>TITLE</b>	<b>Page No.</b>
2.1	History of Alkali-activated cement systems and alkaline cements	18
2.2	Classification of Alkali activators	24
2.3	Typical physical and engineering properties of steel slag	40
2.4	Typical range of composition of steel slag	40
3.1	Properties of OPC used in the present study	46
3.2	Chemical and Physical properties of GGBFS	47
3.3	Chemical and Physical Properties of Fly Ash (Class-F)	48
3.4	Physical Characteristics of aggregates	49
3.5	Gradation of aggregates used for the study	50
3.6	Chemical composition of Steel Slag (% by weight)	50
3.7	Free lime contents in steel slag aggregates	52
3.8	Properties of Conplast SP 430	54
3.9	Properties of Liquid Sodium Silicate	55
3.10	Properties of Sodium Hydroxide (97% purity)	55
3.11	Parameters considered for mix design of AASC and AASFC mixes	60
3.12	Details of Mix designations and Mix proportions of concrete mixes	62
3.13	Specimen details for various tests	63
4.1	Compressive strength of various concrete mixes	74
5.1	Water absorption and VPV of concrete mixes	86
6.1	Fatigue life of OPCC and AASC (100:0) concrete mixes	103
6.2	Fatigue life of AASFC (75:25) concrete mixes	104
6.3	Fatigue life of AASFC (50:50) concrete mixes	105
6.4	Fatigue life of AASFC (25:75) concrete mixes	106
6.5	Relationship between fatigue cycle (N) and stress level (SR)	108
6.6	Weibull parameters for AASC (100:0) mixes at different stress ratios	110
6.7	Weibull parameters for AASC (75:25) mixes at different stress ratios	111

6.8	Weibull parameters for AASC (50:50) mixes at different stress levels	111
6.9	Weibull parameters for AASC (25:75) mixes at different stress ratios	112
6.10	Kolmogorov–Smirnov test of fatigue life for 4-A-100 at S=0.70	113
7.1	Input data for calculation of EE, ECO <sub>2e</sub> and Cost	118
7.2	Parameters considered for the analysis	119
7.3	EE, ECO <sub>2e</sub> and Cost of concrete mixes per kilometre	120
7.4	Thickness requirement for safe design for various concrete mixes for zone 1	124
A 4-1	Detailed calculation for total EE per kilometer of highway	160
A 4-2	Detailed calculation for total ECO <sub>2e</sub> per kilometer of highway	161
A 4-3	Detailed calculation for total cost per kilometer of highway	162
A-5-1	Axle Load Spectrum	164
A-5-2	Axle load category-wise design axle load repetitions	166
A-5-3	Bottom-up Cracking Fatigue Analysis	168
A-5-4	Top-Down Cracking Fatigue Analysis	169

## NOMENCLATURE

MORTH	Ministry of Road Transport and Highways
IRC	Indian Roads Congress
FRC	Fiber Reinforced Concrete
HPC	High Performance Concrete
NHDP	National Highway Development Project
SARDP-NE	Special Accelerated Road Development Program for the North-East region and Left Wing Extremist
NHIIP	National Highways Interconnectivity Improvement Project
NHAI	National Highway Authority of India
OPC	Ordinary Portland Cement
FA	Fly Ash
GGBFS	Ground Granulated Blast Furnace Slag
AAB	Alkali Activated Binders
AAS	Alkali Activated Slag
AASF	Alkali Activated Slag Fly Ash
AAFA	Alkali Activated Fly Ash
RHA	Rice Husk Ash
BOF	Basic Oxygen Furnace
EAF	Electric Arc furnace
OHF	Open Hearth Furnace
AASC	Alkali Activated Slag Concrete
AASFC	Alkali Activated Slag-Fly Ash Concrete
SF	Silica Fume
C-S-H	Calcium Silicate Hydrate
A-S-H	Alumino Silicate Hydrate
HM	Hydration Modulus
GBFS	Granulated Blast-Furnace Slag

Ms	Activator Modulus
w/b	water to binder ratio
SR	Stress Ratio
SCRC	Self Compacting Rubberized Concrete
SFRC	Steel Fibre Reinforced Concrete
ASTM	American Society for Testing and Materials
Na <sub>2</sub> O	Sodium oxide
OPCC	Ordinary Portland Cement Concrete
RTPS	Raichur Thermal Power Station
LSS	Liquid Sodium Silicate
NaOH	sodium hydroxide
PQC	Pavement Quality Concrete
VPV	Volume of Permeable Voids
N	Fatigue life
M-S-H	magnesium silicate hydrate
EE	Embodied Energy
ECO <sub>2</sub> e	Embodied Carbon Dioxide Emission

# **CHAPTER 1**

## **INTRODUCTION**

### **1.0 GENERAL**

Transportation is one of the most important elements for the economic, industrial, social, and cultural development of any country. Lack of proper transportation facilities retards the progress of the country. Road networks are one of the most important modes of transportation in any country. Among all other modes of transportation, road transport is the only mode, which provides maximum ease, flexibility and serviceability to the passengers in selecting the route, time and speed of travel (MORTH 2012a). Moreover, the road networks alone connect the remote areas to the urban areas. Most of the developing countries have focused on the development of road infrastructure in order to boost the economy, by providing proper road connectivity, which facilitates the safe and economic conveyance of goods between the source and the business hubs. Good road connectivity also serves the safe movement of passengers in the overland traffic. An extensive road network is one of the most important elements to promote the growth and development of any country.

India, being one of the fastest developing nations, has concentrated its focus on the development of large scale road networks. With around 4.9 million km road network, India has the second largest road network in the world. The Indian road network is constituted of 0.9 million km national highways, 0.14 million km of state highways and 4.65 million km of major district roads and rural roads, which also include other district roads and village roads. Roads in India account for about 85% of the passenger traffic and 60% of the freight traffic (MORTH 2014)

Road projects need to be economically and ecologically sustainable apart from being safe, in order to benefit from the huge investments made on the road infrastructure projects. Roads in India are subjected to tremendous overloading due to the rapid growth

of passenger vehicular traffic and also due to considerable increase in freight traffic. This has led to the premature performance failure of highway pavements (Sharma et al. 1995). Moreover, the maintenance of roads is not carried out periodically, thus causing inconvenience to the travelers, along with higher maintenance cost. The demand for increased highways, reconstruction and maintenance of prematurely failed pavements has also resulted in faster depletion of naturally available road materials. To overcome this, there is a need to construct eco-friendly, sustainable and cost-effective highways. Construction of concrete pavements is generally preferred nowadays, due to lower maintenance, environmental friendly characteristics, lower vehicle operation cost, better riding quality and longer design life, although the initial investment cost is high. Concrete pavements have been used extensively for highways, airports as well as business and residential streets.

## **1.1 RIGID PAVEMENTS**

Concrete pavements are well known as rigid pavements and are widely constructed all over the world. Concrete roads are considered for construction of expressways, bypasses, urban roads, etc. Concrete roads are generally preferred in coastal areas and places where rainfall is heavy (Bhattacharya 2005).

Concrete Pavements are considered to have several advantages over conventional bituminous pavements. Concrete pavements exhibit long service life, can withstand heavy axle roads, provide better riding quality and durability, even in extreme weather conditions such as heavy rainfall, water logging, high temperature regions and chemical environment, as compared to the bituminous pavements. Concrete roads also have the adaptability to use locally available road materials and industrial waste materials, thus saving scarce natural resources (Naik 2008). Concrete pavements provide better skid resistance, visibility and hence improved safety for the drivers (CPAM 2012). The adoption of rigid pavements over bituminous pavements is also encouraged due to the cement production scenario, as the raw materials for cement production are available in plenty. The Indian Roads Congress (IRC) recommends rigid pavements as an alternative

to flexible pavements for rural roads, where the soil strength is weak, aggregates are scarce and at places where drainage conditions are poor. (IRC: SP: 62-2004).

Concrete pavements are generally constructed using conventional Ordinary Portland Cement (OPC) concrete along with aggregates, water and additives. However, various other types of concrete such as Fiber Reinforced Concrete (FRC), Pervious Concrete, Blended Cement Concrete, High Performance Concrete (HPC), Alkali Activated Concrete, etc., can also be used for the construction of rigid pavements. In India, until the year 2000, Ministry of Road Transport and Highways (MoRTH), specified the use of conventional OPC concrete with a minimum grade of M40 or higher for construction of rigid pavements. However, in the year 2008, the IRC revised the specifications through Amendment No.3 to IRC: 21:2000, which allows the use of blended cements such as Portland Slag Cement (PSC) and Portland Pozzolona Cement (PPC) to be used for construction of rigid pavements.

## **1.2 RIGID PAVEMENTS - IN INDIAN CONTEXT**

In India, until mid 90's, most of the roads constructed were mainly flexible pavements, with a concrete roads contributing to a meagre 1%, which was mainly due to the high investment cost associated with the construction of rigid pavements. However, after mid 90's, Indian road engineers took into consideration the long term benefits of concrete pavements and found rigid pavements as a more attractive alternative to flexible pavements. The first major concrete highway (Agra-Mathura Road) was constructed during 1960; however the second major highway between Delhi and Mumbai was constructed after 30 years during 1990. The construction of Mumbai-Pune 95 km six lane highways during 90's boosted the construction of concrete roads. In order to improve the country's infrastructure facilities, the government of India launched the prestigious National Highway Development Project (NHDP), which initially was involved in the conversion of existing two lane highways into four lane highways. The government of India formulated the seven-phase program NHDP for the development extensive national highway network in the country. Under the NHDP, the government sanctioned to

construct a total road length of 46880 kms in seven phases. Under the scheme, in the year 2001, the project included the construction of prestigious Golden Quadrilateral highway network with a total road stretch of 5846 km connecting the four metros and North-South-East-West corridor with a total road stretch of 7300 km (MORTH 2014).

Now with a new government in place, India is hoping to see a revival of its economy through proper road and transport connectivity. The current government has launched major initiatives to upgrade and strengthen the highways and expressways in the country. The government of India has formulated several programs such as Bharat Nirman, Special Accelerated Road Development Program for the North-East region and Left Wing Extremist (SARDP-NE), National Highways Interconnectivity Improvement Project (NHIIP), that are designed to promote nationwide rural connectivity linking all the unconnected villages with fair weather roads. In order to boost the highway sector, the government of India has targeted to construct highways at the rate 30 km/day, which amounts for about 11,000 km of highways every year (PPPII 2015). The government of India has set a target to complete 1,00,000 kms of highways by the end of 2017 from existing 92,850 kms in 2013-14. The value of roadways and bridge infrastructure in India is expected to reach USD 10 Billion between 2012-17. The National Highway Authority of India (NHAI) and the Ministry of Road Transport and Highways (MoRTH) had sanctioned projects for 3,700 kms in 2013-14, while around 8,470 kms of national highways are to be improved along with 10 bypasses (MII 2015). The boost in the highway infrastructure will lead to the requirements of thousands of tons of concrete production, which in turn leads to depletion of natural resources.

### **1.3 CONCRETE**

Concrete is one of the most basic and critical components for any type of construction and plays an important role in building the nation's infrastructure. Concrete is a composite material which is composed of coarse and fine aggregates embedded in a matrix and bound together by a binder, which fills the space or voids between the aggregates (Mindess et al. 2003). Basically, concrete is a mixture of binder, water,



aggregates and additives. The binder generally used in concrete production is OPC, which is mainly responsible for the mechanical strength.

It is well known that the production of OPC is associated with release of green house gases in huge quantities and also is highly energy intensive process. The production of one ton of cement lead to carbon dioxide (CO<sub>2</sub>) emission in the range of 0.8-1.3 ton, along with high energy consumption in the range of 100-150 kWt (Chandra 2002). The production of OPC also consumes huge quantities of virgin raw materials. The cement industry is making significant research through improvements and advancements in the cement production technology and process efficiency; in order to reduce the CO<sub>2</sub> emissions. However, further improvements may be limited as CO<sub>2</sub> generation is inherent and inevitable during the basic process of calcination of limestone. Moreover, the mining of limestone, which is one of the main raw materials for cement production, has an impact on the land use patterns, local water bodies and ambient air quality. The cement industry, along with consumption of raw materials, is one of the major consumers of coal for production of cement. Dust emissions from the cement industry also have adverse effects on the ambient air quality.

Considering the crucial importance of infrastructure development in India and other emerging countries, the demand for cement production has increased rapidly, which has led to increased concern on the environmental aspects associated with the utilization and production of concrete. An eco-friendly and sustainable development is the need of the day, which demand new concrete technologies that consume lower natural resources, lower energy and generate less CO<sub>2</sub>, without compromising on the strength and durability performance. Eco-friendly technologies and effective management of natural raw materials are necessary to counter to ill-effects occurring from concrete production.

In the context of increased awareness to reduce the production of OPC, the research community is mainly focused on the use of industrial waste materials such as Fly Ash (FA), Ground Granulated Blast Furnace Slag (GGBFS), Silica Fume, etc., in concrete production. Attempts to replace OPC partially with FA, GGBFS have proved to

be successful. The use of GGBFS, FA as partial replacement to OPC have displayed improved workability, reduced segregation, bleeding, heat evolution, permeability and durability properties of conventional OPC concrete. Apart from improving the properties of OPC concrete, the use of such marginal materials have ecological and economic benefits and hence may be used as partial replacement to cement in concrete production (Tripathy and Mukherjee 1997, Chandrashekhar 2010). Apart from techniques which involve partial replacement of OPC binder with industrial waste materials in conventional OPC concrete, there are techniques which involve the complete replacement of OPC binders with industrial waste materials such as Alkali Activated Binders (AAB) mixes. Alkali Activated Slag (AAS), Alkali Activated Slag Fly Ash (AASFC), Alkali Activated Fly Ash (AAFA or Geopolymers), etc., are few examples of AAB's. Alkali activated binders can be looked upon as an alternative to OPC binders, which have the capabilities to be used in the construction industry, causing significant reduction in the production of OPC (Rashad et al. 2012). Along with reduced emission of CO<sub>2</sub> and consumption of energy, the alkali activated binders also exhibit superior mechanical and durability performance than OPC binders (Morsy et al. 2008, Rashad et al. 2013).

#### **1.4 ALKALI ACTIVATED BINDERS (AAB)**

Alkali activated binders are new generation binders which include a clinker-free binder matrix such as AAS, Geopolymers, AASF, etc. The alkali activated binders are produced by alkali activation of finely divided materials (generally industrial waste materials) such as FA, GGBFS, Rice Husk Ash (RHA), Metakaolin, etc., using strong alkaline activators such as sodium silicate, sodium hydroxide, potassium silicate, potassium hydroxide, sodium bicarbonate, etc., or combination of these. Over the past few decades, extensive studies on AAS and AAFA have been carried out. In case of AAS binders, GGBFS is used as the sole binder material, while in AAFA; FA is used as the sole binder. Although, the activation techniques for AAS and AAFA are quite similar, they differ in their chemical reactions and also in their mechanical and durability properties. The AAS based concrete are characterized by high strength even at room

temperatures, rapid setting, improved fire resistance, high early strength, etc. (Shi 2006, Fernandez- Jimenez and Palomo 2001). On the other hand, AAFA based concrete exhibit better resistance to acid environments, high heat resistance, etc. (Lee and van Deventer 2002, Thokchom et al. 2011). However, AAFA based concrete do not achieve sufficient strength at room temperature and hence require heat curing to gain sufficient strength (Fernandez-Jimenez et al. 1999). It has been studied that joint activation of GGBFS and FA as a combined binder, has reported sufficient strength even when cured at room temperatures. Such a type of binder is termed as Alkali Activated Slag Fly Ash, may be considered as a separate type of binder, whose properties are vary with the ratio of GGBFS and FA. The primary difference between AAS and AASF is that, AAS contains only GGBFS as the binder, while AASFC contains GGBFS along with FA mixed in different proportions. The main reaction product in AAS is Calcium Silicate Hydrate (C-S-H) with low Ca/Si ratio; whereas Alumino Silicate Hydrate (A-S-H) is mainly formed reaction product in AAFA (Chen and Brouwers 2007; Fernández-Jimeénez and Palomo 2005). Studies carried out by researchers (Puertas et al. 2000) claim the main product formed in AASF to be C-S-H with no existence of A-S-H; while others (Chi and Huang 2013) have reported the existence of both. Idawati et al. 2013 found the existence of C-A-S-H phase and hybrid C-(N)-A-S-H phases as well. The addition of higher amounts FA in AASF concrete has resulted in the reduction of strength, however the workability was found to increase (Rashad 2013). The AASF containing up to 50% FA (% by weight of binder) develop sufficient strength even at room temperature, however the strength development reduces with higher contents of FA greater than 50% (% by weight of binder) (Rajamane 2013). The strength and durability of AAB are strongly affected by various parameters such as curing regime, type of alkaline activators, dosage and activator modulus of alkaline activator, type of source materials, water to binder ratio, total water content, chemical composition of the binder and alkaline activators etc. (Rashad 2013). Several studies carried out by researchers have claimed AAB's develop better mechanical and durability properties as compared to conventional OPC and hence can be considered as a potential alternative to OPC.

## 1.5 STEEL SLAG

With large scale construction and infrastructure projects being carried out in the recent years, the production of concrete has increased rapidly along with consumption of natural resources. The demand for aggregates has increased and has resulted in over-exploitation of natural rock beds, mountains and river beds, thus causing ecological imbalance. To meet the growing demand of aggregates and to protect the aggregates for future, there is a need to identify alternative materials.

Steel slag, a by-product obtained the manufacture of steel, can be used as a substitute for natural aggregates in concrete. Steel slag is an unavoidable by-product obtained during the manufacturing process of steel and is composed of various metal oxides. However, steel slag is non metallic in nature and does not contain any hazardous materials. The steel slag may be available as Basic Oxygen Furnace (BOF) slag, Electric Arc furnace (EAF) slag or Open Hearth Furnace (OHF) slag, based on the production technique employed. The chemical composition of EAF slag and BOF slag may be different depending upon the fluxes or additives used during the production of steel (Fruehan 1985). The acceptability of steel slag for construction purposes is related to certain problems such as high density of aggregates and volume expansion. The free CaO and MgO present in steel slag, react with water and atmospheric CO<sub>2</sub> to form CaCO<sub>3</sub> and MgCO<sub>3</sub>, which lead to volume expansion of around 91.7% and 119.6% respectively (Bernard and Dipayan 2003). However, the problems related to volume expansion of steel slag aggregates can be countered by exposing the aggregates to a process of weathering for a period more than six months, in order to bring the free lime or magnesia within acceptable limits, beyond which no further volume expansion occurs (ASA 2002). After being subjected to weathering, the steel slag exhibit slight alterations in their physical properties which appears on the surface of the aggregates in the form of development of a thin layer of calcite (CaCO<sub>3</sub>) (van Der Laan et al. 2008).

Steel slag is used extensively for various applications in many countries, including in USA, the European Union, Brazil, Australia and China. Australia utilizes

more than 60- 70% of the steel slag generated, while US and other developed countries utilize around 70-80% of steel slag generated. The steel slag is used for various applications ranging from agriculture, landfills, cement making, paver blocks, and construction of roads to railway ballast. In India, the current production of steel slag is around 12 million tonnes per annum. While only a little quantity of the steel slag generated in India is recycled, a large portion of the steel slag generated is disposed off in stockpiles or dump yards. This is causing a problem due to paucity of land, dumping costs and other environmental aspects. The utilization of steel slag in concrete can lower the environmental impacts along with reduction in valuable landfill space and protection of natural aggregates for future. Instead of disposing steel slag into landfills, use of steel slag as aggregates in the construction industry will help to improve the efficiency as well as the economy. Research carried out on the use of steel slag aggregates in road making applications have reported it as a potential road material. The utilization and awareness of steel slag as road material is very limited in India. With proper support from the steel industries and government agencies, steel slag can prove to be a cheap and useful road material with several economical as well as environmental benefits. However, before promoting such a material, there is a need for extensive research to be carried out to check its suitability in road applications. Proper guidelines and statutory approvals from various government agencies and bodies such as the Indian Roads Congress, Central Road Research Institute etc., would encourage the acceptance of steel slag in Indian road industry (FICCI 2014).

## **1.6 NEED AND SIGNIFICANCE OF PRESENT INVESTIGATION**

The growth of vehicular traffic has led to the construction of new highways. Improved road connectivity is very essential for any country's progress. Due to the poor construction and maintenance methods adopted in most of the road constructions in India, the road conditions have become poor, which results in depletion of raw materials, high fuel consumption, delay in transportation of materials etc. The roads also need to be durable and sustainable; hence well designed concrete pavements have the potential to

overcome this deficiency. The high demand for concrete roads and other construction purposes has resulted in the augmented production of OPC, which is one of the basic constituents required for concrete production. However, the production of OPC is associated with emissions of large amounts of CO<sub>2</sub>, with the cement industry accounting for about 5-8% of worldwide CO<sub>2</sub> emissions (Rashad and Zeedan 2011). In addition to CO<sub>2</sub> emissions, the production of OPC requires considerable amounts of natural raw materials and energy.

The development of eco-friendly and sustainable construction materials has gained major attention by the construction industry. With the augmented emissions of greenhouse gases, high energy consumption and environmental hazards occurring from the increased OPC production; the researchers are focusing on the development of possible alternatives to OPC. Alkali activated binders can be looked upon as an alternative to conventional OPC binders, which have the capabilities to be used in the construction industry, causing significant reduction in OPC production (Rashad et al. 2012). Alkali activated binders include clinker-free binders, such as AAS, AASF, Geopolymers etc., which include the use of a strong alkaline activator along with calcium or silicate rich precursor material such as GGBFS, FA, etc., to form a final product, having properties equivalent or better than OPC. The energy required for the production of alkali activated binders is less than that required for OPC concrete and are further associated with low CO<sub>2</sub> emissions.

Over the years, the natural aggregates have been used as the filler material in concrete. However, the faster depletion of natural aggregates has created concern to the construction industry for future works. The present day research has been concentrated on seeking alternative low cost materials as a replacement for natural aggregates in concrete. Steel slag, which is generally considered as a waste product from the iron and steel industry, can be viewed as a potential replacement for natural aggregates. A little quantity of the steel slag generated in India is recycled and a large portion of the steel slag generated is disposed off in stockpiles or dump yards. The utilization of steel slag in

concrete mixes will have several advantages such as elimination of cost of dumping, minimization of environmental problems related to disposal of steel slag, conservation of natural aggregates, etc. Despite of satisfactory performance of steel slag as coarse aggregates in both normal and high performance OPC concrete, there is limited research available regarding the incorporation of steel slag as coarse aggregates to produce AAB based concrete mixes.

The present experimental study focuses on the possible utilization of industrial waste materials such as GGBFS, FA and steel slag in the production of a sustainable concrete for the construction industry. The aim of the study is not just to protect the natural raw materials, but to recycle the disposal wastes generated from the industries. Since the kind of curing adopted in the present research is air curing, this type of concrete will be of great advantage in arid and desert regions, where there is acute shortage of water. Presently in India, there is no field application of AAB based concrete in pavements or no any other structures, which is mainly due to limited research, non-acceptability of new materials, lack of expertise and confidence, etc. The scenario can be changed by conducting a proper research and communicating the performance of AAB concrete for different applications.

## **1.7 OBJECTIVES OF THE PRESENT RESEARCH WORK**

It is observed that attempts have already been made by researchers to understand the mechanism of Alkali Activated Slag Concrete (AASC) and Alkali Activated Slag-Fly Ash Concrete (AASFC). However, there is limited research on the incorporation of steel slag as coarse aggregates to produce AASC and AASFC mixes. The aim of the proposed study is to focus on detailed experimental investigation to address the suitability and performance of air cured AASC and AASFC incorporating steel slag as coarse aggregate for rigid pavements.

The main objectives of the present research work are identified as follows:

- To evaluate the mechanical properties of AASC and AASFC mixes incorporating steel slag as coarse aggregate.
- To study durability properties of AASC and AASFC mixes containing steel slag as coarse aggregate.
- To study the flexural fatigue behaviour of AASC and AASFC mixes incorporating steel slag as coarse aggregate.

## **1.8 SCOPE OF WORK**

The IRC: 58:2011 recommends a minimum grade of M40 with minimum flexural strength of 4.5 MPa for high volume concrete roads. As per the requirements, AASC and AASFC mixes were designed to attain a minimum strength of M40 and compared with a conventional OPC concrete mix of similar grade. AASC mixes were prepared with 100% GGBFS as sole binder, while AASFC mixes were prepared by mixing GGBFS and FA in different proportions i.e. 75:25, 50:50 and 25:75. Preliminary tests were carried out to identify the optimal activator modulus and dosage of alkaline activators for each of the AASC and AASFC mixes. Steel slag as coarse aggregates were incorporated in the AASC and AASFC mixes by replacing the natural coarse aggregates by volume replacement method at different levels of replacement, i.e. 0%, 25%, 50%, 75% and 100%. The fresh and hardened properties such as workability, compressive strength, split tensile strength, flexural strength, and modulus of elasticity of different concrete mixes was evaluated as per standard test procedures. The durability of concrete mixes in terms of resistance to sulphuric acid, magnesium sulphate, water absorption and volume of permeable voids are investigated. Flexural fatigue performance of various concrete mixes is determined by carrying out repeated load tests on beam specimens using repeated load testing equipment. The fatigue life data obtained are represented and analyzed using S-N curves to establish fatigue equations. Probabilistic analysis of fatigue data is carried out using two parameter Weibull distribution methods. Further, goodness-of-fit test is done to ascertain the statistical relevance of the fatigue data using Weibull distribution model.



Survival probability analysis to predict the fatigue lives of concrete mixes with a required probability of failure is carried out. The impact of the properties of AASC and AASFC mixes on the rigid concrete design is analyzed by carrying out standard pavement design. The ecological and economical benefits of AASC and AASFC mixes in comparison with conventional OPC concrete are analyzed and discussed.

## **1.9 ORGANIZATION OF THESIS**

This thesis is organized into eight chapters followed by the list of references and Appendixes.

### **CHAPTER 1**

The background on the road network and the need for use of concrete roads in India; brief note on alkali activated binders and steel slag; need and significance, objectives and scope of the research are presented in this chapter.

### **CHAPTER 2**

A comprehensive literature review has been carried out to collect adequate information about alkali activated binders, steel slag and other materials. Information gathered about the research works carried out so far on mechanical, durability properties and flexural fatigue studies of alkali activated binders, steel slag is also presented.

### **CHAPTER 3**

The details of various materials used, basic properties of concrete ingredients and the design for M<sub>40</sub> concrete are discussed in this chapter. Further, the preliminary tests carried out for obtaining the optimal design mix for AASC and AASFC mixes. The test methodology for determining the mechanical, durability and flexural fatigue performance of concrete mixes are discussed in detail.

## CHAPTER 4

This chapter presents the detailed discussion on results and observations of the mechanical properties of concrete mixes.

## CHAPTER 5

The results of durability test carried out on AASC and AASFC mixes are studied and discussed in detail in this chapter.

## CHAPTER 6

This chapter deals with results and discussions of the fatigue strength studies of AASC and AASFC mixes with/without steel slag carried. A probabilistic analysis is carried out on the fatigue data of the concrete mixes.

## CHAPTER 7

The ecological and economical benefits of AASC and AASFC with/without steel slag aggregates are studied and the results are presented in this chapter. The pavement analysis and design are carried out using properties of AASC and AASFC mixes.

## CHAPTER 8

Observations and conclusions drawn based on the investigation; recommendations and scope for the future study are presented in this Chapter.

## **CHAPTER 2**

### **LITERATURE REVIEW**

#### **2.0 GENERAL**

Alkali activated binders (AAB) are the new generation binders which include the use of a alkali rich, clinker-free binder matrix such as Alkali Activated Slag (AAS), Geopolymers, Alkali Activated Slag Fly ash (AASF), etc. (Puertas 1995). AABs are generally produced by activating industrial waste materials such as Ground Granulated Blast Furnace Slag (GGBFS), Fly Ash (FA), Silica Fume (SF). (Bernal et al. 2011a). The alkali activation is the method in which the alkali ions are used to trigger pozzalanic reactions or the release of latent cementitious properties of finely divided inorganic materials (Jiang 1997). The source materials can be either natural minerals or marginal materials primarily rich in calcium, aluminosilicates and silica.

Generally, three types of binder can be produced, one is AAS with raw materials, which are rich in calcium and silica such as GGBFS, and the second is geopolymers in which the raw materials are rich in silica and alumina, such as Class-F FA (Fernandiz and Palomo 2003). However, a third type of binder may be produced by a combination of GGBFS and FA as a raw material, and it is termed as Alkali Activated Slag Fly ash (AASF).

Based on the composition of hydration products, Krivenko (1994) classified the alkali activated binders as follows:

1. The alkaline aluminosilicate systems (R-A-S-H, where R= Na or K) are called “geocements”, whose formation process is similar to geological process of natural zeolites. An exceptional case in such systems was named ‘geopolymer’ in which the formation process included poly-condensation rather than hydration (Davidovits 1994).

2. The alkaline –alkaline earth systems (R-C-A-S-H) in which the products of hydration included the formation of calcium silicate hydrates, i.e. Calcium Silicate Hydrate (C-S-H) with low Ca/Si ratio. AAS and alkaline Portland cement are some of the alkaline earth systems. (Adam 2009)

The activation and synthesis of AAS and geopolymer are quite similar; however they vary widely in their reaction products (Palomo et al. 1999). Amorphous hydrated alkali aluminosilicate (A-S-H) is the major reaction product formed in geopolymer, while C-S-H with low Ca/Si ratio is formed in AAS (Duxson 2007, Glukhovsky 1959). Studies carried out by researchers (Puertas et al. 2000) claim the main product formed in AASFC to be C-S-H with no existence of A-S-H; while others (Chi and Huang 2013) have reported the existence of both. Idawati et al. (2013) reported the existence of C-A-S-H phase and hybrid C-(N)-A-S-H phases in AASF binders.

The raw materials used for the production of AAB's may be classified as pozzolans or latent hydraulic materials (Shi et al. 2006). Pozzalons are the materials rich in silica and alumina, which possess little or no cementitious properties, but in finely divided form and in the presence of moisture undergo chemical reactions with calcium hydroxide at ambient temperatures to form compounds consisting cementing properties (Malhotra and Mehta 1996). Low calcium (class-F) fly ash and silica fume are the most widely used pozzolonic materials. Latent hydraulic materials are finely divided materials similar to pozzolans, which contain sufficient amount of calcium to form compounds with cementitious properties after reacting with water (Popovics 1992). The latent hydraulic materials cannot undergo direct setting and hardening after reacting with water in normal conditions. The hardening energy is quiescent and requires an activator such as calcium hydroxide or some other strong alkaline compound to release the cementitious properties. The latent hydraulic materials when blended with Portland cement and water gets activated under the influence of calcium hydroxide, which is generated during the hydration reaction of cement (Jiang 1997). GGBFS is one of the examples of latent hydraulic materials. The pozzolons or latent hydraulic materials may be naturally

occurring in nature or may be artificially produced from industrial processes (Adam 2009).

## **2.1 HISTORICAL DEVELOPMENT OF ALKALI ACTIVATED BINDERS**

Alkali as a component of cementing material was investigated first by Kuhl (1930), by studying the setting behaviour of mixes, by combining ground slag powder and caustic potash solution in concrete. Chassevent (1937) measured the reactivity of slag by mixing caustic potash and soda solution. Purdon (1940) carried out an extensive laboratory study on clinker-free cements that consisted slag as the binder and caustic alkalis, produced by a base and an alkaline salt. Glukhovsky (1959) discovered a new group of binders composed of low basic calcium or calcium-free aluminosilicate and alkali metal solutions, which were termed “soil cements” and the corresponding concretes, were termed as “soil silicates”. In 1979, Davidovits developed a new group of binders produced by combining sintering products of kaolinite and limestone or dolomite as the aluminosilicate constituents and called those binders as “geopolymer” due to the presence of a polymeric structure. Davidovits (1994) proposed any source, either from natural geological origin or industrial by-product materials such as fly ash, rice husk ash, etc., rich in silica and alumina can be activated using highly alkaline liquid solutions. The classification of alkali activated binders based on their chemical composition and characterization of hydration products was done by Krivenko (1994). Pacheco-Torgal et al. (2008) suggested to use the term ‘geopolymer’ in alkali activated cementitious materials only if there is a presence of a zeolite phase with amorphous to semi-crystalline characteristics.

The important historical developments of alkali activated binders are summarized by Roy (1999) shown in Table 2.1.

Table 2.1 History of alkali-activated cement systems and alkaline cements (Roy 1999).

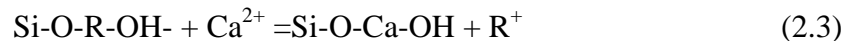
Author(s)	Year	Significance
Feret	1939	Slags used for cement
Purdon	1940	Alkali-slag combinations
Glukhovskiy	1959	Theoretical basis and development of alkaline cements
Glukhovskiy	1965	First called "alkaline cements" because natural substances used as components
Davidovits	1979	"Geopolymer" term—emphasizes greater polymerization
Malinowski	1979	Ancient aqueducts characterized
Forss	1983	F-cement (slag-alkali-superplasticizer)
Langton and Roy	1984	Ancient building materials characterized (Roman, Greek, Cyprus)
Davidovits and Sawyer	1985	Patent leading to "Pyrament"
Krivenko	1986	D.Sc. Thesis, $R_2O-RO-R_2O_3-SiO_2-H_2O$
Malolepsy and Petri	1986	Activation of synthetic melilite slags
Malek et al.	1986	Slag cement-low level radioactive waste forms
Davidovits	1987	Ancient and modern concretes compared
Deja and Malolepsy	1989	Resistance to chlorides shown
Kaushal et al.	1989	Adiabatic cured nuclear waste forms from alkaline mixtures including zeolite formation
Roy and Langton	1989	Ancient concrete analogs
Majumdar et al.	1989	$C_{12}A_7$ -slag activation
Talling and Brandstetr	1989	Alkali-activated slag
Wu et al.	1990	Activation of slag cement
Roy et al.	1991	Rapid setting alkali-activated cements
Roy and Silsbee	1992	Alkali-activated cements: overview
Palomo and Glasser	1992	CBC with metakaolin
Roy and Malek	1993	Slag cement
Glukhovskiy	1994	Ancient, modern and future concretes
Krivenko	1994	Alkaline cements
Wang and Scrivener	1985	Slag and alkali-activated slag microstructure

The field of alkali activated binders saw major contributions from many researchers such as Davidovits, J.J. 1979, Wang et al.1994, Palomo et al.1999, Puertas et al. 2000, Bakharev et al. 2000, Fernández-Jiménez and Puertas 2001, Wallah and Rangan (2005), Pacheco -Torgal et al. 2007, Shi et al. 2006, Bernal et al. 2010, Idawati et al. 2013, Rashad 2013, etc.

## 2.2 ACTIVATION MECHANISMS OF ALKALI ACTIVATED BINDERS:

### 2.2.1 Alkali Activation of Slag Systems

During the activation process of slag (GGBFS), the reaction begins with the attack of alkalis on slag particles, thus breaking the outer layer and then continued by polycondensation of reaction products. Although, the initial reaction products are formed due to the process of dissolution and precipitation, at later stages, a solid state mechanism is followed, where the reaction occurs on the surface of formed particles dominated by slow diffusion of the ionic species into the unreacted core (Wang et al.1994). In the initial stages of hydration, alkali cation ( $R^+$ ) behaves like as a mere catalyst in cation exchange with the  $Ca^{2+}$  ions, as shown in the following equations (Eq 2.1,2.2 and 2.3) (Glukhovsky 1994, Krivenko 1994).



While the alkaline cations act as structure creators, the nature of anion in the solution play a significant role in activation, especially during the early stages particularly with regard to paste setting (Fernández-Jiménez and Puertas 2001). A descriptive model showing the reaction mechanism is presented in Figure 2.1. The final hydration products in case of activation of slag are similar to the products of OPC hydration i.e. C-S-H, but with low Ca/Si ratio. However, the rate and intensity of activation of slag differ majorly as compared to that hydration of OPC. It is reported that the alkalis are not freely available in the pore solution, since they are bound to the reaction products, thereby negating the potential for alkali-silica reactivity, however this depends on the concentration of alkali used.





precursors. A descriptive model showing the activation mechanism of fly ash is presented in Figure 2.2.

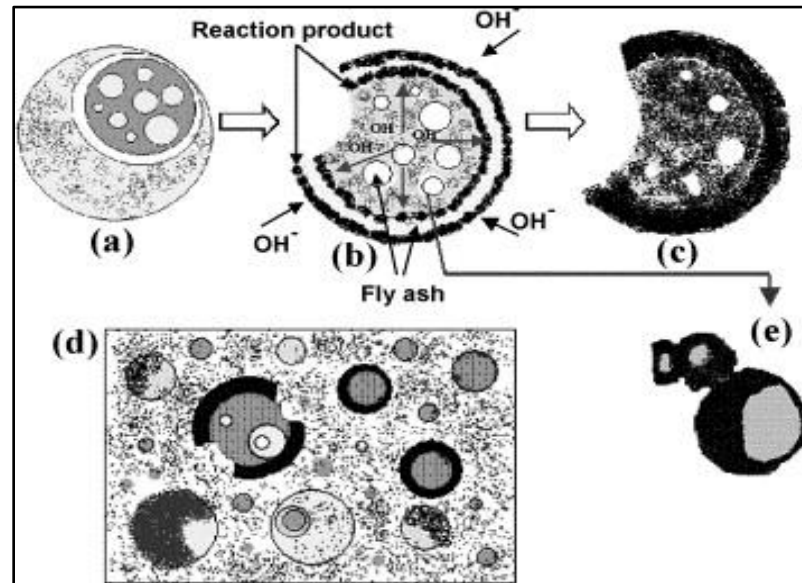


Fig. 2.2 Mechanism of gel formations in alkali activated fly ash binder (Fernandez-Jimenez et al. 2005)

### 2.2.3 Alkali Activated Slag-Fly Ash

The hydration mechanism of AASF is very similar to that of AAS; however, they slightly differ in the rate of hydration. There have been certain contradictions on the reaction products in hydration of AASF. Studies carried out by Puertas et al. (2000) claim the main product formed in AASF to be C-S-H, with no existence of A-S-H; whereas Chi and Huang (2013) have reported the existence of both. Puertas et al. (2000) reported that the reaction products of AASF pastes were C-S-H rich in Al that contains Na in its structure and alkaline A-S-H with a three dimensional structure. Chi and Huang (2013) reported that amorphous alkaline A-S-H and C-S-H gel, to be the products of hydration of AASF. Idawati et al. (2013) found C-A-S-H phase and hybrid C-(N)-A-S-H phases in AASF binders. Sravanthi and Paramita (2013) reported that the dissolution of calcium present in GGBFS affects the both early and later age properties significantly, and

availability of free calcium prolongs the FA dissolution and enhance geopolymer gel formation. They proposed that the hardening process initiated with the precipitation of C-S-H/C-A-S-H, while rapid hardening continues due to accelerated geopolymerization. It was also reported AASF display a basic network formation due to the formation of aluminosilicate geopolymer at a very early age and that product formation was observed on both GGBFS as well as FA spheres.

## **2.3 SOURCE MATERIALS AND ALKALINE ACTIVATORS**

### **2.3.1 Fly Ash (FA)**

Fly Ash (FA) is a by-product generated from the combustion of coal in thermal power plants which are transported by flue gases and captured by electrostatic precipitators before the gases reach chimneys. The FA has fine particles with sizes ranging from 1 to 100  $\mu\text{m}$ . The FA is usually divided into two types based on the amount of calcium content (CaO) present in it, i.e., Class-C and Class-F fly ash. Class-C fly ash is generally obtained from the combustion of lignite and bituminous coals and contains 15 to 35 percent of CaO content. Class-F fly ash is obtained from the combustion of anthracite coals and contains CaO content less than 20 percent. The FA is used as supplementary cementitious material and has been used extensively to partially replace OPC in concrete. Unused FA is dumped into landfills and hence contributes to air, water and soil pollution (Palomo et al.1999, Duxon et al. 2007).

FA is considered as a pozzolanic material due to the presence of high contents of silica and alumina that react with the calcium hydroxide formed during hydration of cement to provide cementitious properties. Due to the high availability of reactive silica and alumina, Class-F FA is preferred for synthesis of geopolymer concrete. Class-F FA is also preferred as a source material due to the presence of low calcium, since the presence of high calcium content may hinder the geopolymerisation process and alter the microstructure (Gourley 2003). The fineness of FA plays a significant role in the development of mechanical strength (Fernandez and Palomo 2003). The breakdown of

glassy surface of FA requires high activation energy, and can be overcome by providing higher temperature and higher alkaline environment (Rajamane 2013).

### 2.3.2 Ground Granulated Blast Furnace Slag (GGBFS)

Granulated Blast-Furnace Slag (GBFS), a by-product of iron and steel industry, is granular material generated when the molten blast furnace slag is rapidly quenched with water. When this granular GBFS is ground to the fineness of cement, it is called GGBFS. The GGBFS is majorly constituted of oxides of calcium (CaO), silica (SiO<sub>2</sub>), alumina (Al<sub>2</sub>O<sub>3</sub>), magnesia (MgO), with some other oxides SO<sub>3</sub>, FeO or Fe<sub>2</sub>O<sub>3</sub>, TiO<sub>2</sub>, K<sub>2</sub>O, Na<sub>2</sub>O, etc. in small quantities. GGBFS is one of the most widely investigated, used and probably the most effective cement replacement material used for concrete manufacturing.

The hydraulic activity of GGBFS can be determined by calculating the basicity coefficient, which is ratio between the total content of basic constituents to total content acidic constituents as given in the equation 2.5 (McGannon 1971).

$$K_b = \frac{CaO + MgO + Fe_2O_3 + K_2O + Na_2O}{SiO_2 + Al_2O_3} \quad (2.5)$$

However, the equation for calculation of basicity coefficient was simplified by excluding minor components such as Fe<sub>2</sub>O<sub>3</sub>, K<sub>2</sub>O, and Na<sub>2</sub>O (less than 1%) in the GGBFS (Wang et al. 1994; Bakharev et al. 2000).

$$K_b = \frac{CaO + MgO}{SiO_2 + Al_2O_3} \quad (2.6)$$

Based on the basicity coefficient (K<sub>b</sub>), the GGBFS can be classified into three groups, i.e. acidic (K<sub>b</sub><1), neutral (K<sub>b</sub>=1), and basic (K<sub>b</sub>>1). However, neutral or alkaline slags are preferred as starting materials for activation of AAS binders. Chang (2003) introduced a parameter termed as the Hydration Modulus (HM) given in equation 2.7 and

suggested it to be greater than 1.4 in order to ensure good hydration properties (Adam 2009).

$$HM = \frac{CaO + MgO + Al_2O_3}{SiO_2} \quad (2.7)$$

### 2.3.3 The Influence of Type, Dosage and Modulus of Alkaline Activators

The source materials for alkali activated binders need to be activated using strong alkalis in order to form the resulting binding material. Caustic alkalis or alkaline salts are the most widely used alkaline activators. The alkaline activators are classified into six groups based on their chemical composition and are tabulated in Table 2.2.

Table 2.2 Classification of alkali activators (Fernandez-Jimenez et al. 2005)

Alkali Activator	Chemical Formula
Hydroxides	MOH
Non-silicate weak acid salts	M <sub>2</sub> CO <sub>3</sub> , M <sub>2</sub> SO <sub>3</sub> , M <sub>3</sub> PO <sub>4</sub> , MF
Silicates	M <sub>2</sub> O · nSiO <sub>2</sub>
Aluminates	M <sub>2</sub> O · nAl <sub>2</sub> O <sub>3</sub>
Aluminosilicates	M <sub>2</sub> O · Al <sub>2</sub> O <sub>3</sub> · (2–6)SiO <sub>2</sub>
Non-silicate strong acid salts	M <sub>2</sub> SO <sub>4</sub>

M - Metal

The alkaline activators generally consist of mixtures of silicates and hydroxides of alkali. Sodium silicate (Na<sub>2</sub>SiO<sub>3</sub>), sodium hydroxide (NaOH), sodium carbonate (Na<sub>2</sub>CO<sub>3</sub>) or a mixture of sodium – potassium hydroxide (NaOH, KOH) with sodium silicate - potassium silicate or any other combinations are the most widely used alkaline activators. A combination of sodium hydroxide with liquid sodium silicate has been agreed to provide the best strength performance for activation of alkali activated binders (Rashad 2013). The strength of AAB's is governed by the type of alkaline activator, activator modulus and dosage of alkaline activator (Fernandez-Jimenez et al.1999). The

Activator Modulus ( $M_s$ ) is the ratio of the mass ratio of  $\text{SiO}_2$  to  $\text{Na}_2\text{O}$  components present in the alkaline activator, while the Dosage (usually referred as % $\text{Na}_2\text{O}$ ) is the total sum of the mass of  $\text{Na}_2\text{O}$  present in the alkaline activator (mass of  $\text{Na}_2\text{O}$  present in liquid sodium silicate + mass of  $\text{Na}_2\text{O}$  equivalent in sodium hydroxide if combination of sodium silicate and sodium hydroxide used as alkaline activator).

Wang et al. (1994) reported that mechanical strength and other properties of AAS mortars were influenced by the nature of the alkaline activators. The dosage and the activator modulus have significant effects on the properties of AAB's. They provided a range of activator modulus within maximum compressive strength may be obtained based on the type of GGBFS.

a) Acid slag 0.75 – 1.25,

b) Neutral slag 0.90 – 1.3 and

c) Basic slag 1.0 – 1.5

Figure 2.3 presents the variation of 28-day strength with activator modulus for different type of GGBFS. It may be noticed that the strength increases with higher activator modulus up to an optimal activator modulus; however, with further increase in activator modulus, the strength decreases.

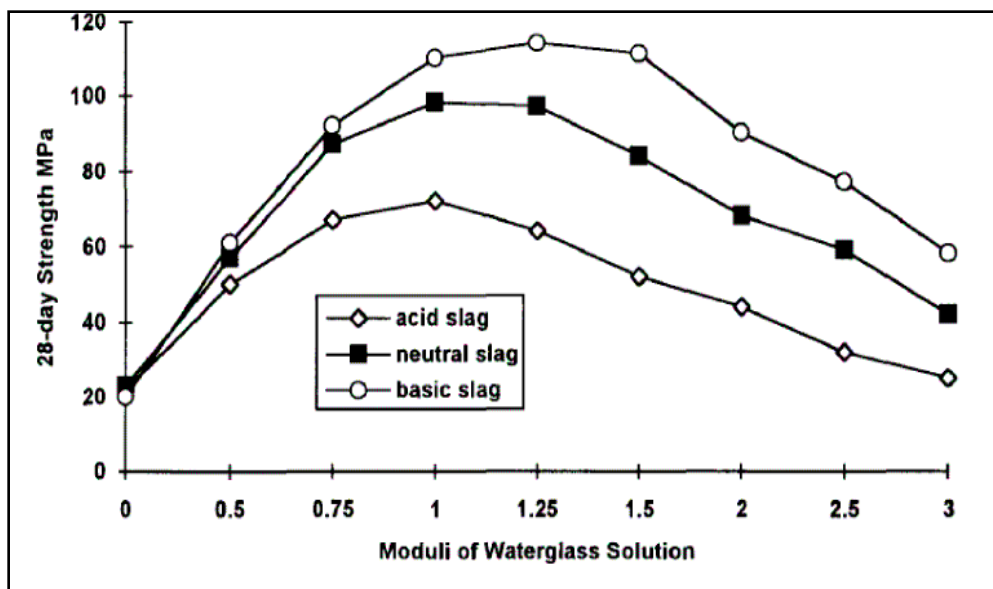


Fig. 2.3 Moduli of sodium silicate solution Vs 28-day strength for different types of GGBFS (Wang et al. 1994)

Bakharev et al. (1999) investigated the activation of Australian GGBFS using different activators such as sodium silicate, sodium hydroxide, sodium carbonate, sodium phosphate, and combinations of these activators and recommended sodium silicate solution with 5%  $\text{Na}_2\text{O}$  dosage with an activator modulus of 0.75 for better results. Fernandez-Jimenez et al. (1999) reported that the mechanical strength of AAS mortars is mostly influenced by the type and nature of alkaline activator, dosage of alkaline activator and observed that the optimum dosage of alkaline activator varies from 3% and 5.5 % of  $\text{Na}_2\text{O}$  by the mass of GGBFS.  $\text{Na}_2\text{O}$  dosage above this limit may cause efflorescence problems along with inefficient uneconomical mixtures. Ultimate strength higher than OPC can be achieved with GGBFS cements activated using sodium silicate with modulus between 0.6 and 1.5 with the appropriate  $\text{Na}_2\text{O}$  dosage (Krizan and Zivanovic 2002). Fernandez and Palomo (2005) studied the activation of FA using different types of alkaline activators and by varying the  $\text{Na}_2\text{O}$  dosage between 5% to 15% (mass of binder). They reported that the activator modulus along with a water/binder (w/b) ratio, affect the mechanical strength. They observed that the  $\text{Na}_2\text{O}$  dosage of 5.5% (mass of fly ash) led to very low pH, that affected the reaction development negatively;

while the increase in Na<sub>2</sub>O dosage led to higher strength with 14% Na<sub>2</sub>O dosage (mass of FA) providing the maximum compressive strength. Garcia et al. (2006) studied activation of AASFC mixes with different GGBFS: FA ratios of 100:0, 75:25, 50:50, 25:75 and 0:100 activated using sodium silicate solution. The Na<sub>2</sub>O dosages 4%, 6% and 8% (mass of binder) were selected and the activator modulus was varied from 0, 0.75, 1, 1.5 and 2. The pastes were subjected to heat curing at 75°C for 24 h and then at 20°C up to 28 days. The results indicated that the best modulus for all the mixes were in the range of 1 to 1.5. Cengiz et al. (2009) investigated the AAS mortars using different types of activators such as sodium hydroxide, sodium carbonate, and sodium silicate, with varying activator modulus and with Na<sub>2</sub>O dosages in the range of 4-8% (mass of GGBFS). It was observed that the compressive and tensile strengths of AAS mortars increased with Na<sub>2</sub>O dosage of alkaline activators, and also suggested that there exists an optimal alkaline modulus for which the highest compressive and tensile strengths can be obtained. Law et al. (2012) reported that the activator modulus between 1.0 to 1.25 may be considered optimal for AAS mixes. Wardhano et al. (2012) reported that activator modulus to have significant influence on the early strength of AAS mixes. Chi (2012) reported that the mechanical and durability properties of AAS concrete mixes were significantly dependent on Na<sub>2</sub>O dosage of the alkaline activators. Kovtun et al. (2013) carried out studies on the activation of basic and neutral types of GGBFS and reported that 4% of the Na<sub>2</sub>O dosage (by weight of GGBFS) as the optimal dosage for AAS mixes for both kinds of GGBFS. Shekhovtsova et al. (2014) studied the effect of Na<sub>2</sub>O dosages on the compressive strength of AAFA pastes in the range of 3% to 15% (by weight of FA) and reported that increase in the Na<sub>2</sub>O dosage greatly affected the compressive strength of AAFA pastes, with the highest strength reported at 9% of Na<sub>2</sub>O dosage (by weight of FA).

## **2.4 PROPERTIES OF ALKALI ACTIVATED BINDERS**

### **2.4.1 Mechanical Properties of Alkali Activated Slag**

The mechanical properties of AAS mixes are influenced by various parameters such as the type and nature of alkaline activators, Na<sub>2</sub>O dosage and activator modulus,

curing regime, water to binder ratio, chemical admixtures, etc. Various studies have reported that the AAS concretes display similar or better mechanical properties as compared to Ordinary Portland Cement Concrete (OPCC). Collins and Sanjayan (1999) investigated AAS concrete mixes with the emphasis of achieving reasonable workability and equivalent one-day strength as compared to OPCC under normal curing temperature, and concluded that AAS concrete displayed similar one-day strength and superior ultimate strength as compared to OPCC. Sakulich et al. (2009) reported AAS concrete achieved compressive strengths up to 45 MPa and flexural strength up to 4 MPa, when cured for 28 days under normal room temperatures, activated using NaOH-activated solution. Bernal et al. (2010) studied the mechanical properties of AAS concretes reinforced with steel fibers at early ages and concluded AAS concrete to be a potential building material with or without steel fibers. Bernal et al. (2011) studied the effect of binder content on the strength performance of AAS concretes and reported that regardless of the binder content, AAS concrete developed higher compressive strength when compared to conventional OPCC mixes; however, higher binder content led to increase in strength in both AAS concrete and OPCC mixes at 28 days. Wardhono et al. (2015) reported high early strength with AAS mixes, however the 28-days compressive strength was found to be lower than OPC. It was also reported that the modulus of elasticity and density showed reduced values with age, which was attributed to the occurrence and propagation of micro-cracks with increasing age. The use of AAS concrete mixes is associated with certain problems such as high shrinkage and poor workability impede its practical application (Bakharev et al. 2000). Investigations on the use of chemical admixtures to overcome problems related to high shrinkage and poor workability have been carried out by researchers. Bakharev et al. (2000) investigated the use of various chemical admixtures, which were used for OPC concrete, such as superplasticiser based on modified naphthalene formaldehyde polymers, air-entraining agent, water-reducing, shrinkage-reducing admixtures at dosages of  $6\pm 10$  ml/kg, and gypsum (6% by GGBFS weight), on AAS mixes. It was observed that the use of air-entraining agent, shrinkage-reducing admixtures and gypsum reduced the shrinkage significantly. While the



naphthalene-based superplasticizer significantly increased the shrinkage and reduced the strength of AAS concrete, the air-entraining agent improved the workability without any negative effects on the compressive strength and recommended its use in AAS concrete. Similar observations were made by several other researchers (Douglas and Brandstetr 1990, Wang et al. 1994).

#### **2.4.2 Curing Regime**

The properties of AAS mixes are affected considerably with the curing condition to which they are subjected. Over the years, the properties of AAS mixes have been studied by subjecting the AAS mixes to different curing conditions such as heat curing, steam curing, normal room temperature curing (open air curing), water curing, etc. Altan and Erdogan (2012) studied AAS mortar mixes activated using a combination of sodium silicate and sodium hydroxide at room and elevated temperatures. They observed that the heat cured samples gained strength rapidly, however samples cured at room temperature also gained comparable strengths with time. It was also reported that the heat evolution of AAS hydration was lesser compared to OPC hydration and the use of lower water to binder (w/b) ratio provide higher strength at early ages. Aydın and Baradan (2012) reported that high strength mortars with compressive strength up to 70 MPa can be produced with alkaline activators having alkali content as low as low 2% (by mass of binder) when subjected to autoclave curing. They also observed that AAS mixes provided similar performance as compared to autoclave curing, when activated using activator solutions with high activator modulus. In case of heat curing, the curing time and temperature are one of the critical factors in determining the strength of alkali activated mixes (Datta and Ghosh 2014, Shekhovtsova et al. 2014). Qureshi and Ghosh (2013) studied the effect of curing regime on the strength behaviour of AAS pastes under different curing conditions such as water curing at 27<sup>0</sup>C, heat curing at 50<sup>0</sup>C and controlled curing with relative humidity 50%, 70% and 90 % at 27<sup>0</sup>C and reported that maximum strength was obtained at water curing condition. They concluded that mechanical behaviour AAS paste was significantly affected by the curing conditions.

Bilim et al (2015) investigated the AAS mixes with Na<sub>2</sub>O dosages of 4% and 6% by mass of slag to study the effect of curing conditions on AAS mixes and reported that curing conditions affected the mechanical behaviour of AAS mixes as compared to OPC mixes. The AAS mixes attained high early strength as compared to OPC mixes when subjected to elevated temperatures.

### **2.4.3 Mechanical Properties of Alkali Activated Slag-Fly Ash**

The performance of AASF mixes is significantly dependent on the proportion of GGBFS and FA used in the mix, apart from various other parameters such as the type and nature of alkaline activators, Na<sub>2</sub>O dosage and activator modulus, curing regime, water to binder ratio, chemical admixtures. The strength properties of AASF are strongly dependent on the amount of GGBFS present in the AASFC binder. Puertas et al. (2000) studied the strength behaviour of AASF mixes and reported increases in compressive strength with increase in GGBFS content. Similar observations have been made by several other researchers (Li and Lui 2007, Rajamane 2013). Increase in the compressive strength with increased Na<sub>2</sub>O dosage has been studied by Guerrieri and Sanjayan (2009) as in case of AAS mixes. Higher content of FA in the AASF mixes tends to decrease compressive strength drastically, mainly due to the lower reactivity of FA as compared to GGBFS. The breakdown of glassy surface of FA requires high activation energy. The higher activation energy may be induced by higher temperature and higher alkaline environment (Rajamane 2013). However, AASF mixes with proper proportions of GGBFS: FA ratios can achieve sufficient strength even at ambient room temperatures without any need for heat curing (Manjunath et al. 2011, Nath and Sarker 2012). Compressive strength up to 50 MPa have been achieved for AASF mixes with equal blending (50:50) of GGBFS and FA without heat curing (Narasimhan et al. 2011). Rajamane et al. (2013) reported that GGBFS when replaced beyond 50% by FA in AASF systems resulted in reduction in strength and suggested higher concentrations of alkaline activator solution for mixes containing more than 50% of FA, to achieve sufficient strength. It was concluded that AASF mixes containing FA content up to 50%, develop a

considerable amount of strength at ambient temperature, and can be easily adopted for practical applications. Idawati et al. (2013) observed that the reduction in the strength of mixes with high contents of FA can be countered by lowering the water to binder ratios and stated that water to binder ratios can be controlled to achieve the desired strength in AASF concrete mixes with high amounts of FA.

#### **2.4.4 Effect of Fly Ash on the Workability of Alkali Activated Slag-Fly Ash**

The inclusion of FA in alkali activated concrete mixes has a significant effect with respect to the strength and workability of the mixes. Several studies have reported the use of FA has a positive effect on the workability; however the compressive strength reduced with the increase in the FA content. Rashad a (2013) investigated with workability properties of slag-FA-based mixes and reported an increase in the workability of the mixes. Yang et al. (2008) investigated the workability properties of AAS and AAFA mortar mixes with a constant w/b ratio of 0.5 and binder to sand ratio of 1: 3, and observed that the AAS mortar had lower workability than FA-based alkali-activated mortar. Rashad b (2013) presented a comprehensive overview of the previous works carried out using different additives in AAS system and the influence of different additives on the properties of AAS. It was concluded that the inclusion of FA in AAS matrix increased the workability. The improved workability with higher FA contents is mainly due to the particle size and morphology of this precursor (Wang et al. 2003). Although, most of the researchers reported that inclusion of higher content FA resulted in a reduction of strength in the AASF mixes, few others believe that the optimal content of FA in AASF mixes can provide the highest compressive strength, which again is further dependent on other parameters such as activator type, activator concentration, modulus ratio and curing conditions (Chi and Huang 2013). Apart from improving the workability, the inclusion of FA has a positive effect on the setting time of alkali activated mixes. The setting time of AAS and AASF mixes increased with the inclusion of FA (Rashad *b* 2013; Nath and Sarker 2012). One of the major limitations of AAS mixes related to poor workability can be improved with the inclusion of proper amount of FA. AASF mixes

formulated with the proper amount of FA, with optimal contents of Na<sub>2</sub>O dosage and activator modulus of alkaline activators and reduction of water binder ratios can achieve sufficient strength with desired workability along with prolonged setting time even at ambient room temperature (Idawati et al.2013).

## **2.5 DURABILITY PROPERTIES OF ALKALI ACTIVATED BINDERS**

Durability is one of the most important properties of concrete. Concrete is inherently a durable material. However, concrete is susceptible to attack in a variety of different exposure conditions, unless some precautions are taken. Concrete is well known for its strength, ease of production, water tightness and durability properties. However, concrete are most of the times exposed to aggressive environments. The aggressive environments can be naturally occurring (such as sea-waters, soils rich in sulphates, etc..) or man-made (such as chemical effluents from industries, waste water from drainage infrastructure, etc.), that affect the long term performance of concrete. Concrete undergoes degradation under the influence of such aggressive environments due to chemical processes involving exchange of ions, thus causing changes in the microstructure of the binding matrix, leading to reduction in the mechanical strength. The cement paste is affected by the presence of acids, sulphates, chlorides, etc. The durability of concrete subjected to chemical attacks such as acids and sulphates are the main aspects of concern. Due to the presence of high calcium compounds in chemical composition of OPC, the resistance of OPC to acid and sulphate resistance is low. The acids and sulphates usually attack the products of hydration of cement to form products such as gypsum and ettringite along with changes in the C-S-H structure. The formation of the additional products leads to internal expansive stress, causing the deterioration of the concrete. Water absorption, total porosity and sorptivity are related to the ability of water or fluid to move into mortar and concrete and therefore have significant importance in the durability related properties of concrete structures. The water absorbed in the presence of oxygen may initiate the corrosion of reinforcement in concrete structures. Water may enter into the concrete through the capillary action of pore systems (Alexander et al.

2013). However, better durability properties of OPCC are reported with addition of pozzalonic materials such as FA, GGBFS, etc. in the binder (Gambhir 2004).

Efforts to study the durability properties of alkali activated binders have been carried out by several researchers (Bakharev 2005, Fernandez-Jimenez et al. 2007, Adam 2009, Pacheco-Torgal et al. 2012, Rajamane 2013 etc.). The AAS and AASF mixes are known to have reported better durability properties when exposed to aggressive environments (Duxson et al. 2007, Mithun and Narasimhan 2015). The better durability properties of AAS and AASF mixes are mainly due to the absence of calcium hydroxide (Portlandite) and low calcium content in the reaction products (Bakharev et al. 2003). The durability properties of alkali activated binders are affected by various parameters such as the type and concentration of the alkaline activator, activator modulus, binder type, fineness, curing conditions, water/binder ratio, use of admixture as well as fibers, etc. (Palacios and Puertas 2005, Rodriguez et al. 2008, Hafa et al. 2011). The mechanism of sulphate attack on OPC, AAS and AASF mixes is expected to be different, due to differences in the binder chemistry, reaction products, large differences in the amount and role played by calcium in these systems (Bakharev et al. 2003). Bakharev et al. (2002) studied the sulphate resistance of AAS systems and reported that AAS samples did not expand; however, it showed visible cracks and traces of gypsum. Increase in the strength of AAS and AASF concrete samples have been reported when immersed in sodium sulphate solution due to ongoing binder formation reactions; however the strength decreased when immersed in magnesium sulphate solution (Bakharev et al. 2002). Varaprasad (2006) reported that ambient cured alkali activated binders mixes containing fly ash, GGBFS blended in proper proportions as source material can attain excellent durability properties. Rajamane et al. (2013) investigated sulphuric acid resistance of AAS and AASF in comparison with Portland pozzolana cement containing FA and reported that AAS and AASF mixes when immersed in 2% and 10% of sulphuric acid, displayed lower weight loss, thickness loss and strength loss as compared to Portland pozzolana cement concrete. Chi (2012) investigated the effect of Na<sub>2</sub>O dosages and curing conditions on the sulphate attack resistance of AAS concrete and concluded that

sulphate resistance improved with increase in dosage of  $\text{Na}_2\text{O}$  and also stated that AAS concrete cured at  $60^\circ\text{C}$  proved the best durability performance followed by air and limewater curing. Law et al. (2012) studied the durability properties of AAS concrete such as water sorptivity, chloride and carbonation resistance and reported lower durability performance as compared to OPC and blended concrete mixes. The lower performance was attributed to surface micro cracking in AAS concrete. Chi and Huang (2013) studied the water absorption properties of AAS and AASF activated at 4% and 6% of  $\text{Na}_2\text{O}$  dosages with an activator modulus of 1 and reported that a reduction in the percentage of water absorption with increasing GGBFS and decreasing FA content at both concentrations. Datta and Ghosh (2014) studied the effect of incorporation of GGBFS on the magnesium sulphate resistance of AAFA mixes and reported that addition of GGBFS in AAFA resulted in high residual strength after immersion in 10% of magnesium sulphate solution for 15 weeks.

## **2.6 FATIGUE CHARACTERISTICS OF CONCRETE PAVEMENTS**

Fatigue failure is one of the major modes of failure in structures like concrete pavements that subjected to repeated application of loads. The fatigue failure in concrete pavements occurs under the influence of repetitive loads or cyclic load, whose peak values are considerably lower than the safe loads estimated through static tests. In fatigue failure, the material fails by repeated application of load, which is not large enough to cause failure due to single application. The fatigue failure in concrete structures causes progressive, localized and permanent damage due to dynamic or moving or cyclic loads. Usually, this change leads to cracking or failure. The failure due to fatigue occurs as a result of development of internal cracks and progressive growth of cracks under the action of cyclic loadings, which leads to failure of the pavements at stresses smaller than the modulus of rupture of the concrete (Hui et al. 2007, Lee and Barr 2004). Although studies on fatigue failure began over many decades, there is still a lack of understanding regarding the nature of fracture mechanism in cementitious composite materials due to fatigue. This is due to the complex nature of cementitious composite materials and their

properties, that are influenced greatly by a large number of parameters. The fatigue failure in plain concrete is influenced by several parameters such as composition and quality of the concrete, age of the concrete, moisture conditions, load frequency, minimum stress used in load cycle, stress levels, rest period, waveform of cyclic load, etc. (Naik et al. 1993). Fatigue loading can be classified as low cycle and high cycle loading. Low cycle loading involves application of few load cycles at higher stress levels; while high cycle loading involves application of a large number of load cycles at lower stress levels. Generally, concrete pavements in highways and airport pavements are classified as high cycle loading (HSU 1981). Hence, fatigue strength is one of the important parameters to be considered while designing concrete pavement for roads and airfields. The development of reliable flexural fatigue life prediction model is one of the toughest challenges in research (Phull and Rao 2007).

Over the years, the fatigue behaviour of plain OPCC mixes, OPCC containing mineral admixtures, fiber reinforced concrete, high performance concrete, etc., have been studied. However, there is very meagre research available on the fatigue performance of alkali activated concrete mixes. The performance of AASF mixes incorporating steel fibres under fatigue was investigated by Kumar (2011). It was concluded that AASF mixes with 1% steel fibres displayed better strength as compared 0.5% steel fibres. The addition of steel fibres improved the fatigue life of AASF concrete mixes. Silva et al. (2004) evaluated the performance of AAS concrete in comparison to OPC concrete with emphasis to the fatigue behaviour and reported that the AAS concrete performed better than OPCC, mainly due to the strong matrix/aggregate bonding in AAS concrete, due to the massive nature of the AAS matrix. The fatigue behaviour of OPCC made with two different lightweight aggregate, at stress levels of 40, 50, 60, 70, and 80 percent of the ultimate static compressive strength was studied by Gary et al. (1961) and it was reported that the fatigue behaviour of light weight concrete and normal concrete was essentially the same. Klaiber et al. (1979) investigated the effect of aggregate types, gravel and crushed limestone on the fatigue behaviour of plain OPC concrete in flexure and reported that the flexural fatigue performance of plain OPC concrete are influenced by the type of

coarse aggregates used in the concrete. It was observed that the concrete made with gravel displayed better fatigue performance as compared to limestone aggregates. Hui Li et al. (2006) investigated the flexural fatigue performance of plain concretes containing nano-particles ( $\text{TiO}_2$  and  $\text{SiO}_2$ ) and reported improved fatigue life and sensitivity to change in stress. Heeralal et al. (2009) investigated the fatigue behaviour of OPC concrete with steel fibers and different proportions of recycled aggregate under both static and fatigue loading at different stress levels. The study suggested the inclusion of steel fibers improved the fatigue performance of recycled aggregate concrete. Li-Ping Guo et al. (2010) reported that the addition of FA and GGBFS to OPC concrete have considerable impact on the fatigue crack propagation and damage accumulation under high/low stress levels, and concluded that materials with such admixtures display improved fatigue resistance.

### **2.6.1 S-N Curves and Probabilistic Approach**

The fatigue behaviour of concrete mixes is most commonly characterized with two important terms; firstly the Stress Ratio (SR), i.e. the ratio of stress applied to the modulus of rupture of concrete and secondly the Fatigue Life (N), i.e. the number of cycles to failure. Most of the studies on the fatigue behaviour of concrete are intended to arrive at a relationship between the stress ratio and fatigue life. This relationship is commonly plotted on so-called S-N curve (or Wohler curve). The S–N curve in which ‘S’ denotes stress level and ‘N’ denotes the fatigue life; represents a plot between with linear S verses log N scale and is the most commonly used in engineering. The employment of S–N curves for the representation of fatigue data gives a clear idea on the distribution of fatigue lives under different stress ratios. It is also generally accepted that non dimensionalized S-N curve is independent of the shape of the specimen, strength of concrete, curing conditions, age, moisture condition at loading, etc. A typical S-N curve is presented in Fig.2.4 (Naik et al. 1993).



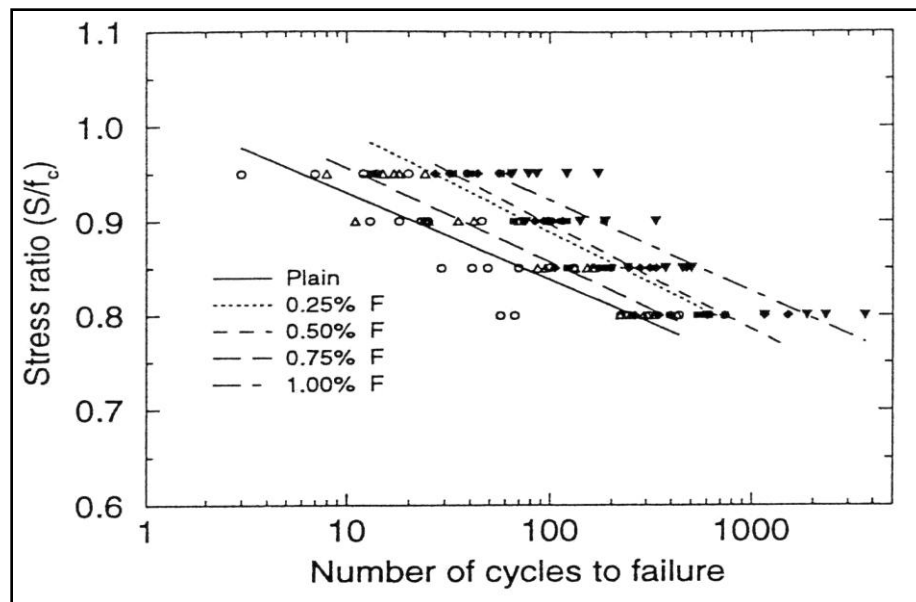


Fig.2.4 A typical S-N curve

(Source: <http://www.columbia.edu/cu/civileng/meyer/research/fati1.html>)

In order to obtain statistically reasonable information on the fatigue behaviour of concrete mixes, it is necessary to test several specimens at every stress level, due to the fact that the fatigue tests display large scatter and variability in the number of cycles to failure. This variability and scatter in fatigue data of concrete is mainly due to influence of several parameters like material strength and variability, applied loads, testing conditions, etc. Therefore, the fatigue design process is associated with lots of uncertainties from the numerous assumptions made in analysis and material variability and hence probabilistic concepts need to be implemented to model the fatigue data, in order to evaluate fatigue resistance of concrete structures (Naik et al. 1993). Probabilistic procedures can be used to obtain the number of cycles to failure at any required probability of failure. A probabilistic approach to determine the fatigue reliability of concrete was introduced by Oh (1986) and it was found that fatigue life data on concrete under a given stress level followed the Weibull probability law. The results of the study reported that Weibull distribution provided a better representation of the experimental data than the log normal distribution and suggested that it can be used to describe the fatigue behaviour of concrete. Oh (1991) investigated the distributions of fatigue life of

concrete at different stress ratios, i.e. 0.85, 0.75 and 0.65 using specimens of size (100 x 100 x 500) mm loaded using the third-point loading system at a frequency of 250 cycles/min. The results indicated that the probabilistic distributions of fatigue life of concrete were dependent on stress ratios and hence, the shapes of Weibull distribution to describe the fatigue life of concrete, depended upon levels of applied fatigue stress. Singh and Kaushik (2001) carried out a study on the fatigue strength of Steel Fibre Reinforced Concrete (SFRC) on specimens of size (100 x100 x 500) mm under four-point flexural fatigue loading. The results indicated that the statistical distribution of equivalent fatigue life of SFRC was in agreement with the two-parameter Weibull distribution. Ganesan et al. (2013) investigated the flexural fatigue behaviour of Self Compacting Rubberized Concrete (SCRC) with and without steel fibers, and concluded that the probabilistic distribution of fatigue life of SCRC at a given stress level can be approximately modelled by the two-parameter Weibull distribution.

## **2.7 STEEL SLAG**

Steel slag is an industrial by-product obtained from the iron and steel industry either during the conversion of iron into steel in Basic Oxygen Furnace (BOF) or by melting scrap to produce steel in an Electric Arc Furnace (EAF). The steel slag may be available as Basic Oxygen Furnace (BOF) slag, Electric Arc furnace (EAF) slag or Open Hearth Furnace (OHF) slag based on the production technique employed. The chemical composition of EAF slag and BOF slag may be different depending upon the fluxes or additives used during the production of steel (Fruehan 1985). As per American Society for Testing and Materials (ASTM) steel slag is defined as a non-metallic product, consisting essentially of calcium silicates and ferrites combined with fused oxides of iron, aluminium, manganese, calcium and magnesium that are developed simultaneously with steel in basic oxygen, electric arc, or open hearth furnaces (Kalyoncu 2001). Steel slag may be produced in Basic Oxygen Furnace (BOF) or Electric Arc Furnace (EAF) and hence named accordingly. In BOF technique, hot liquid metal generated from blast furnace, consisting of scraps, fluxes, lime and dolomite are charged into the furnace and

then the lance is lowered into the convertor, continued with injection of oxygen under high pressure (Shi 2004). The oxygen injected combines and removes the impurities. These impurities are mainly composed of carbon in the form of gaseous carbon monoxide along with silicon, manganese, phosphorous and some iron as liquid oxides, which react and combine with lime and dolomitic lime to produce steel slag. The steel slag generated is molten and floats on the top of molten steel, and is then skimmed off into a separate pot from an outlet, while the molten steel removed from another outlet. The molten steel slag is then sprayed with a strong jet of water for cooling and after cooling the hardened steel slag is crushed and subjected to magnetic separation to remove metallic impurities. After the metallic separation, the steel slag may be further crushed and hence made available for use in various applications. In case of Electric Arc Furnace (EAF), cold steel scraps are heated and melted using electric current, unlike the BOF process that uses hot metal liquid from the blast furnace. During the melting process, the fluxes and other metals are added to the charge to obtain the required chemical composition, along with injection of oxygen to purify the steel. The steel slag then generated is poured off from a separate outlet and is subjected to cooling, crushing, magnetic separation and other operations (Patel 2008).

Currently, the steel slag finds its use in various applications like aggregates for bituminous roads, road bases and sub-bases, manufacture of blended cement, base application, construction of unpaved parking lots, railroad ballast, landfill, shoulder material for highway, construction of berms and embankment, agricultural purposes, soil stabilization, and for remediation of industrial waste water run-off, etc. (NSA 2003).

### **2.7.1 Physical and Chemical Composition of Steel Slag Aggregates**

The physical appearance of steel slag is generally black in colour, having a sharp angular shape with porous texture surface and stone-like appearance. The steel slag aggregates display high bulk density and specific gravity. Some of the typical physical and engineering properties of steel slag are listed in Table 2.3. The chemical composition is generally expressed in term of oxides usually determined by elemental analysis carried

out using X-ray fluorescence spectrometer. The typical chemical composition of steel slag is tabulated in Table 2.4.

Table 2.3 Typical physical and engineering properties of steel slag

Specific gravity	3.1-3.6
Maximum dry unit weight (kN/m <sup>3</sup> )	15.7-18.9
Water absorption (%)	0.2-2
California Bearing Ratio (CBR)	Up to 300
Los Angeles Abrasion	20-25%
Porosity (%)	Up to 3

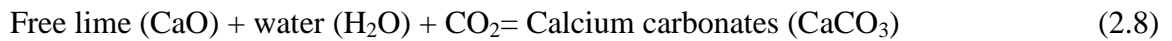
Table 2.4 Typical range of composition of steel slag (FHWA 2012)

Oxide Composition	Percentage (by weight)
CaO	40 - 52
SiO <sub>2</sub>	10 -19
MgO	5 -10
Al <sub>2</sub> O <sub>3</sub>	1 - 5
MnO	5- 8
FeO	10-40
P <sub>2</sub> O <sub>5</sub>	0.5-1.0
SO <sub>3</sub>	less than 0.1
Metallic Fe	0.5-6

### 2.7.2 Acceptability of Steel Slag Aggregates

The acceptability of steel slag aggregate in the construction industry (especially concrete) is associated with few issues that limit the use of such aggregates. The two main issues related to the use of steel slag aggregates include volume expansion and high density of steel slag. The volume expansion of steel slag aggregate is mainly due to the presence of free calcium and magnesium oxides, which remain undissolved in the steel slag. This unhydrated free calcium (free lime) and magnesium oxides when comes in contact with water and in the presence of carbon dioxide, undergoes hydration and leads

to volume expansion. The following chemical reactions explain the conversion of free calcium and magnesium oxides into calcium carbonates ( $\text{CaCO}_3$ ) and magnesium carbonates ( $\text{MgCO}_3$ ) after coming in contact with water.



The reaction primarily begins with the reaction of free lime with water to form calcium hydroxide ( $\text{Ca(OH)}_2$ ), and further this calcium hydroxide ( $\text{Ca(OH)}_2$ ) in the presence of carbon dioxide reacts to form calcium carbonate ( $\text{CaCO}_3$ ). As a result of this hydration, there is an increase in the volume of the aggregates. The volume changes may either occur within a few weeks of production or after a few months, if the steel slag is protected initially from coming in contact with water. The hydration of free lime occurs rapidly, causing large volume changes in a relatively short period of time, however hydration of free magnesia occurs slowly and contributes to the long term expansion (GeoPave 1993). To overcome the expansion related problems, the steel slag aggregates are generally subjected to a process of weathering or aging for a period of over six months, before using it for construction purposes. Weathering of steel slag reduces the amount of free lime within acceptable limits. After being subjected to weathering, the steel slag aggregates exhibit slight alterations in their physical properties which show a thin layer of calcite ( $\text{CaCO}_3$ ) on the surface (van Der Laan 2008).

Another issue related to the use of steel slag aggregates is its high density. Steel slag are quite heavier than other naturally available rock aggregates such as limestone, granite, etc. Such denser aggregate would require higher tonnage than other aggregates for a given volume that may create economic disadvantage especially at locations where transportation costs are significant (GeoPave 1993). Also, the use of heavier aggregates such as steel slag would increase the density of concrete, which again will affect the structural design and hence the economy if used for structural applications. However,

high density aggregates if used for highway applications may not affect much with regard to the pavement design.

### **2.7.3 Previous Studies on Steel Slag Aggregates in Concrete**

Several researchers have investigated the possible use of steel slag as fine and coarse aggregates in conventional OPC concrete and its effects on the different mechanical and long-term properties of mortar and concrete. The engineering properties along with physical and chemical properties of steel slag aggregates have been investigated. Studies conducted in the past have reported the use of steel slag aggregates to be advantageous in conventional concrete (Alizadeh et al. 1996, Maslehuddin et al. 2003, Shekarchi 2003, Taha et al. 2014). Although studies related to the incorporation of steel slag aggregates in conventional concrete have proved to enhance the mechanical properties; however, for few researchers, the inclusion of steel slag aggregates in conventional concrete resulted in similar or slightly lower performance than natural aggregates (Manso et al. 2004, Ivanka et al. 2011, González-Ortega et al. 2014). Kawamura et al. (1983) reported reduction in compressive strength with weathered BOF slag aggregates when used in OPC concrete, mainly due to slow hydration of free lime on or near the surface of BOF slag. Maslehuddin et al. (2003) examined the mechanical and durability performance concrete containing steel slag aggregates in comparison with crushed limestone aggregates and reported better performance of steel slag aggregates. Manso et al. (2006) observed that the mechanical and durability of steel slag concrete was acceptable, though slightly lower than that of conventional concrete with traditional aggregates. Ameri et al. (2012) reported an increase in the compressive strength of cement concrete containing up to 25% BOF slag aggregate as compared to control concrete; however, concrete mixes containing higher quantities of BOF slag displayed a decrease in the compressive strength. Papayianni et al. (2010) achieved compressive strength up to 60 MPa and superior abrasion resistance with the use of steel slag in concrete quality pavement and reported steel slag to be cost effective and advantageous. Ivanka et al. (2011) investigated concrete mixtures prepared with coarse steel slag

fractions by evaluating the hardened state properties, such as compressive and flexural strength, static modulus of elasticity, volume changes and corrosion susceptibility and compared it with the properties of reference concrete made of commonly used natural aggregate materials, namely dolomite. The results concluded that concrete with steel slag aggregates achieve slightly lower strength as compared to conventional concrete. Concrete pavements with expansive steel slag aggregates were constructed in Tampa, Florida in 1980, which reported pavement failure showing longitudinal cracks and crack openings (Armaghani et al. 1988). Concrete pavement constructed using EAF slag aggregates was monitored and surveyed over 10 years of service life and it was reported that the compressive strength and tensile properties of the cores extracted had superior strength than conventional concrete (Papayianni and Anastasiou 2010). However, there is limited research available on the effect of steel slag aggregates on the properties of alkali activated binder concrete mixes.

## **2.8 SUMMARY**

From the detailed literature review, it is observed that the strength and durability of alkali activated concrete mixes are affected by many factors such as type of binder, chemical composition of the binder, water-to-binder ratio, percentage of sodium oxide dosage ( $\text{Na}_2\text{O}$ ), type of alkali activator, modulus of alkaline activator, water content, type of curing, etc. The AAS and AASF mixes if designed properly, may obtain higher strength and better durability as compared to conventional OPCC. AAS and AASF mixes containing higher quantities of GGBFS can attain sufficient strength even at room temperatures, when subjected to air curing, without any need for heat curing or other methods. The inclusion of higher amounts of FA in AASF concrete mixes results in a decrease in the strength properties, however the workability increases. The activation energy required for alkali activated mixes containing large proportions of FA is higher and hence replacement of GGBFS with FA beyond 50% in AASF mixes will require a higher dosage of the alkaline activator solution. The combination of sodium hydroxide and liquid sodium silicate if used as alkaline activator provides the best activation for

alkali activated binders. The strength and durability properties of alkali activated concrete mixes are significantly influenced by the sodium oxide dosage ( $\text{Na}_2\text{O}$ ) and activator modulus ( $M_s$ ) of the alkaline solution. There exists an optimal activator modulus ( $M_s$ ) and sodium oxide dosage ( $\text{Na}_2\text{O}$ ) at which the maximum strength of alkali activated binders can be attained. The optimal sodium oxide dosage varies between 3% and 5.5% of  $\text{Na}_2\text{O}$  (by weight of binder) for AAS mixes, whereas higher dosages may lead to uneconomical mixtures and efflorescence problems. The optimal activator modulus ( $M_s$ ) varies between 0.75 and 1.75 for AAS and AASF mixes. The water to binder ratio, sodium oxide dosage ( $\text{Na}_2\text{O}$ ), activator modulus ( $M_s$ ) etc., needs to be controlled in order to obtain mixes of the required strength and workability. Steel slag, an industrial by-product can be looked upon as a potential replacement for traditional aggregates in concrete. Improved or satisfactory performance of steel slag aggregates have been reported by various researchers when used in conventional OPC concrete. The use of steel slag as coarse aggregates in concrete is associated with problems related to volume expansion and higher density. Steel slag aggregates must be allowed to undergo the weathering process before using as an aggregate for concrete production. However, there is limited research available on strength, durability and fatigue performance of alkali activated concrete mixes incorporating steel slag as coarse aggregate. The present research is focussed to study the properties of sustainable air-cured AAS and AASF mixes with steel slag as coarse aggregate with the aim of conserving natural raw materials and to use marginal materials.



## **CHAPTER 3**

### **MATERIALS AND METHODS**

#### **3.0 GENERAL**

The selection of materials for the production of concrete is one of the important steps in the mix design procedure. This chapter provides a detailed description of the various steps involved in the mix design process for OPCC, Alkali Activated Slag Concrete (AASC) and Alkali Activated Slag Fly Ash Concrete (AASFC) mixes. The materials used, preliminary mix design, preparation of specimens and procedures adopted for the evaluation of hardened concrete in terms of compressive strength, split tensile strength, flexural strength, modulus of elasticity, water absorption, volume of permeable voids, etc., are explained in this chapter in detail.

#### **3.1 INGREDIENT MATERIALS**

The constituent materials to be used for the production of concrete mix should satisfy the basic requirements as per the relevant standard codes. Proper understanding of the basic properties of these ingredients plays a vital role in the mix design procedure, strength and durability behaviour performance of the concrete. The basic properties of various materials used for the preparation of OPCC, AASC and AASFC mixes are discussed in the following sections.

##### **3.1.1 Cement**

Cement is one of the important constituents of the concrete mix. In the present investigation, OPC of 43 grade conforming to IS 8112:2013 was used. The properties of the cement are tabulated in Table 3.1.

Table 3.1 Properties of OPC used in the present study

Sl.No	Test	Result	Limits as per IS 8112-2013
1	Specific Gravity	3.14	-
2	Standard Consistency,%	30	
3	Fineness of cement (m <sup>2</sup> /kg) (Blaine's air permeability)	330	>225
4	Setting time - Initial (minutes)	65	> 30
	- Final (minutes)	375	<600
5	Compressive Strength ( MPa ) 3 Days	29	23
	7 Days	40	33
	28 Days	57	43-58

### 3.1.2 Ground Granulated Blast-Furnace Slag (GGBFS)

GGBFS is the generally used as cement replacement material in concrete. In the present investigation, GGBFS produced from M/s JSW Iron and Steel Company, Bellary, Karnataka, India was procured from a local supplier. The chemical composition and physical properties of GGBFS are presented in Table 3.2.

Table 3.2 Chemical and Physical properties of GGBFS

Constituent	Oxide Content (% by weight)
CaO	37.34
Al <sub>2</sub> O <sub>3</sub>	14.42
Fe <sub>2</sub> O <sub>3</sub>	1.11
SiO <sub>2</sub>	37.73
MgO	8.71
Na <sub>2</sub> O	0.16
K <sub>2</sub> O	0.07
SO <sub>3</sub>	0.39
Insoluble Residue	1.59
Loss of Ignition	0.24
Blaine's Fineness (m <sup>2</sup> /kg)	370
Specific gravity	2.9

### 3.1.3 Fly Ash (FA)

Fly Ash, is a by-product obtained from coal burning in Thermal power plants. FA (class-F) procured from Raichur Thermal Power Station (RTPS), Karnataka, India was used for the present investigation and the chemical and physical properties of FA are tabulated in Table 3.3.

Table 3.3 Chemical and Physical Properties of Fly Ash (Class-F)

Constituent	Oxide Content (% by weight)	Requirement as per IS 3812 (Part II) - 2003
SiO <sub>2</sub>	59.75	35% min
Al <sub>2</sub> O <sub>3</sub>	26.06	SiO <sub>2</sub> + Al <sub>2</sub> O <sub>3</sub> + Fe <sub>2</sub> O <sub>3</sub> combined 70% min
Fe <sub>2</sub> O <sub>3</sub>	6.73	
CaO	3.05	5% max
Na <sub>2</sub> O	0.93	Total alkalis, 5% max
K <sub>2</sub> O	1.54	
SO <sub>3</sub>	0.65	2.75% max
Loss of Ignition	1.26	12% max
Fineness (m <sup>2</sup> /kg)	350	320
Specific Gravity	2.2	-

### 3.1.4 Fine Aggregates

In the present investigation, locally available river sand conforming to Zone II of IS: 383-1970 was used as fine aggregate. The river sand was tested according to IS: 2386 (Part I-IV)-1963 and the physical properties and gradation of river sand are presented in Tables 3.4 and 3.5 respectively.

### 3.1.5 Coarse Aggregates

Crushed granite aggregates of maximum aggregate size of 20 mm (20mm to 4.75mm) conforming to IS: 383-1970 was used for the present investigation. The physical properties and sieve analysis of natural coarse aggregates are evaluated as per IS: 2386 (Part I-IV)-1963 and the results are tabulated in Tables 3.4 and 3.5 respectively.

### 3.1.6 Steel Slag Aggregates

In the present investigation, the steel slag coarse aggregates (Basic Oxygen Furnace slag) were procured from JSW Iron and Steel Industry, Bellary, India. The steel slag procured was black in colour, having a sharp angular shape with a porous texture surface and stone like appearance. Maximum aggregate size of 20 mm is considered for

the present study. Physical properties and gradation of steel slag aggregates are tabulated in Tables 3.4 and 3.5 respectively. The chemical composition of steel slag aggregates is tabulated in Table 3.6.

Table 3.4: Physical Characteristics of aggregates

SI. No	Test	Crushed granite aggregates	Steel slag	River sand	Method of Test, reference to
1	Specific Gravity	2.69	3.35	2.64	IS 2386 (P-III) -1963
2	<u>Bulk Density</u> a) Dry loose	1495 kg/m <sup>3</sup>	1726 kg/m <sup>3</sup>	1475 kg/m <sup>3</sup>	
	b) Dry compact	1653 kg/m <sup>3</sup>	1935 kg/m <sup>3</sup>	1548 kg/m <sup>3</sup>	
3	Aggregate Crushing Value	24%	20%	-	IS 2386 (PIV)-1963
4	Los Angeles Abrasion value	20%	18%	-	
5	Aggregate Impact value	21%	16%	-	
6	Water Absorption	0.50%	2.00%	0.80%	

Table 3.5 Gradation of aggregates used for the study

Fine aggregates			Coarse aggregates			
Sieve No (mm)	IS:383-1970 requirement	Passing (%)	Sieve No (mm)	IS:383-1970 requirement	Passing (%)	
					Crushed granite	Steel slag
10	100	100	20	95-100	98	96
4.75	90-100	98.5	10	25-55	40	42
2.36	75-100	95.4	4.75	0-10	5	2
1.18	55-90	71.5				
0.6	35-59	47				
0.3	8-30	12				
0.15	0-10	3.1				

Table 3.6 Chemical composition of Steel Slag (% by weight)

Constituent	Oxide Content (% by weight)
CaO	41.52
Free CaO	5.33
Al <sub>2</sub> O <sub>3</sub>	4.12
Fe <sub>2</sub> O <sub>3</sub>	22.54
SiO <sub>2</sub>	15.04
MgO	6.17
Na <sub>2</sub> O	0.14
K <sub>2</sub> O	0.05
SO <sub>3</sub>	0.08
Insoluble Residue	9.97
Loss of Ignition	0.25

### 3.1.6.1. Weathering of steel slag aggregates

Steel slag aggregates must be allowed to undergo the weathering process before using as aggregates for construction purposes, because of its expansive nature due to the presence of free lime and free magnesia. The presence of free lime content more than 1% cause adverse effects on the properties of steel slag aggregates. Free CaO present in steel slag reacts with atmospheric CO<sub>2</sub> to form calcium carbonate (CaCO<sub>3</sub>); which gets

deposited on the surface of aggregates in the form white powder (FHWA 2012). The FHWA (2012) specifies a maximum free lime content of 7% and 4% in steel slag aggregates when used in unbound applications and hot mix bituminous pavements respectively. Maximum free lime content in steel slag aggregates for use in cement bound layers is not specified. However, it is advisable to subject the steel slag to weathering until the free lime content is brought to a level, beyond which the volume expansion becomes minimal. Studies carried out by researchers (Mathur et al. 1999, Motz and Geiseler 2001) have reported that weathered steel slag aggregates with free lime content lower than 1% are found to be non expansive. Kandhal and Hoffman (1997) carried out investigations on steel slag aggregates collected from 10 different sources and reported that steel slag when subjected to weathering for 6 months displayed negligible expansion in the range 0.0 to 0.3%, while the un-weathered raw steel slag showed expansion in the range 1.1 to 2.8%. Hence, in the present investigation, free lime content in steel slag lower than 1% was considered as the “acceptable limit” and the steel slag were weathered for a period more than 6 months. The steel slag aggregates were exposed to open air conditions and water was sprayed for over 6 months (including monsoon season), in order to bring the free lime and free magnesia contents within acceptable limits. It was observed that the steel slag after undergoing the weathering process display appearance of thin white film or coating of calcium carbonate (calcite) on the surface. The weathered steel slag aggregates were subjected to washing in order to check if the coating or film could be removed; however the bond between the coating and aggregate surface was strong enough and hence calcite coating could not be washed off. The free lime contents before and after the weathering were identified using Ethylene Glycol Extraction method (Gebhardt 1988). The volume stability was also conducted using modified auto-clave technique developed by Edw. C. Levy Company (Alexander and Jeffery 2014) and the volume expansion was found to be 0.091%, which may be considered negligible. The free lime results determined by the ethylene glycol extraction method and the average of 3 trials are presented in Table 3.7. From Table 3.7, it may be noticed that the free lime content was reduced from 5.33% before weathering to 0.16% after weathering. After the

free lime content and volume stability were found to be within acceptable limits, the steel slag aggregates were used in AASC and AASFC mixes. Fig.3.1 presents the images of steel slag aggregate before and after undergoing the weathering process.

Table 3.7: Free lime contents in steel slag aggregates

Sample type	Free CaO (%)
Un-Weathered Steel slag	5.33
Weathered Steel slag	0.16





(a) Steel slag aggregates before weathering process



(b) Formation of thin film of calcite on slag aggregates after weathering process



(c) Enlarged image of steel slag aggregate showing coating of calcite

Fig. 3.1 Images showing steel slag aggregates before and after the weathering process

### 3.1.7 Water

Potable tap water available in the institute laboratory was used for casting of all specimens and for the curing of OPC based concrete specimens in the present

investigation. The same water was utilized for the preparation of alkaline activator solutions.

### 3.1.8 Super-plasticizer

The super-plasticizer used was commercially available sulfonated naphthalene formaldehyde polymer admixture (“Conplast SP 430”) supplied by FOSROC, Chemicals (India) Pvt. Ltd. Properties of super-plasticizer are tabulated in Table 3.8.

Table 3.8 Properties of Conplast SP 430

Specific Gravity	1.20
Chloride Content	nil
Solid content	40%
Operating Temperature	10 to 40°C
Colour	Dark brown liquid

### 3.1.9 Alkaline Activators

The mixture of sodium hydroxide (NaOH) and Liquid Sodium Silicate (LSS) ( $\text{Na}_2\text{SiO}_3$ ) have proved to deliver the best performance in alkali activated binders (Rashad 2013). Hence, in the present investigation, a combination of sodium hydroxide and LSS is used as the alkaline activator.

Laboratory grade sodium hydroxide flakes (97% purity) and LSS were procured from local suppliers. The LSS was tested as IS: 142112-1995 for the physical properties and the results are tabulated in Table 3.9. The physical properties of sodium hydroxide are presented in Table 3.10. The alkaline activator solution was prepared by dissolving the sodium hydroxide flakes in LSS in proper proportion, in order to achieve the desired activator modulus ( $M_s = \text{SiO}_2/\text{Na}_2\text{O}$ ) and sodium oxide ( $\text{Na}_2\text{O}$ ) dosage. The solution was stirred properly and water was added in order to bring the solution to contain a total water content, equivalent to the water/binder (w/b) of 0.20 of total binder content. The solution was stored in tight plastic container one day prior to mixing. The solution was brought to

the required total water content (water/binder ratio) by mixing extra water during the time of casting of specimen.

Table 3.9 Properties of Liquid Sodium Silicate

Constituent	
Molecular formula	Na <sub>2</sub> SiO <sub>3</sub>
Na <sub>2</sub> O% (by weight)	14.7
SiO <sub>2</sub> % (by weight)	32.8
water% (by weight)	52.5
% of solids (by weight)	47.5
Ms (SiO <sub>2</sub> /Na <sub>2</sub> O)	2.23
Specific gravity	1.57

Table 3.10 Properties of Sodium Hydroxide (97% purity)

Molecular formula	NaOH
Molar mass	39.9971 g/mol
Appearance	White solid
Specific Gravity	2.1
Solubility in water	114 g/100 ml (25°C)

### 3.2 PRELIMINARY STUDIES ON ALKALI ACTIVATED CONCRETE MIXES

The activator modulus (Ms) and sodium oxide (Na<sub>2</sub>O) dosage have significant influence on the strength properties of the alkali activated binders. For each type of binder, there exists an optimal activator modulus for which the mix attains highest strength activated at constant sodium oxide dosage. Hence, it is necessary to identify the optimal activator modulus based on the strength requirement. Preliminary studies were carried out to determine the strength of AASC and AASFC mixes at different activator modulus and sodium oxide dosages. Based on the results, the optimal activator modulus for different mixes were identified and later these mixes further optimized to identify the sodium oxide dosages to obtain the required strength. According to the Indian standard code IRC: 58:2002, Pavement Quality Concrete (PQC) should have a minimum compressive strength of M40 and a slump value in the range 25-50 mm.

Preliminary mix design was carried out for AASC and AASFC mixes in order to identify the optimal activator modulus to achieve the desired strength grade of M40 with slump value in the range 25-50 mm. The AASC and AASFC mixes were prepared using binder content of  $425 \text{ kg/m}^3$  with water to binder ratio (w/b) of 0.40. In case of AASC, 100% GGBFS was used as the binder; while in case of AASFC, GGBFS: FA in the ratios 75:25, 50:50 and 25:75 were used as binders. The mixes were activated at sodium oxide ( $\text{Na}_2\text{O}$ ) dosages of 4% and 5% (by weight of binder content) and the activator modulus was varied between 0.75 to 1.75. The activator modulus for which the mix attained the maximum compressive strength was considered for further optimization for determining the sodium oxide dosage as per the desired strength. Cube specimens of size 100 mm were prepared and tested for compressive strength after 28 days of air curing. The workability tests, i.e. the ease of compaction, was also determined using the slump tests, as it would help to carry out water content correction based on the required slump and the strength of the mixes.

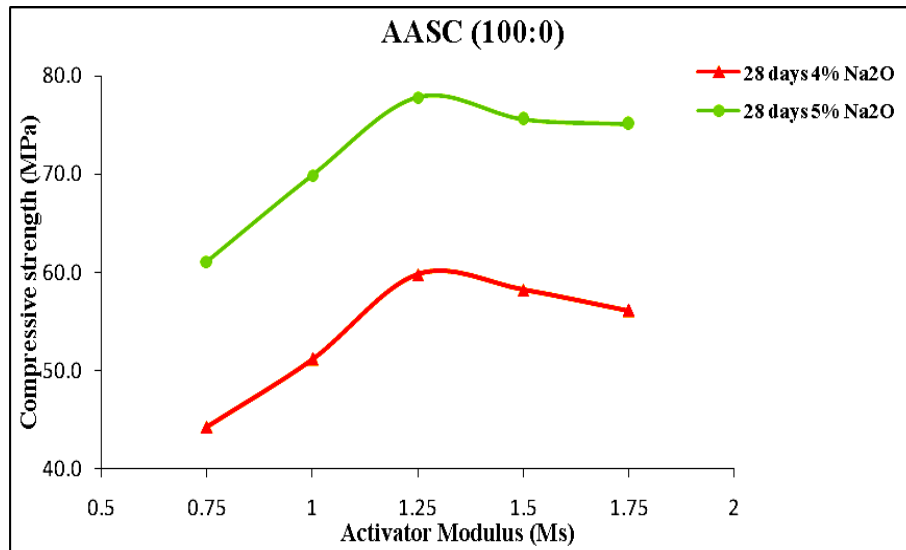


Fig.3.2 Compressive strength v/s activator modulus for AASC mix (100:0)

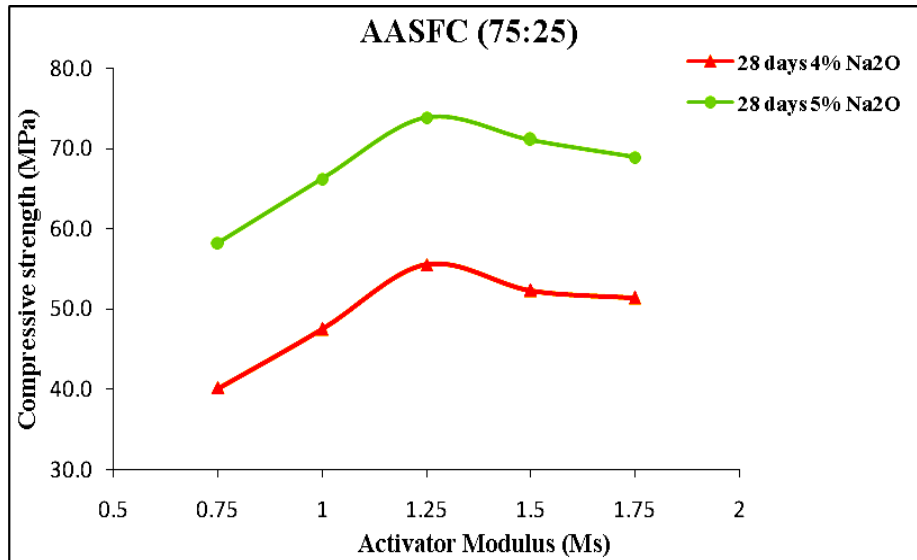


Fig.3.3 Compressive strength v/s activator modulus for AASFC mix (75:25)

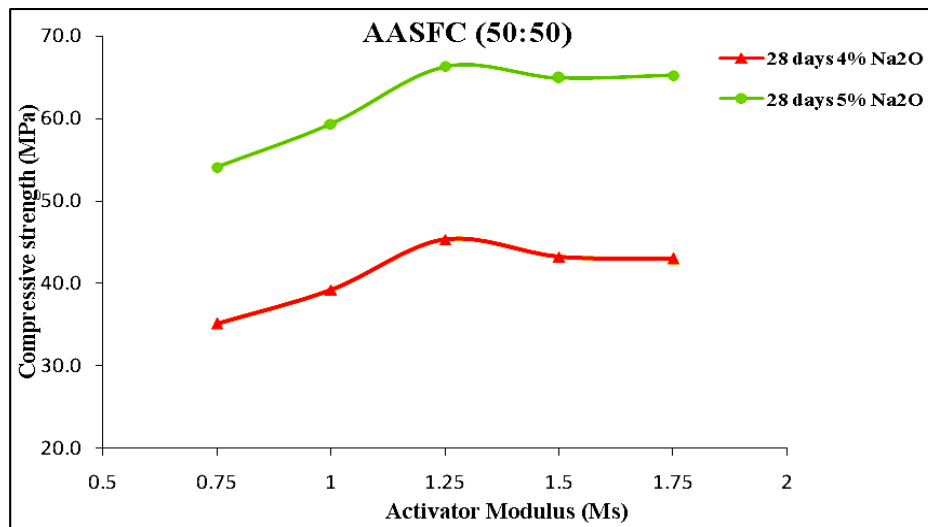


Fig.3.4 Compressive strength v/s activator modulus for AASFC mix (50:50)

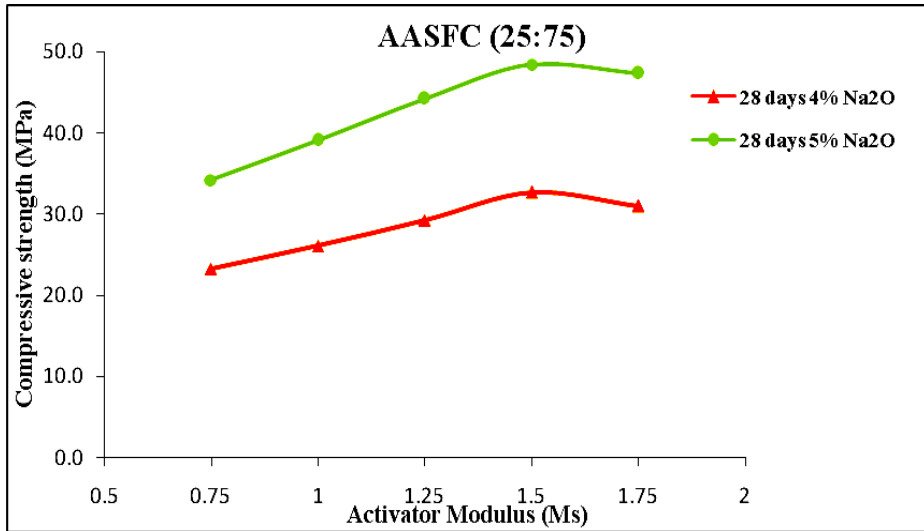


Fig.3.5 Compressive strength v/s activator modulus for AASFC mix (25:75)

The 28-day compressive strength results for AASC (100:0) and AASFC (75:25, 50:50 and 25:75) mixes at 4% and 5% sodium oxide dosages and for different activator modulus are depicted in Figs 3.2 to 3.5. From the results, it can be noticed that the activator modulus of the solution has significant influence on the compressive strength of AASC and AASFC mixes. All the mixes follow a similar and definite trend line. The compressive strength increases with the increase of activator modulus, until an optimal point is reached and later decreases with further increase of activator modulus. The increase in activator modulus implies the increase in the concentration of the anions of sodium silicate in the activator solution, which helps the dissolution process of the binder materials contributing higher strength to the mix (Shi and Li 1989).

It can be noticed that the mixes 100:0, 75:25 and 50:50 mixes attain the highest compressive strength at an optimal activator modulus of 1.25 at both 4% and 5% sodium oxide dosages; however, for a mix of 25:75, the optimal activator modulus is 1.50. The strength of AASC mixes (100:0) is higher than AASFC mixes (75:25, 50:50 and 25:75) at all dosages. AASC mix at an activator modulus of 1.25 exhibited the highest strength at 5% Na<sub>2</sub>O dosage. The compressive strength of the mixes reduced with the incorporation of FA at a constant Na<sub>2</sub>O dosage. This may be attributed to the lower

reactivity to FA as compared to GGBFS. However, the reduction in the strength is not significant at lower levels of replacement (i.e. for mix 75:25). Replacement of GGBFS beyond 50% (by weight of binder content) with FA resulted in a crucial reduction in the compressive strength in AASFC mixes at a constant  $\text{Na}_2\text{O}$  dosage. This indicates that under the activation conditions used, the inclusion of more than 50% (by weight of binder content) FA in the binder, affects the kinetics of reaction at early times of curing. This is likely to be due to the alkalinity supplied by the activator, under the formulation conditions assessed, not being sufficient to promote the extensive reaction of the FA at an early age. AASFC mixes containing higher content of FA (> 50% by weight of binder content) at 4%  $\text{Na}_2\text{O}$  dosage show the lower compressive strength, due to slow reactivity of the starting material when cured at room temperature (Idawati et al. 2013). However, AASFC (25:75) still achieved a compressive strength up to 30 MPa at an activator modulus of 1.5 and at 4% sodium oxide dosage. Mixes with higher contents of FA displayed low early and ultimate strength due to the lower reactivity of FA, when cured at room temperature (Nath and Sarker 2012) However, at higher sodium oxide dosages i.e. 5% the AASFC mixes (25:75) developed adequate strength after 28 days of curing. It was noticed that, at constant water/binder ratio of 0.40, the mixes containing FA displayed higher workability.

From the preliminary investigation, it was found that mixes AASC (100:0) and AASFC (75:25) mixes satisfied both desired strength and workability at an activator modulus of 1.25 and at 4% sodium oxide dosage (by weight of binder). The mixes AASFC (50:50) and AASFC (25:75) on the other hand achieved higher slump values, but did not satisfy the compressive strength requirements at 4% sodium oxide dosage. Therefore, revision of sodium oxide dosages for AASFC (50:50) and AASFC (25:75) was done with simultaneous reduction in the water/ binder ratio for the optimal activator modulus. Based on trials, sodium oxide dosage of 4.5% with 0.38 w/b ratio for AASFC (50:50) and 5.5% with 0.37 w/b ratios for AASFC (25:75) was adopted. The revised dosages and water binder ratios were selected such that the compressive strength and workability of all the mixes fall in the similar range, i.e. M40 and a slump value of 25-50

mm. Table 3.11 presents the sodium oxide dosages and activator modulus adopted for the AASC and AASFC mixes.

Table 3.11 Parameters considered for mix design of AASC and AASFC mixes

Mix ID	Sodium oxide dosage (%)	Water/binder	Activator Modulus (Ms)
A	4.0	0.40	1.25
B	4.0	0.40	1.25
C	4.5	0.38	1.25
D	5.5	0.37	1.50

Note: **A** represents AASC (100:0), **B** represents AASFC (75:25), **C** represents AASFC (50:50) and **D** represents AASFC (25:75).

### 3.3 MIX DESIGN

The mix design for OPC concrete is based on the procedure suggested by IS: 10262-2009. The total binder content is restricted to  $425 \text{ kg/m}^3$ , with water/binder ratio of 0.40 and coarse aggregate: fine aggregate ratio of 0.64:0.36. The mixes are designed to achieve a slump value of 25-50mm. A super plasticizer dosage of 0.40% (by weight of binder content) is added to the mix to arrive at the designated slump.

The AASC mixes are proportioned to contain same binder content ( $425 \text{ kg/m}^3$ ) and water/binder ratio (0.4) as that of OPCC mix. The AASFC mixes were prepared using same binder content by mixing GGBFS: FA in the ratios 75:25, 50:50 and 25:75 and using water /binder ratios as obtained from preliminary results (Table 3.11). The total water content in the activator solution for the AASC and AASFC mixes, constituted the sum of water readily available in LSS plus the extra water added, to arrive at the required content. The alkali activator solutions were proportioned separately for each type of mix to provide desired dosage of  $\text{Na}_2\text{O}$  (by weight of binder), with an optimal activator modulus (Ms) and total water/binder ratio as provided in Table 3.11 (as identified from preliminary investigation). No super-plasticizers are added for the AASC and AASFC mixes. Further AASC and AASFC mixes were prepared with steel slag coarse aggregate



by replacing the natural aggregates by 25%, 50%, 75% and 100% (by volume) keeping the volume of total coarse aggregates constant. The aggregates used were in saturated surface dry condition. The details of mix proportions for OPCC, AASC and AASFC mixes are tabulated in Table 3.12. A sample of mix design procedure for OPCC and AASC are presented in Appendix I and II respectively.

Table 3.12: Details of mix designations and mix proportions of concrete mixes  
(all ingredients are in kg/m<sup>3</sup>)

Mix ID	GGBFS	FA	Sand	Natural coarse aggregate	Steel slag	LSS	NaOH flakes	Added Water	Total water	SP
OPCC	425	-	660	1196	0			169	170	1.7
4-A-0	425	0	647	1172		64.78	9.64	136		
4-A-25				879	365					
4-A-50				586	730					
4-A-75				293	1094					
4-A-100				0	1460					
4-B-0				319	106					
4-B-25	864	359								
4-B-50	576	717								
4-B-75	288	1076								
4-B-100	0	1434								
4.5-C-0	212.5	212.5	628	1127	0	72.88	10.52	123		
4.5-C-25				845	351					
4.5-C-50				564	702					
4.5-C-75				272	1052					
4.5-C-100				0	1404					
5.5-D-0	106	319	583	1121	0	106.9	9.88	101		
5.5-D-25				841	349					
5.5-D-50				561	698					
5.5-D-75				280	1047					
5.5-D-100				0	1396					

**Note:** OPCC - represents Portland cement based control mix; 4-A-0 represents AASC mix with 100% natural coarse aggregates at 4% Na<sub>2</sub>O dosage. 'Y-A-X' represents AASC mixes with 'X' (% by volume) of natural aggregates replaced with steel slag, at 'Y' Na<sub>2</sub>O dosage (%.wt binder). The first number denotes the Na<sub>2</sub>O dosage (%.wt binder), while second number denotes the percentage volume of normal aggregates replaced with steel slag. Similarly B, C and D represent AASFC mixes 75:25, 50:50 and 25: 75 respectively. SP represents superplasticizers.

### 3.4 MIXING, PLACING, COMPACTION AND CURING OF CONCRETE MIXES

The mixing, placing and compaction of AASC and AASFC mixes were done in a similar way as that of conventional concrete. The solid constituents of the mix i.e. the aggregates and the binder were dry mixed in the ribbon mixer of 125 kg capacity for about three minutes. Later the activator solution is added to the dry mix and wet mixing continued for another four minutes. After proper mixing, the fresh concrete was poured into moulds for preparation of specimen, in three layers for proper compaction. The wet mix is thoroughly compacted on a vibrator and then allowed to stand in humid and cool place at ambient room temperature and relative humidity ( $85\pm 5\%$ ) for about 24 hours. After 24 hours, the specimens were demoulded. After demoulding, the OPCC specimens were cured in the water tank at room temperature, while the AASC and AASFC specimens were subjected to air curing (general laboratory conditions) at relative humidity of  $85\pm 5\%$  and room temperature ( $27\pm 3^\circ\text{C}$ ). In order to evaluate the strength and other characteristics, the various specimens were cast. The details of the specimens used for various tests are given in Table 3.13.

Table 3.13 Specimen details for various tests

No.	Types of test	Specimen type	Specimen dimension (mm)	Relevant Standards
1	Compressive strength	Cube	100	IS 516-1959
2	Flexural strength	Beam	100*100*500	IS 516-1959
3	Split tensile strength	Cylinder	100(dia)*200(ht)	IS 5816-1999
4	Modulus of Elasticity	Cylinder	150(dia)*300(ht)	IS 516-1959
5	Water absorption and Volume of Permeable Voids	Cube	100	ASTM C642-06
6	Acid Attack	Cube	100	-
7	Magnesium sulphate attack	Cube	100	-
8	Flexural fatigue testing	Beam	100*100*500	-

Note : dia-Diameter, ht-height.

### **3.5 TESTING OF CONCRETE MIXES**

After proper mixing of the ingredients, the specimens of different dimensions (as given in Table 3.13) are prepared in order to test the hardened and durability properties. All the tests were conducted as per relevant standard codes at different ages.

#### **3.5.1 Workability of Fresh Concrete**

In the present investigation, the workability i.e. the ease of compaction was determined using the slump cone tests in conformation to IS: 1199:1959. The test was conducted immediately after the mixing the ingredients.

#### **3.5.2 Mechanical and Durability Properties of Hardened Concrete Mixes**

The concrete specimens are tested at different ages to determine the mechanical and long term durability properties. An average of three samples was tested for each mix using calibrated machines. The mechanical properties such as compressive strength, static flexural strength, modulus of elasticity and split tensile strength were determined as per relevant Indian standards. The test for water absorption and Volume of Permeable Voids (VPV) were performed as per procedure suggested by ASTM C642-06. The test procedures for the sulphuric acid attack and magnesium sulphate attack were adopted from the literature.

##### ***3.5.2.1 Acid Attack***

Sulphuric acid resistance tests conducted on 100 mm concrete test specimens immersed in containers filled with 1% sulphuric acid solution (pH = 1). The pH levels of the sulphuric acid solutions were examined using a portable digital pH meter (standard error  $\pm 0.05$ ). Concentrated sulphuric acid was often added to the solutions to maintain the pH level. Acid solution was replaced with fresh 1% solutions after every 30 days. The compressive strength was measured up to 120 days at an interval of 15 days.

### ***3.5.2.2 Sulphate Attack***

Sulphate resistance tests on concrete samples were carried out on 100 mm cubes using the test method suggested by Metha and Gjorv (1974). Concrete specimens after 28 days of curing, were immersed in a solution, containing 10%  $\text{MgSO}_4$  by maintaining a constant pH in the range 6.5 to 7.5. The pH was checked every 15 days using a portable digital pH meter (standard error  $\pm 0.05$ ). The pH was balanced to the required level (6.5 to 7.5) by adding calculated amount of concentrated nitric acid ( $\text{HNO}_3$ ) to the magnesium sulphate solution, whenever solution became alkaline after immersion of cubes. The solutions in containers were replaced every month for the first 2 months, and then replaced after every two months up to 12 months. The compressive strength was measured at regular intervals up to 360 days.



Fig. 3.6 Immersion of cubes in plastic containers for durability tests

### ***3.5.2.3 Flexural Fatigue Testing***

The flexural fatigue tests on OPCC and alkali activated concrete samples were carried out on beam specimens of dimensions (100x100x500) mm on a MTS servo-

controlled hydraulic repeated load testing machine having a capacity of 5 tonnes. The fatigue tests were conducted on OPCC and AASC/AASFC samples containing 0%, 50% and 100% steel slag aggregates. Five specimens were tested for each mix at each stress level. The static flexural strength of the mixes was recorded at 90 days of curing, before the fatigue test was conducted. The beam specimen was loaded at the same span (i.e. 400 mm) as it was loaded in case of static flexural tests. The specimens were subjected to loading using constant amplitude waveform at a frequency of 4 Hz without any rest period. The test setup was calibrated applying initial loading and the frequency of loading was maintained constant throughout the test for all specimens. The minimum load is maintained at zero, while the maximum load was adjusted based on the required stress ratio (ratio of applied stress to the modulus of rupture of concrete). Fatigue testing is a very time consuming and expensive process and a large number of samples have to be tested. An upper limit of 1,00,000 cycles was selected in this investigation. The test was terminated when the failure of the specimen occurred or the upper limit was reached, whichever was earlier. In the experimental investigation, it was found that the specimen reached the upper limit at stress ratio 0.65. Hence, in this study, the stress ratios were limited to 0.70, 0.75, 0.80 and 0.85. As the uncertainty involved in this test is very high, the maximum stress level was restricted to 0.85. The fatigue tests were conducted at different stress ratios, i.e. 0.70, 0.75, 0.80 and 0.85 to obtain a relationship between different stress ratios (SR) and the number of cycles to failure (N). The test was conducted at the end of 90 days of curing of concrete specimens in order to eliminate the errors occurring, due to the strength development of concrete mixes after 28 days of curing. The Fatigue life (N) i.e. the number of cycles up to failure for each sample was recorded.

#### ***3.5.2.4 Accelerated Fatigue Testing Equipment***

The equipment used in the present study for fatigue analysis was manufactured by M/s Spranktronics, Bangalore. Fig 3.7 shows the Accelerated Fatigue testing equipment used in this study and it has the following main components:

- 1) Loading Frame and loading system: consists of a double acting hydraulic cylinder with suitable mounting flanges. It is associated with a power pack unit consisting of pump coupled with motor (1 HP, 3-phase, 1440 rpm), valves and filters, heat exchanger (cooling system), servo valve, pressure gauge etc.
- 2) Load sensing devices were used to sense the applied load to the specimen during testing. The load cell used for testing was of capacity 50 kN (5000 kg).
- 3) Deflection Recorder: LVDTs are used to sense the deflections with the help of suitable signal conditioners and display panels.
- 4) Frequency and Waveform of loading: The loading is generally with half sinusoidal waveform (zero -maximum load-zero). The application frequency can be between 1-5 Hz with or without rest periods.
- 5) Servo Amplifier System: It is used to link the function generator and the servo valve.
- 6) Control Unit is used to monitor the load and the repetitions. It is connected to the PC with an ADD ON Card to acquire or log the data.



Fig. 3.7 Repeated load testing set up

### 3.6 SUMMARY

In this chapter, investigations are carried out to characterize the constituent materials which are used in the present investigation. Preliminary investigations are carried out to arrive at the optimized mix design. The mix design for OPCC is carried out as per standard available guidelines. The sodium oxide dosage, optimal activator modulus and water content for different binder types was identified as per the strength (M40) and workability (slump value of 25-50 mm) requirements and the mix design for the AASC and AASFC mixes was optimized. The AASC and AASFC mixes were prepared using binder content of  $425 \text{ kg/m}^3$  with water to binder ratio (w/b) of 0.40. In case of AASC, 100% GGBFS was used as the binder; while in case of AASFC, GGBFS: FA in the ratios 75:25, 50:50 and 25:75 were used as binders. The mixes were activated at sodium oxide



(Na<sub>2</sub>O) dosages of 4% and 5% (by weight of binder content) and the activator modulus varied between 0.75 to 1.75. The mixes 100:0, 75:25 and 50:50 mixes attain the highest compressive strength at an optimal activator modulus of 1.25 at both 4% and 5% of sodium oxide dosages; however, for mix 25:75, the optimal activator modulus is 1.50. The compressive strength of the AASFC mixes reduced with the incorporation of FA for a constant Na<sub>2</sub>O dosage. At a constant water/binder ratio of 0.40, the mixes containing FA displayed higher workability. The mixes AASC (100:0) and AASFC (75:25) satisfied both strength and workability at sodium oxide dosage of 4% and activator modulus of 1.25. However, the mixes AASFC (50:50) and AASFC (25:75) achieved higher slump than the required, but did not satisfy the compressive strength requirements at the optimal activator modulus. Therefore, revision of sodium oxide dosages for AASFC (50:50) and AASFC (25:75) was done with subsequent reduction in the water/ binder ratio for the optimal activator modulus. Based on trials, sodium oxide dosage of 4.5% with 0.38 w/b ratio for AASFC (50:50) and 5.5% with 0.37 w/b ratios for AASFC (25:75) mixes was adopted. Steel slag as coarse aggregate are incorporated in the optimized AASC and AASFC mixes at different replacement levels, i.e. 0%, 25%, 50%, 75% and 100% (by volume). The mixing, placing, curing and specimen sizes are explained in detail. The preparation of the concrete specimen, properties investigated, the test methodologies followed for testing specimens are also explained in detail here.



## **CHAPTER 4**

### **MECHANICAL PROPERTIES OF CONCRETE MIXES**

#### **4.0 INTRODUCTION**

In this chapter, the observations made on the mechanical properties of AASC and AASFC mixes with partial or complete replacement of natural coarse aggregates with steel slag, both in the fresh and hardened state are discussed. The workability and unit weights are initially discussed and this is followed by a detailed discussion on the strength related properties like compressive strength, flexural and split tensile strength and modulus of elasticity. The results obtained from the experiments are analyzed and discussed.

#### **4.1 WORKABILITY AND UNIT WEIGHT**

The slump cone test was performed according to the procedure suggested in IS 1199:1959. The slump values obtained for different concrete mixes are tabulated in Table 4.1. The OPCC, AASC and AASFC mixes attained the target slump values, for which they were designed. During the preliminary investigation, it was observed that the slump increased with the inclusion of higher FA content in AASFC mixes. It was noticed that the workability increased drastically after inclusion of more than 50% of FA in the AASFC mix. The inclusion of FA required less water to achieve desirable workability due to the particle size and morphology of this precursor (Wang et al. 2003), thus facilitating a lower water/binder (w/b) ratio with equivalent workability. Hence the water/binder (w/b) ratios for AASFC (50:50, 25:75) were reduced in order to achieve a slump in the range 25-50 mm. Incorporation of steel slag in the AASC and AASFC mixes resulted slight decrease in slump. This is due to the fact that steel slag aggregates are sharp, porous and angular in shape, which cause a reduction in the mobility of the matrix, thus reducing the workability (Carlo et al. 2013; Gambhir 2004). Concrete prepared with steel slag aggregates require slightly higher water/binder ratio to achieve a designated

slump as compared to the traditional aggregates. However, the slump loss was not significant at 25% replacement of steel slag in alkali activated concrete mixes. It can be observed from Table 4.1, that the unit weight of the AASC mixes increase with the incorporation of steel slag from 2470 kg/m<sup>3</sup> (for mix 4-A-0) to 2765 kg/m<sup>3</sup> (for mix 4-A-100). A similar trend is observed in AASFC mixes with incorporation of steel slag. The higher density is due to the higher specific gravity of the steel slag than natural aggregates. The density of AASFC mixes was found to marginally decrease with the higher FA content, mainly due to the lower specific gravity of FA as compared to GGBFS. The unit weights of AASC/AASFC with 100% natural aggregates and OPCC were in the same range.

## **4.2 COMPRESSIVE STRENGTH OF CONCRETE MIXES**

Compressive strength tests were conducted as per IS: 516-1959 at 3, 7, 28, and 90 days of curing and the results are tabulated in Table 4.1. It can be noticed that all the OPCC, AASC and AASFC specimens display progressive strength development up to 90 days of curing. The 28-days compressive strength of AASC and AASFC samples with partial or complete replacement of natural coarse aggregates with steel slag are in the range of 55±5 MPa. The AASC mix with 100% natural aggregates exhibit higher compressive strength as compared to OPCC samples. The incorporation of steel slag in the AASC and AASFC mixes led to decrease in the compressive strength. The AASC and AASFC mixes with 100% steel slag exhibit slightly lower compressive strength as compared to traditional aggregates. This may be due to the presence of weak aggregate-paste bond, occurring because of the presence of thin film of calcite (formed during the weathering process) on the surface of steel slag aggregates. Visual inspection of the failed samples after testing exhibited incidents of debonding between the steel slag aggregate and paste. It is a well established fact that the bond between the aggregate and the paste significantly affect the mechanical properties of concrete. If there exists a stronger bond between the paste and coating layer than the bond between the coating and the aggregate surface, it may lead to the development of weak coating–aggregate interface, thus leading

to the reduction in mechanical and durability properties of the concrete (Forster 1994). The AASC and AASFC mixes with higher proportions of steel slag displayed a greater variation in strength in the samples tested for the same mix. This may be attributed to the higher heterogeneity of steel slag particles as compared to natural aggregates. However, the strength variation of AASC and AASFC mixes with steel slag was within normal range of variability. No significant difference in strength is observed in AASC and AASFC mixes with steel slag content up to 25% (by volume). The AASC and AASFC mixes exhibit high early strength as compared to OPCC, i.e., the 3-days and 7-days strength. The high early strength of AASC and AASFC mixes is due to the physical and structural characteristics of binders formed. The hydration process in case of AASC and AASFC mixes depend upon the dissolution and precipitation of GGBFS and is quite faster in the presence of a high alkaline activator than hydration process in OPC (Roy and Silsbee et al. 1992; Wang and Scrivener 1995). However, the rate of strength development slowed down after 7-days and at the end of 90-days the OPCC, AASC and AASFC mixes show similar strength. AASC with 100% natural aggregates achieved the highest strength at the end of 90 days. The AASFC specimens (i.e. 5.5-D-0) mix with FA up to 75% (by weight of binder) exhibit comparable mechanical strength as that of AASC (4-A-0). The lower water/binder ratio and higher sodium oxide dosage used at high FA content mixes, were able to counteract the decrease in strength, which would otherwise have been induced by the incorporation of FA. This indicates that the water/binder ratio and sodium oxide dosage can be controlled to achieve the desired strength in alkali-activated concretes formulated with high FA content. All concrete mixes attained sufficient strength at 28 days of curing necessary for application in pavement quality concrete. The high early strength of AASC and AASFC mixes is of great benefit for pavement quality concrete as it would allow the early opening of the pavements to the traffic. The AASC and AASFC mixes with partial or complete replacement of natural coarse aggregates with steel slag developed acceptable strength required for pavement quality concrete as per IRC: 58:2011.

Table 4.1 Compressive strength of various concrete mixes

Mix ID	Compressive strength (MPa)				Slump (mm)	Density (kg/m <sup>3</sup> )
	3-days	7-days	28-days	90-days		
OPCC	23.1	40.4	56.9	62.8	35	2480
4-A-0	39.6	48.2	59.6	67.4	40	2470
4-A-25	38.2	46.9	56.1	65.9	40	2540
4-A-50	37.5	45.1	53.4	61.6	35	2595
4-A-75	35.1	43.2	52.1	57.1	30	2685
4-A-100	33.2	40.4	50.2	53.5	20	2765
4-B-0	36.3	43.6	55.6	62.4	60	2455
4-B-25	36.1	42.9	54.2	60.2	55	2520
4-B-50	34.2	40.8	52.9	57.6	45	2570
4-B-75	33.1	38.4	50.8	54.1	40	2620
4-B-100	30.4	36.7	48.9	51.7	30	2720
4.5-C-0	32.6	45.3	58.4	65.4	55	2420
4.5-C-25	33.1	43.2	57.1	62.5	55	2510
4.5-C-50	31.7	43.6	55.4	58.2	40	2580
4.5-C-75	30.7	41.6	53.4	55.6	30	2605
4.5-C-100	27.4	38.7	51.2	53.7	30	2685
5.5-D-0	33.5	44.6	56.8	63.4	50	2390
5.5-D-25	31.4	41.6	56.1	61.4	55	2455
5.5-D-50	29.8	40.9	53.4	59.9	35	2530
5.5-D-75	29.4	37.3	52.7	57.6	35	2595
5.5-D-100	26.3	34.5	50.1	55.7	20	2640

### 4.3 STATIC FLEXURAL STRENGTH OF CONCRETE MIXES

The static flexural strengths of all concrete specimens were determined according to IS 516:1959. Figs. 4.1 to 4.4 depict the flexural strength of AASC (100:0), AASFC (75:25), AASFC (50:50) and AASFC (25:75) at 7, 28 and 90 days of curing. From the figures, it can be observed that the flexural strength decreases with the increase in steel

slag content in AASC and AASFC mixes. The flexural strength of AASC/AASFC with 100% steel slag is lower than AASC/AASFC with 100% natural aggregates at all ages. This may be due to the weak aggregate-paste bond, due to the presence of a coating of calcite, as explained in case of compressive strength. AASC and AASFC mixes with 100% natural aggregates display higher flexural strength than OPCC concrete at all ages, which may be due to the presence of highly dense interfacial transition zone between the paste and the aggregates and development of a distinct microstructure in alkali activated concrete mixes as compared to OPC concrete (Bernal et al. 2012). The AASFC mix 5.5-D-0 exhibit lower flexural strength as compared to other AASFC mixes (4-B-0, 4.5-C-0) of similar strength grade. It was observed the inclusion of higher FA in the binder reduced the flexural strength as compared to other AASFC mixes with lower FA content of similar compressive strength grade. This is due to the differences in the binder chemistry between AASC and AASFC mixes (Provis 2013). The flexural strength of concrete is one of the important parameters that influence the design of concrete pavements. Since, the alkali-activated concrete mixes achieved quite higher flexural strength as compared to conventional OPC concrete, it may be beneficial in reducing the pavement thickness to some extent. Although, there was a reduction in the flexural strength of AASC and AASFC mixes with the incorporation of steel slag aggregates, all AASC/AASFC mixes (including 100% steel slag aggregates) achieved the minimum strength requirements of 4.5 MPa as suggested by the Indian Roads Congress for rigid pavement design (IRC:58:2011).

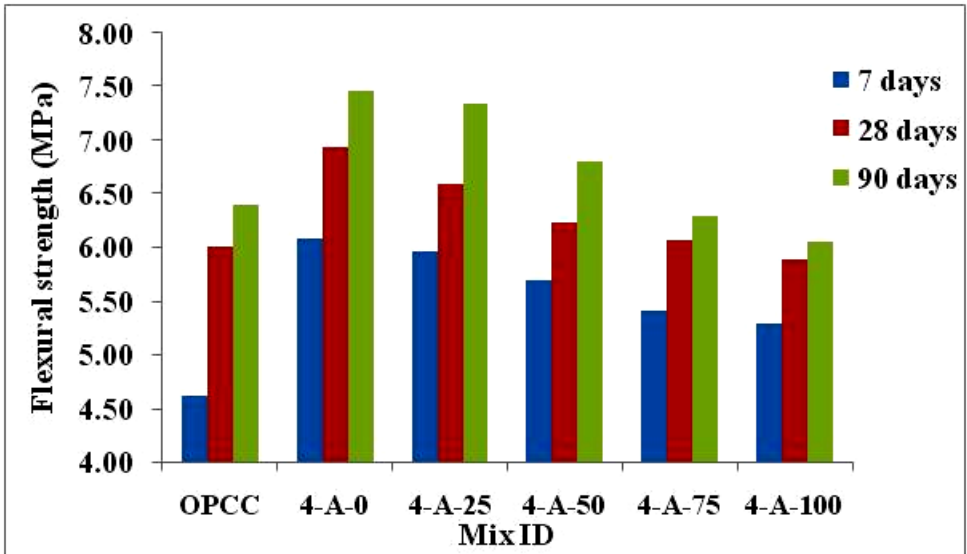


Fig. 4.1 Flexural strength of the AASC mix (100:0) at different ages

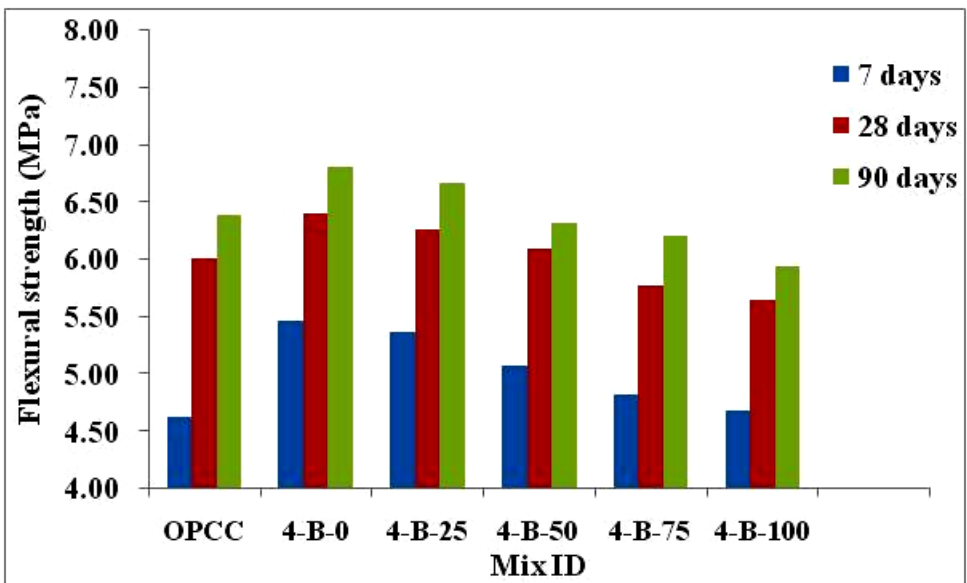


Fig. 4.2 Flexural strength of the AASFC mix (75:25) at different ages



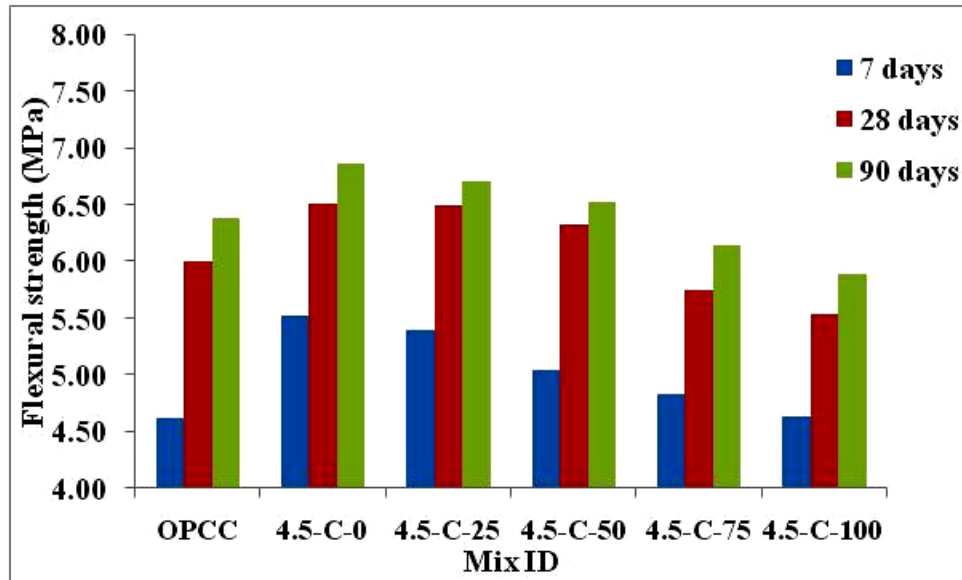


Fig. 4.3 Flexural strength of the AASFC mix (50:50) at different ages

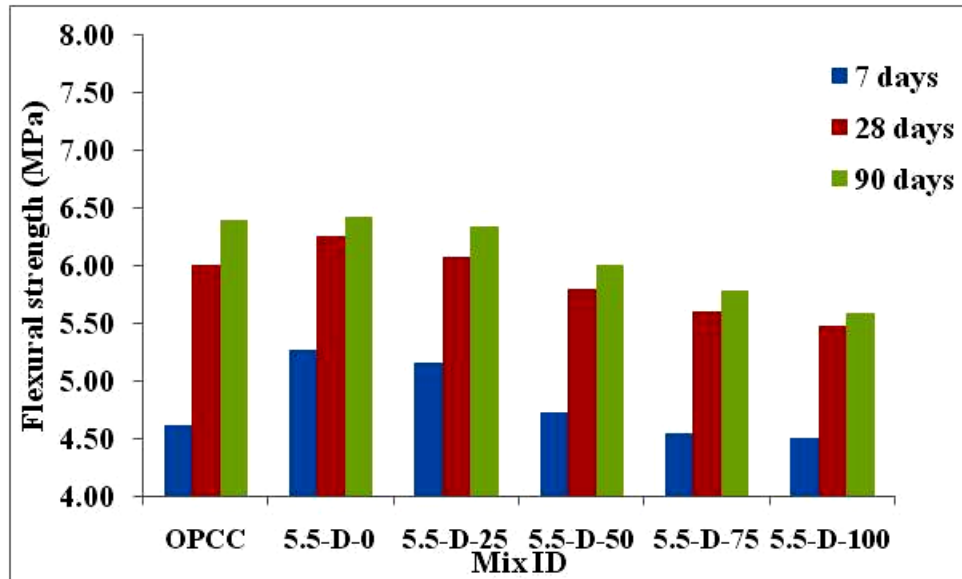


Fig. 4.4 Flexural strength of the AASFC mix (25:75) at different ages

#### 4.4 SPLIT TENSILE STRENGTH OF CONCRETE MIXES

Figs 4.5 to 4.8 present the 28-day split tensile strength values of AASC (100:0), AASFC (75:25), AASFC (50:50) and AASFC (25:75) in comparison with OPCC. The split tensile strength test was conducted as per IS 5816:1999. The split tensile strength of AASC and AASFC mixes with 100% natural aggregates is higher than OPCC. The split tensile strength of AASC and AASFC mixes is found to decrease with replacement of natural coarse aggregates by steel slag. At lower levels of replacement up to 25% (by volume) steel slag; no appreciable change in split tensile strength is noticed, however split tensile strength of AASC/AASFC at 100% steel slag aggregates is found to be lower than AASC/AASFC with natural coarse aggregates.

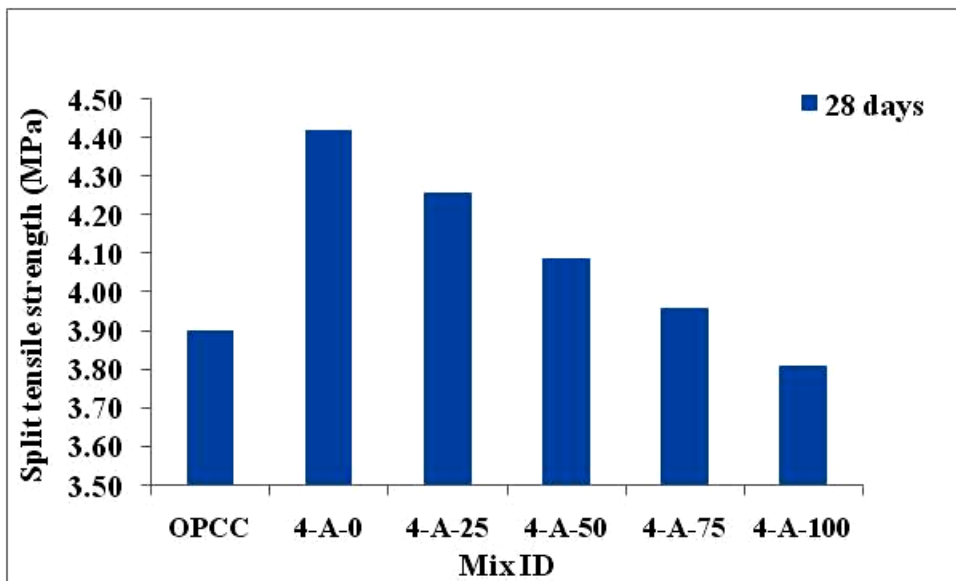


Fig. 4.5 28-day Split tensile strength of the AASC mix (100:0)

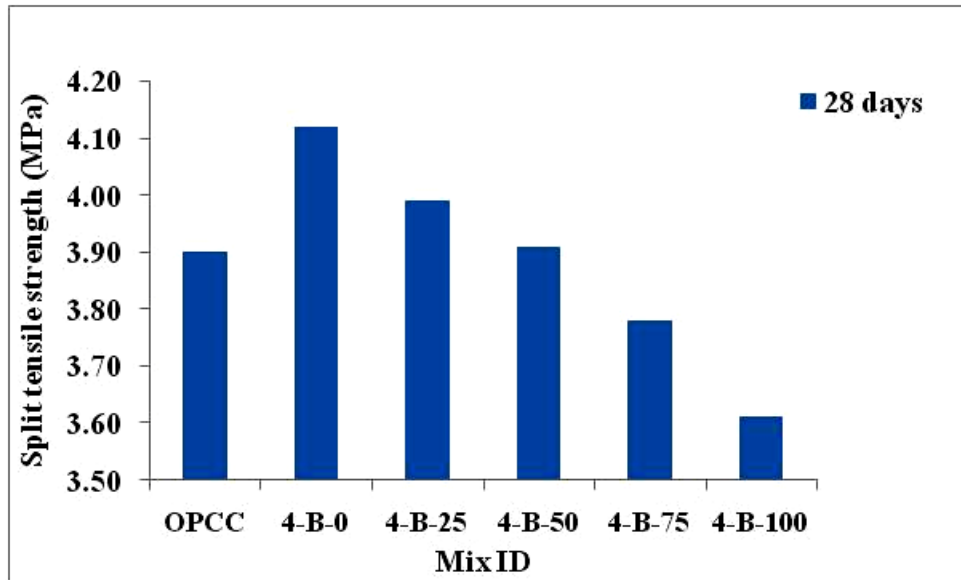


Fig. 4.6 28-day Split tensile strength of the AASFC mix (75:25)

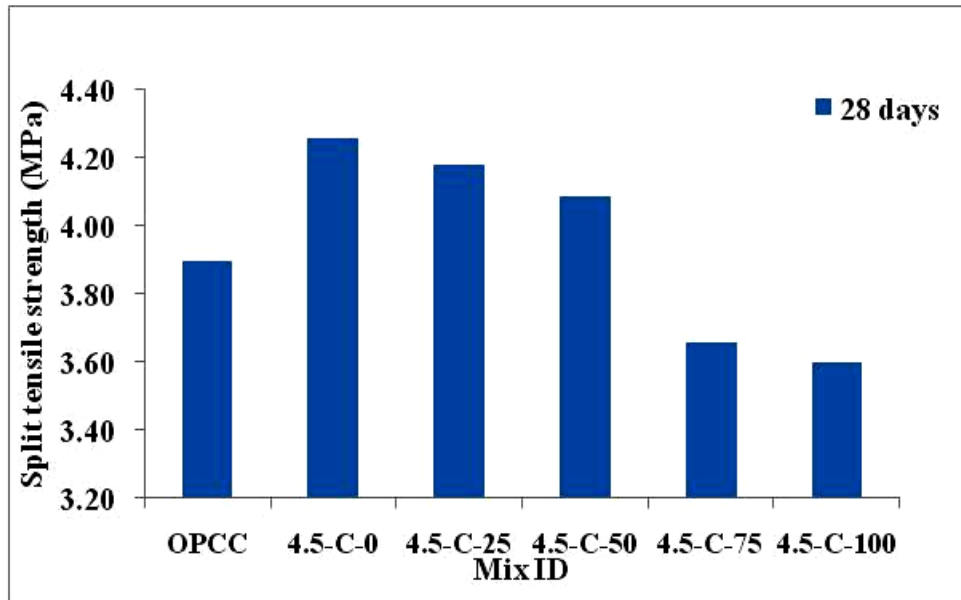


Fig. 4.7 28-day Split tensile strength of the AASFC mix (50:50)

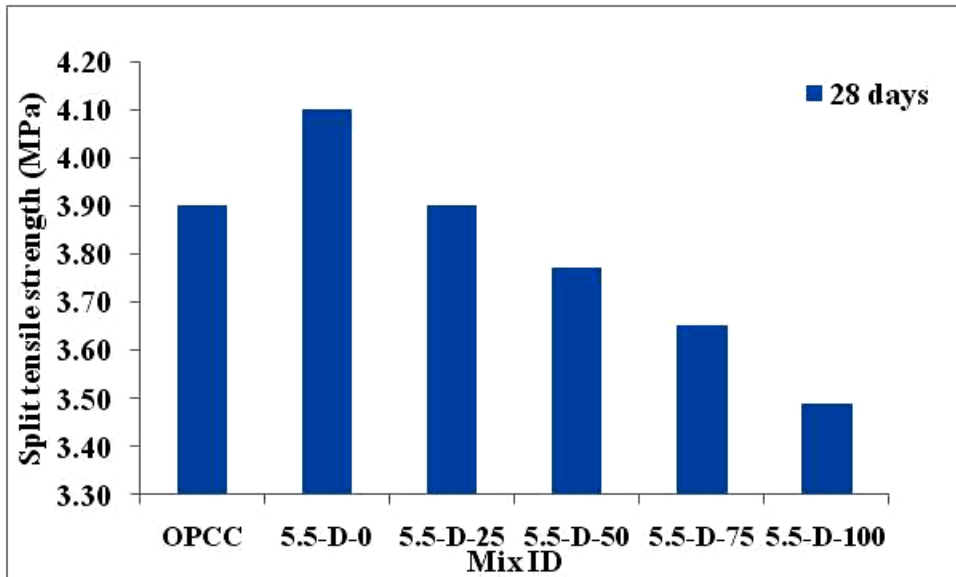


Fig. 4.8 28-day Split tensile strength of the AASFC mix (25:75)

#### 4.5 MODULUS OF ELASTICITY OF CONCRETE MIXES

The test for modulus of elasticity was conducted as per IS 516:1959. Figs 4.9 to 4.12 present the static modulus of elasticity values of AASC (100:0), AASFC (75:25), AASFC (50:50) and AASFC (25:75) in comparison with OPCC after 28 days of curing. It can be observed that the static modulus of elasticity of OPCC mixes is higher than that of AASC and AASFC mixes. The modulus of elasticity of AASFC mixes exhibit lower values with replacement of GGBFS with FA. The relationship between 28-day compressive strength and other mechanical properties such as flexural, tensile, elastic modulus may differ as a function of binder chemistry. It has been reported that flexural strength and elastic modulus of alkali activated materials display different dependence of such properties on the 28-day compressive strength, than the well-known (standardized) relationships that hold good for normal-strength OPC concretes (Sofi et al. 2007, Diaz-Loya et al. 2011, Bernal et al. 2012). AASC and AASFC, both being subsets of the general class of alkali activated materials, show very different strength development rates under the same curing conditions up to 28 days, along with micro-structural differences and hence it may lead to differences in flexural and elastic properties (Provis 2013).

The modulus of elasticity of AASC and AASFC mixes decrease with the replacement of natural aggregates with steel slag, due to the weak aggregate-paste interface formed, due to the presence of a coating of calcite on the steel slag surface. The type and properties of coarse aggregates affect the modulus of elasticity of high performance concretes. The nature of the constituent material and nature of interfacial transition zone between the paste and the aggregates affects the elastic modulus of the concrete (Alexander et al. 1995).

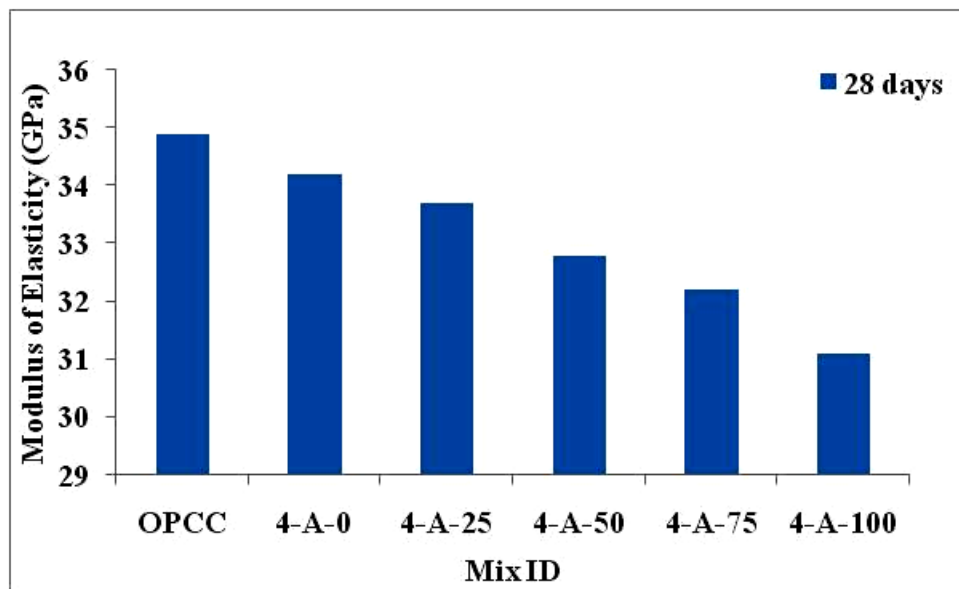


Fig. 4.9 28-day Modulus of elasticity of AASC mix (100:0)

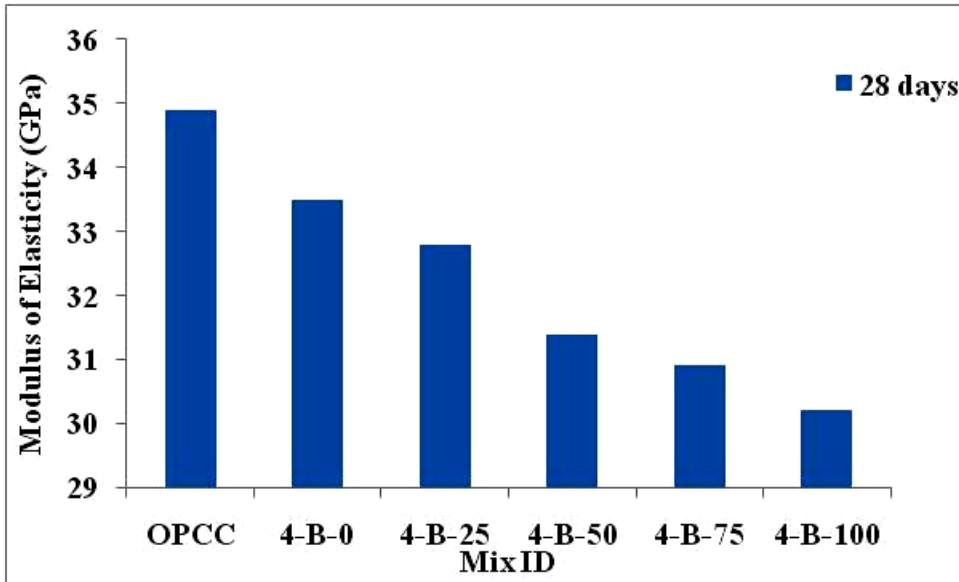


Fig. 4.10 28-day Modulus of elasticity of AASFC mix (75:25)

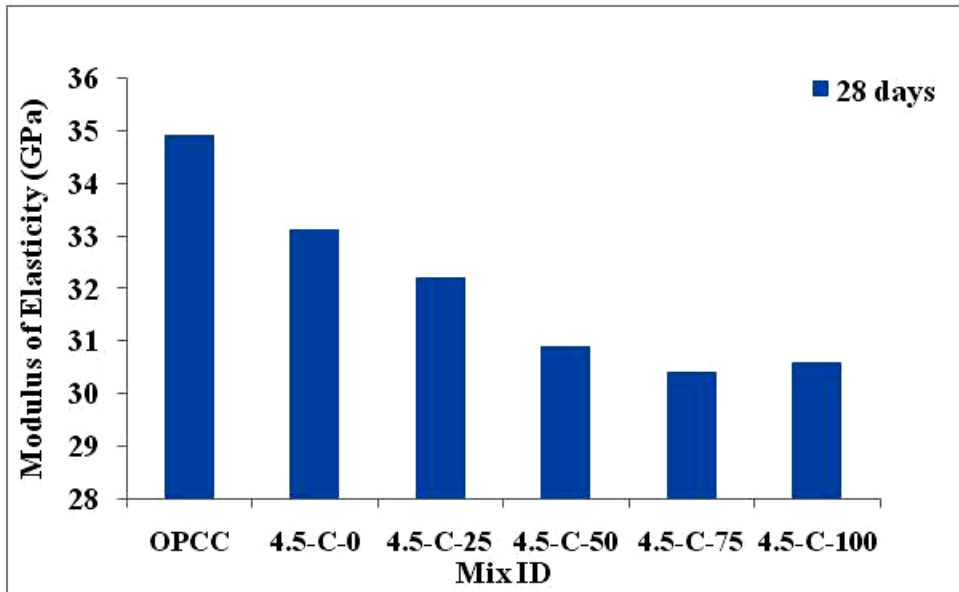


Fig. 4.11 28- day Modulus of elasticity of AASFC mix (50:50)

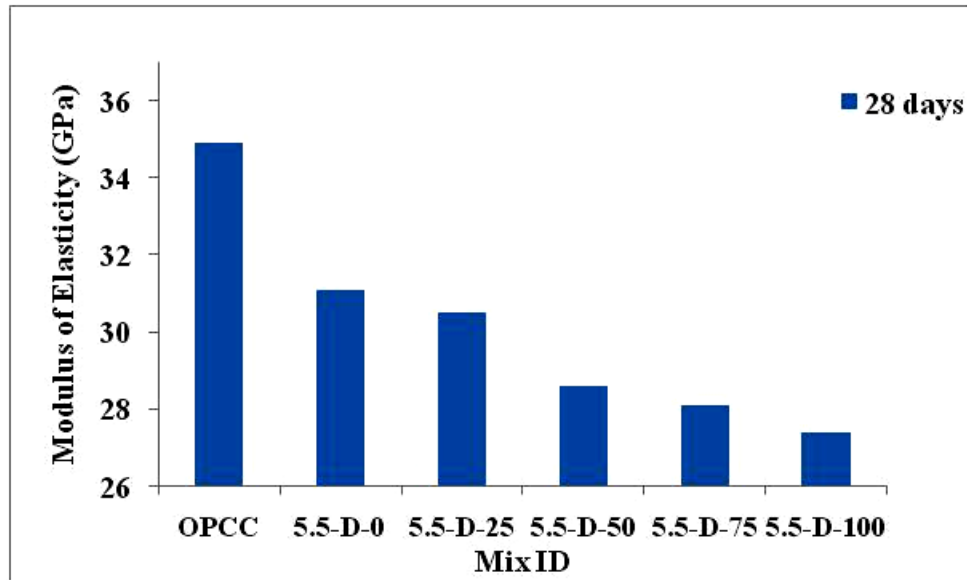


Fig. 4.12 28-day Modulus of elasticity of AASFC mix (25:75)

#### 4.6 SUMMARY

The mechanical properties of AASC and AASFC mixes with partial or complete replacement of natural coarse aggregates with steel slag are discussed in this chapter. It was observed that AASC and AASFC mixes attained sufficient mechanical properties required for application in pavement quality concrete. The incorporation of steel slag in AASC and AASFC mixes slightly affected the workability and the unit weight of the concrete mixes. The AASC and AASFC mixes with steel slag showed reduced workability; along with an increase in the unit weight of the concrete mixes as compared those with natural coarse aggregates. All the AASC and AASFC mixes with partial or complete replacement of natural aggregates with steel slag attained compressive strength in the range of  $55 \pm 5$  MPa and flexural strengths greater than 5.5 MPa after 28 days of curing. The incorporation of steel slag slightly lowered the mechanical properties in both AASC and AASFC mixes, mainly due to the weak aggregate-paste interface, occurring because of the presence of a coating of calcite (formed during the weathering process). The AASC and AASFC mixes displayed high early strength, which is advantageous for pavement quality concrete as it would allow the early opening of the constructed

pavements to the traffic. The inclusion of higher contents of FA in the AASFC mixes slightly resulted in decrease of tensile and modulus of elasticity properties for similar compressive strength grade as compared to AASC mix. AASC and AASFC mixes with partial or complete replacement of natural aggregates with steel slag displayed satisfactory results for its use in highway application.



## **CHAPTER 5**

### **DURABILITY OF CONCRETE MIXES**

#### **5.0 INTRODUCTION**

Concrete and cement based materials finds its application in a diverse environment such as buildings, drainage structures, water supply units, industrial infrastructure, etc. Although concrete provide good mechanical strength, the concrete needs to be durable since it is exposed to various aggressive environments. The aggressive environments are usually aqueous in nature that may either be natural occurring (such as sea waters, soft waters) or may be man-made (such as industrial, waste water or polluted environments). Under such environments, concrete undergoes degradation through the processes of ion exchange and chemical reactions, thus leading to changes in the matrix microstructure and ultimately reduction in the strength of the material. The durability of concrete is rapidly affected by acidic environments, especially sulphuric acid. The sulphuric acid may arise from various ways like acidic soils, industrial effluents, sewage wastes, etc. Concrete are known to undergo degradation in sulphate environment, that may arise from sulphate rich soils, industrial effluents etc. (Shi et al. 2006). In the present chapter, the durability properties of AASC and AASFC mixes with 0%, 50% and 100% (by volume) steel slag as coarse aggregates are evaluated and compared with OPCC. Durability properties such as water absorption, Volume of Permeable Voids (VPV), resistance to the sulphuric acid environment and magnesium sulphate environment are studied in detail.

#### **5.1 WATER ABSORPTION AND VPV**

The water absorption and VPV were evaluated according to ASTM C 642-06. A set of three cubes of 100 mm size was tested for each mix. The water absorption and VPV of different mixes at 28-days of curing are presented in Table 5.1.

Table 5.1 Water absorption and VPV of concrete mixes

Mix ID	Water Absorption (%)	VPV (%)	Mix ID	Water Absorption (%)	VPV (%)
OPCC	3.67	9.4			
4-A-0	3.32	8.05	4-B-0	3.58	9.12
4-A-50	3.61	9.15	4-B-50	3.79	10.3
4-A-100	3.94	10.51	4-B-100	4.14	11.6
Mix ID	Water Absorption (%)	VPV (%)	Mix ID	Water Absorption (%)	VPV (%)
4.5-C-0	3.89	9.78	5.5-D-0	4.55	11.12
4.5-C-50	4.10	11.1	5.5-D-50	4.71	12.7
4.5-C-100	4.51	12.3	5.5-D-100	4.90	13.6

AASC and AASFC (75:25) mixes with normal aggregates having same binder content and water-binder ratio as OPCC, show reduced water absorption and VPV values as compared to OPCC at 28 days of curing. This may be due to the presence of very refined closed pore structure in the AASC samples (Provis et al. 2012; Shi 1996) that restrict the water to penetrate into the structure. The water absorption and VPV values increased with FA replacements in the AASFC mixes. The higher VPV with higher contents of FA is due to the nature of the gel type forming in the binder (Idawati et al. 2013). C-S-H and C-A-S-H binding gels dominate the microstructure of AASFC with GGBFS inclusion up to 50 wt.% of binder, which are more dense than the geopolymer (alkali aluminosilicate) type gels dominating the microstructure of binders mostly composed of activated FA (Bernal et al. 2012). A study conducted by Provis et al. (2012) for activated GGBFS/FA blends, via X-ray microtomography, reported that each binding gel promotes a different pore structure and hence different porosities. The presence of more bound water, induced by the presence of Ca in C-S-H/C-A-S-H type products, provides greater pore-filling capacity for this type of gel, than geopolymer type gels. Furthermore, GGBFS has a much finer particle size, which can fill the pore and result in lower water absorption and VPV in AASC (Idawati et al. 2013). The water absorption

and subsequent VPV increase with the replacement of steel slag in both AASC and AASFC mixes, due to the higher water absorption of steel slag as compared to natural aggregates. The presence of pores in steel slag resulted in the increase in VPV in the mixes. The results obtained are in agreement with the literature (Manso et al. 2004).

## 5.2 SULPHURIC ACID ATTACK

Figures 5.1 to 5.4 present the percentage loss in compressive strength with time for AASC (100:0), AASFC (75:25), AASFC (50:50) and AASFC (25:75) mixes in comparison with OPCC. The Fig. 5.5 and 5.6 depict the images of specimens after being immersed in sulphuric acid solution for 120 days.

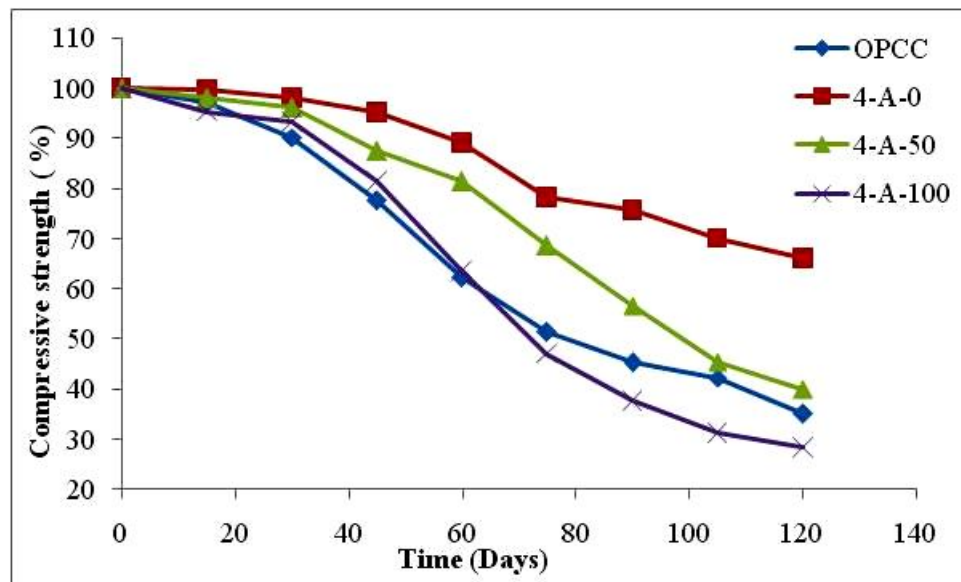


Fig.5.1 Strength loss of AASC mixes (100:0) in pH=1 sulphuric acid

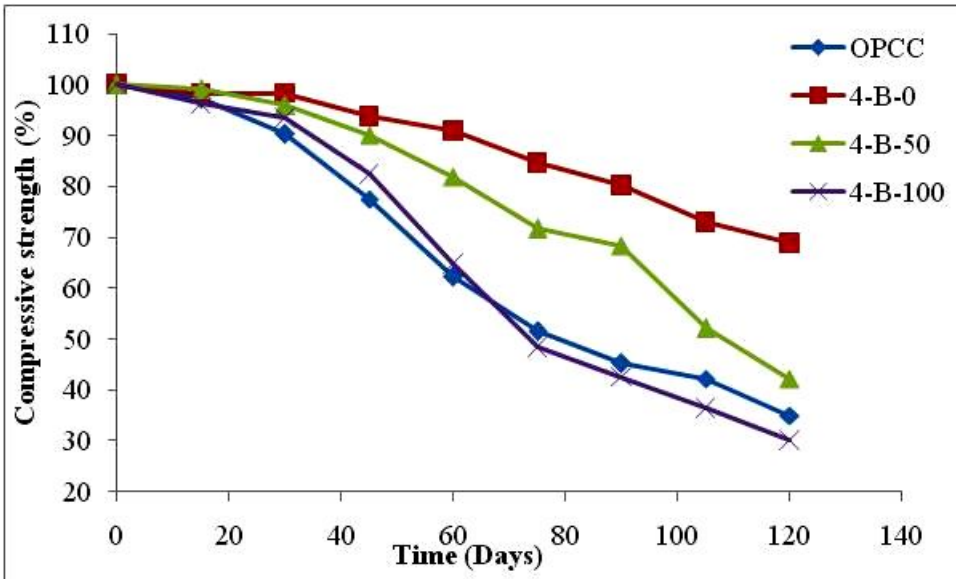


Fig. 5.2 Strength loss of AASFC mixes (75:25) in pH=1 sulphuric acid

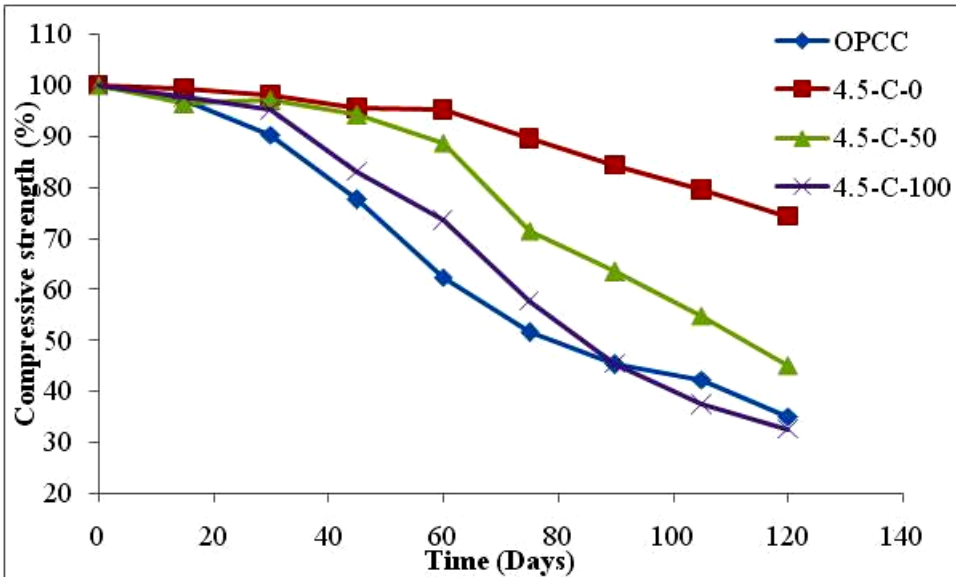


Fig. 5.3 Strength loss of AASFC mixes (50:50) in pH=1 sulphuric acid

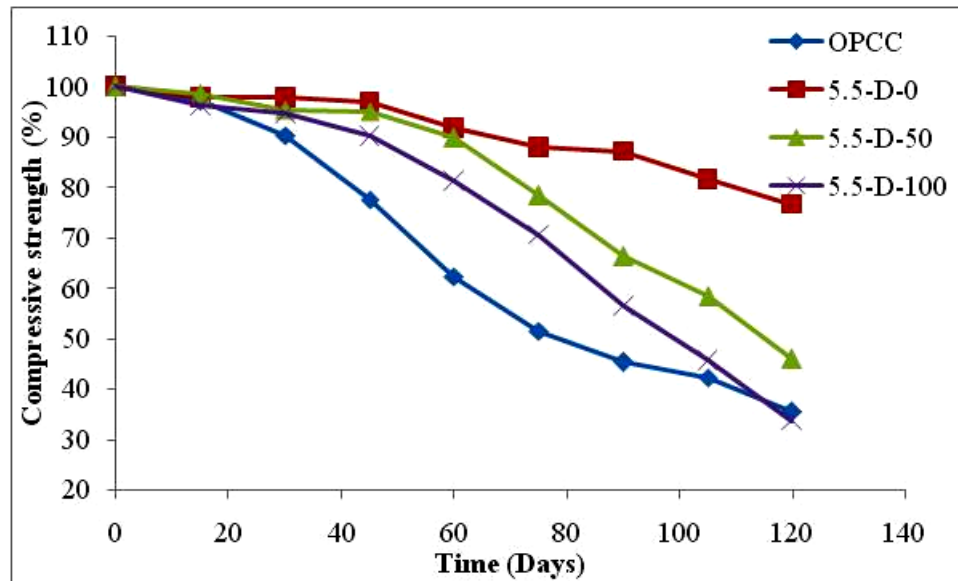


Fig. 5.4 Strength loss of AASFC mixes (25:75) in pH=1 sulphuric acid

All the concrete mixes show progressive strength loss with time after immersion in sulphuric acid solution. The AASFC mixes with high amount of FA (> 50%, say mixes C and D) exhibited better resistance as compared to OPCC, AASC (100:0) and AASFC (75:25) mixes. All alkali activated concrete mixes with 100% natural aggregates exhibited better resistance to sulphuric acid as compared to OPCC, due to the properties and structure of binders. The reaction products formed in OPC i.e. portlandite ( $\text{Ca}(\text{OH})_2$ ) and calcium silicate hydrate (C-S-H) are vulnerable to chemical degradation (Adam 2009). On complete hydration, OPC paste consists of 50-60% of C-S-H with high Ca/Si ratio of 1.5 to 1.8, along with the formation of 20-25%  $\text{Ca}(\text{OH})_2$  and 15-20% calcium sulphoaluminates (AFt and AFm) by volume; while AAS pastes consist mainly of C-S-H with a Ca/Si ratio of around 1, without any formation of  $\text{Ca}(\text{OH})_2$  (Wang and Scrivener 1993). In OPC, the portlandite ( $\text{Ca}(\text{OH})_2$ ) tends to decompose at a pH below 12, while the calcium sulphoaluminates decompose at a pH below 11. With the decrease in pH after immersion in sulphuric acid environment, the C-S-H structure releases  $\text{Ca}^{2+}$  ions. However, when pH goes below 9, C-S-H losses its stability and has released most of the  $\text{Ca}^{2+}$  ions and is left with layer of silica and aluminosilicate gels, which protect the uncorroded paste from further corrosion (Pavlik 1994). The dissolution of hydrated

products of OPC, i.e. portlandite, along with calcium sulphoaluminates and the subsequent decalcification of C-S-H structure leaves a very porous corroded layer in OPC under the influence of acid environment, thus leading to the reduction in compressive strength. The absence of portlandite ( $\text{Ca}(\text{OH})_2$ ) and the low calcium content in AASC and AASFC mixes, is an advantage, which leads to slower degradation and better resistance when subjected to acid environment, as compared to OPCC. However, binder structures formed in AASC and AASFC mixes also undergo degradation, in the form of decalcification of C-S-H/C-(A)-S-H and formation of gypsum, which is reflected by the formation of expansive cracks (as shown in Figure 5.5) on the specimen. The combined effect of decalcification of C-S-H/ C-(A)-S-H (binding phase) and the volume instability caused due to formation of gypsum, lead to decrease in the compressive strength in AASC and AASFC mixes. The replacement of GGBFS with FA slightly improved the acid resistance of the alkali activated concrete mixes i.e. AASFC mixes. It may be noticed that the mix 4-A-0 [AASC (100:0) with 100% natural aggregates] display strength loss of around 33.9% as compared to 23.3% in case of mix 5.5-D-0 [AASFC (25:75) with 100% natural aggregates] after exposure to 120 days of sulphuric solution. This may be due to further decrease in calcium content in the binder with addition of FA content that tends to make the binder further resistant to acid attack. The resistance of cement materials to acid environment is determined mainly by the nature of hydration products (Shi et al. 2006).

The acid resistance of alkali activated concrete mixes decreased with the replacement of natural aggregates with steel slag. The mix 4-A-0 displayed around 33.9% strength loss as compared to 59.6% and 71.6% loss of strength in 4-A-50 and 4-A-100 mixes respectively, after being immersed in sulphuric acid solution for 120 days. A similar trend of decrease in compressive strength with inclusion of steel slag is observed in mixes B, C and D. The high strength loss with steel slag is attributed to the softening and deterioration of steel slag. The deterioration of steel slag is due to leaching out of calcium present in the aggregates. The steel slag aggregates reacted with the sulphuric acid to form expansive paste, which exerted internal pressure on the concrete samples,

leading to pop-outs on concrete surface, thus resulting in strength reduction. The steel slag aggregates apart from forming expansive products, displayed deterioration, and softening/corrosion under the action of sulphuric acid. The mix 5.5-D-100 displayed slightly lower loss in strength and slower rate of strength loss with age as compared to 4-A-100, due to better stability of the binder due to high FA content. The acid resistance of 4-A-100 was found to be lower than OPCC at the end of 120 days of immersion, while the mix 5.5-D-100 performed better at the early days of immersion, which may be due to the contribution of the high FA binder as compared to GGBFS binder, however at the end of 120 days, the strength loss of OPCC and 5.5-D-100 were similar.

### **5.2.1 Visual Inspection of Samples to Acid Solution**

The images of the OPCC and AASC mixes with natural /steel slag aggregates exposed to pH=1 sulphuric acid solution at the end of 120 days are depicted in Fig.5.5 (a-d). The OPCC specimen displayed complete rupture of the surface with the exposure of the aggregates. The AASC specimens with/without steel slag show expansion cracks due to extensive formation of gypsum in the regions close to the surfaces (Allahverdi and FrantišekŠkvára 2000). The AASC specimen with steel slag in addition to formation of expansion cracks, display pop-outs of the concrete surface due to the expansion of the steel slag along with white paste formation on the surface of the aggregates. The Fig. 5.6 (a-d) presents the images showing the deterioration of steel slag in the concrete mix. The Fig.5.6 (a-b) displays the pop-outs on concrete surface due to the internal pressure exerted due to the expansion of the steel slag aggregates. Fig.5.6 (c-d) shows the exposure of the aggregate after the loss of surface cover along with the formation of white paste on the surface of the aggregate. The AASFC mixes (B, C and D) with/without steel slag displayed similar behaviour as that AASC (A) mixes. However, it was noticed that AASC (A) mix displayed slightly wider expansion cracks as compared to AASFC mixes (C and D) at the end of 120 days of immersion.



(a) OPCC



(b) 4-A-0



(c) 4-A-50



(d) 4-A-100

Fig. 5.5 Concrete specimen after immersion in sulphuric acid solution for 120 days

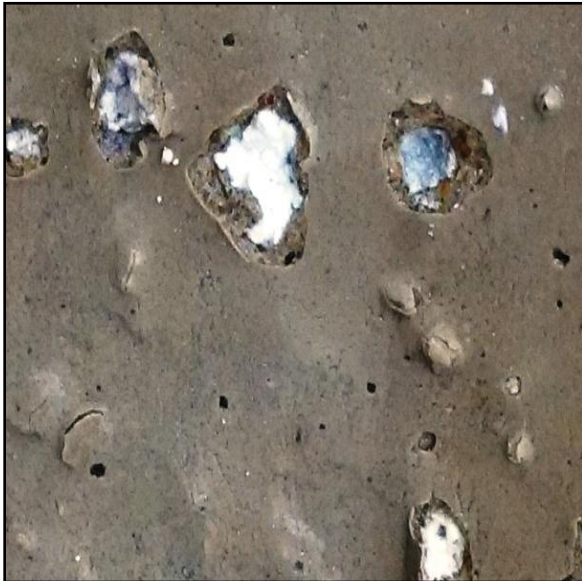




(a) Cube sample after aggregates undergo expansion leading to pop-out of surface



(b) Pop-out on the surface due to internal pressure exerted by aggregates



(c) Loss of cover due to expansion of aggregates and exposure of white paste like formation



(d) Image showing deteriorated steel slag aggregate

Fig.5.6 Deterioration of steel slag aggregates

### 5.3 MAGNESIUM SULPHATE ATTACK

The Figs. 5.7 to 5.10 present the percentage loss in compressive strength with time for AASC (100:0), AASFC (75:25), AASFC (50:50) and AASFC (25:75) in comparison with OPCC after immersion in magnesium sulphate solution up to 360 days.

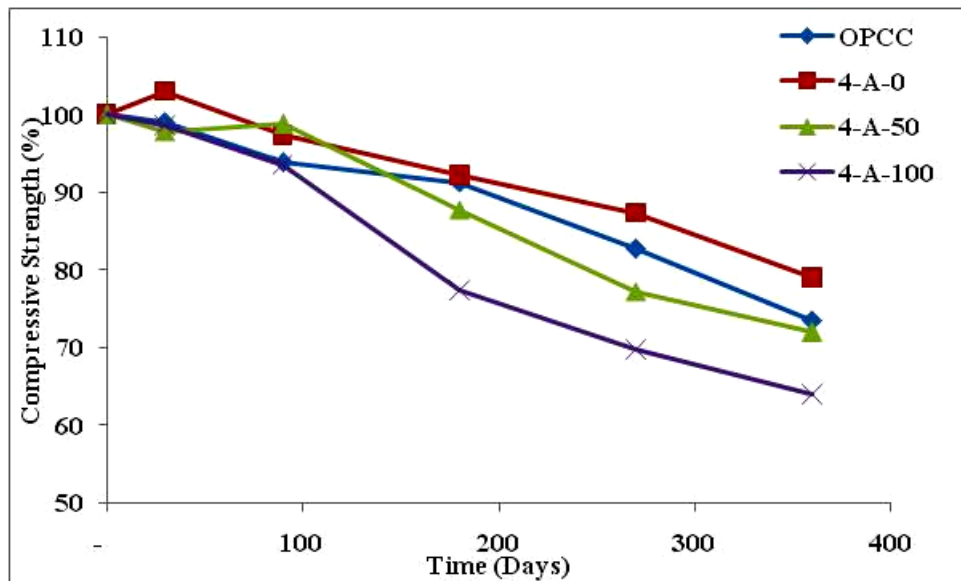


Fig. 5.7 Strength loss of AASC mix (100:0) in magnesium sulphate solution

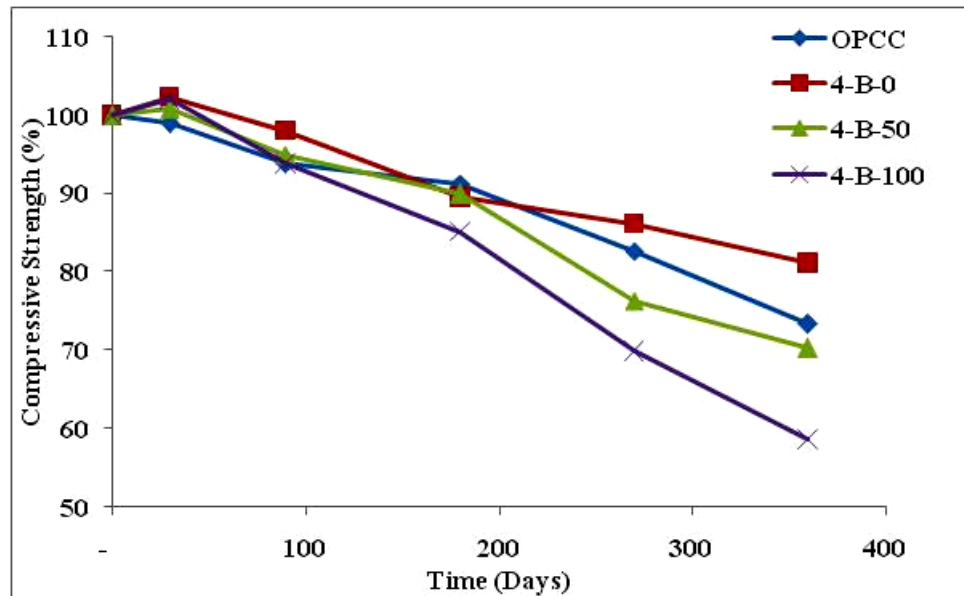


Fig. 5.8 Strength loss of AASFC mix (75:25) in magnesium sulphate solution

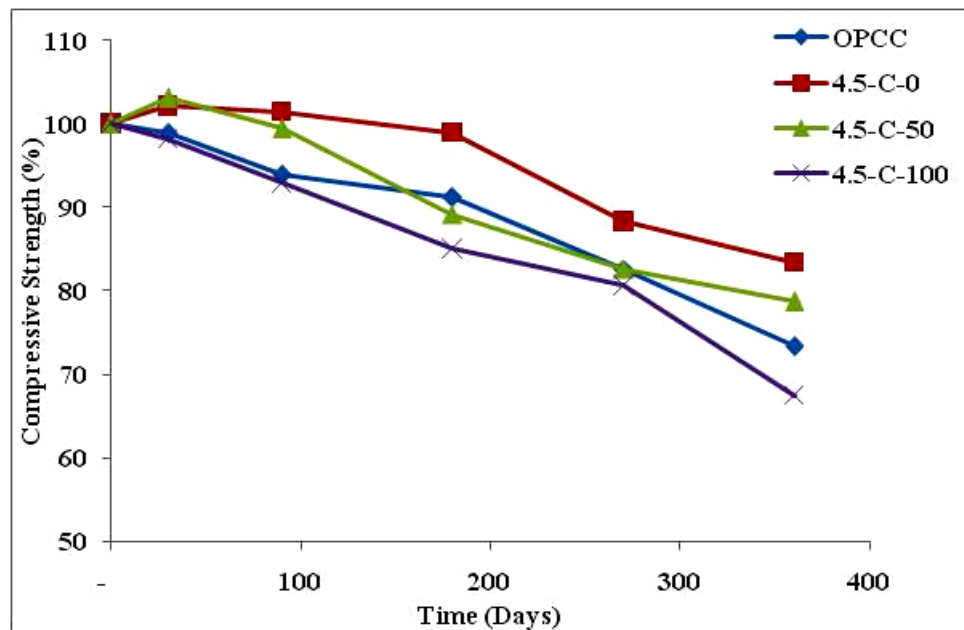


Fig. 5.9 Strength loss of AASFC mix (50:50) in magnesium sulphate solution

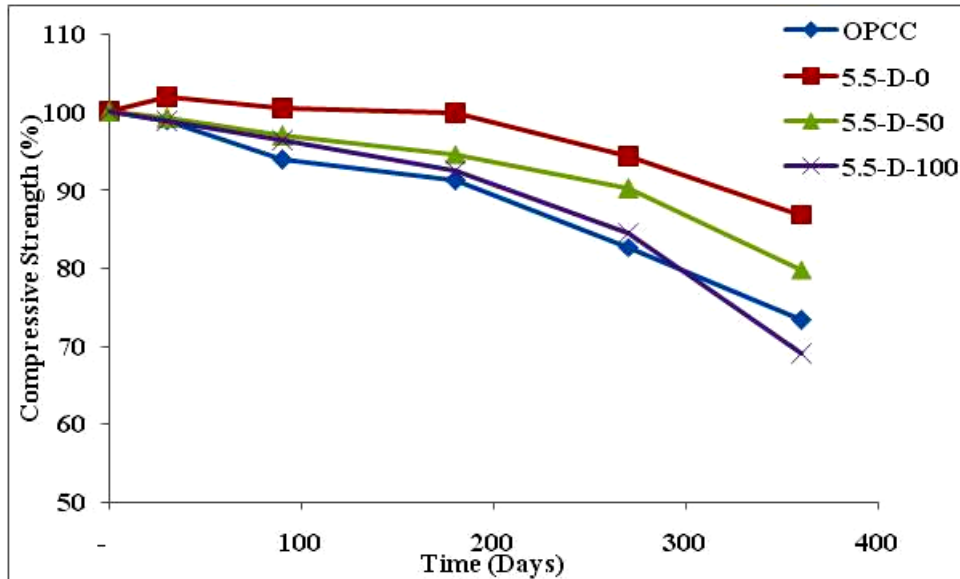


Fig. 5.10 Strength loss of AASFC mix (25:75) in magnesium sulphate solution

It may be observed that all the concrete mixes display gradual strength loss at the end of 360 days after immersion in magnesium sulphate solution. The OPCC samples exhibited lower resistance to magnesium sulphate environment as compared to alkali activated concrete mixes with 100% natural aggregates. The OPCC displayed around 27% reduction in strength, while the mix 4-A-0 displayed reduction in strength up to 21% at the end of 360 days of immersion. The AASFC mixes with 100% natural aggregates i.e. 4-B-0, 4.5-C-0 and 5.5-D-0 displayed a reduction in strength of 20%, 16% and 14%, respectively, when tested at the end of 360 days of immersion. The higher reduction in compressive strength in OPCC may be due to presence of  $\text{Ca}(\text{OH})_2$  in OPCC, which undergoes dissolution after reacting with magnesium sulphate, thus leading to decalcification of C-S-H structure and formation of gypsum. Since, pH of the surrounding environment is maintained in the range 6.5-7.5 (neutral), the consumption of  $\text{Ca}(\text{OH})_2$  occurs, in order to increase the pH of the solution (Metha and Gjorv 1974). With the consumption of  $\text{Ca}(\text{OH})_2$ , the C-S-H structure becomes unstable and releases  $\text{Ca}^{2+}$  ions, along with the further liberation of  $\text{Ca}(\text{OH})_2$  into the surrounding solution, to increase the pH. As the reaction progresses, reduction in the Ca/Si ratio occurs in the C-S-H of OPCC and at advanced stages of attack the  $\text{Mg}^{2+}$  ion can replace  $\text{Ca}^{2+}$  in the C-S-

H, to form magnesium silicate hydrate (M-S-H), which is reported to be non-cementitious (Bonen 1992). The combined effect of dissolution of  $\text{Ca(OH)}_2$  and decalcification of C-S-H, along with the formation of gypsum led to strength reduction in OPCC. The binders in AASC and AASFC mixes with lower Ca/Si ratio and absence of portlandite, undergo slower degradation and display better resistance to sulphate environment as compared to OPCC (Lu 1992). The reduction in the strength of AASC and AASFC mixes may be due to attack on the C-S-H and C-A-S-H structure by  $\text{MgSO}_4$ , which can cause the formation of M-S-H and gypsum (Bonen and Cohen 1992). The  $\text{Mg}^{2+}$  ions present in the solution lead to the decalcification of Ca-rich gel structures in the AASC and AASFC binders, along with precipitation of gypsum, leading to degradation of the binder system. The products resulting from the attack of magnesium sulphate on the binder system are expansive and poorly cohesive, which causes dimensional instability in binder system and thus reduces the mechanical performance (Idawati et al. 2012). It is reported that alkali-activated GGBFS–fly ash cements have very good resistance to acidic, sulphate and seawater attacks (Lu 1992), which can be explained by the low Ca/Si ratio of C–S–H/C-(A)-S-H in the alkali-activated GGBFS–FA cements. Slightly better performance of AASFC (25:75) mix with high FA contents can be explained by further reduction in calcium in the binder with increased content of FA.

The incorporation of steel slag in the alkali activated concrete resulted in higher reduction in the strength after immersion in magnesium sulphate solution. It may be noticed that the 4-A-0 displayed a strength loss of 21% as compared to 28% and 36% in the mix 4-A-50 and 4-A-100 respectively, after being immersed in magnesium sulphate solution for 360 days. The higher strength loss with steel slag may be due to weakening the interfacial transition zone between the aggregates and the paste caused due to volumetric expansion. The volumetric expansion is due to the reaction of calcium carbonate coating (present steel slag surface) with magnesium sulphate solution to form gypsum. A similar trend was noticed in AASFC mixes with steel slag aggregates.

## 5.4 SUMMARY

The durability properties of AASC and AASFC mixes with partial or complete replacement of natural coarse aggregates with steel slag are discussed in this chapter. AASC and AASFC mixes with steel slag displayed higher water absorption and VPV, due to higher water absorption of steel slag aggregates as compared to natural aggregates. The acid resistance of alkali activated concrete mixes decreased with the replacement of natural aggregates with steel slag. Mix 4-A-0 displayed a strength loss of 33.9% as compared to 4-A-50 and 4-A-100 that undergo a strength loss of 59.6% and 71.6% respectively after being immersed in sulphuric acid solution for 120 days. A similar trend of decrease in compressive strength with inclusion of steel slag is observed in mixes B, C and D. The higher reduction of strength with steel slag aggregates may be due to softening and deterioration of steel slag aggregates. This is due to leaching out of calcium present in the steel slag, to form expansive paste that exerted internal pressure on the concrete samples, leading to pop-outs of concrete surface. The incorporation of steel slag in alkali activated concrete resulted in higher reduction in compressive strength after immersion in magnesium sulphate solution. 4-A-0 displayed a strength loss of 21% as compared to a strength loss of 28% and 36% in 4-A-50 and 4-A-100 respectively, after being immersed in magnesium sulphate solution for 360 days. The higher strength loss due to steel slag may be due to weakening the interfacial transition zone between the aggregates and the paste; occurring because of volumetric expansion. The volumetric expansion occurs due to the reaction of calcium carbonate coating (present steel slag surface) with magnesium sulphate solution to form gypsum. The inclusion of steel slag aggregates slightly reduced the durability performance of AASC and AASFC mixes.

## **CHAPTER 6**

### **FATIGUE PERFORMANCE OF CONCRETE MIXES**

#### **6.0 INTRODUCTION**

Concrete pavements may undergo failure in different types under the action of vehicular loads during their service life; one such type of failure may be due to fatigue. The fatigue strength of concrete structures such as pavements, bridges etc., subjected to repetitive loads, is one important parameter to be considered in the design of such structures. Fatigue is often described by a parameter “Fatigue life” which essentially represents the number of cycles the material can withstand under a given pattern of repetitive loading, before failure. The failure due to fatigue occurs as a result of development of internal cracks and progressive growth of cracks under the action of cyclic loadings, that leads to failure of the pavements at loads smaller than the modulus of rupture of the concrete (Li, et al. 2007, Lee and Barr 2004). Fatigue testing is a very time consuming and expensive process and a large number of samples have to be tested. In the present study, the flexural fatigue performance of AASC and AASFC mixes incorporating 0%, 50% and 100% (by volume) steel slag coarse aggregate have been investigated. The specimens were subjected to different stress ratios (0.70, 0.75, 0.80 and 0.85) and the number of cycles for failure of the specimen at each stress ratio was determined. A probabilistic analysis of fatigue test data was carried out to ascertain the fatigue life of the material.

#### **6.1 S-N CURVE**

Most of the researchers adopted the relationship between stress level (ratio of maximum applied stress to the modulus of rupture) and the number of repetitions ‘N’ causing failure, to predict the fatigue behaviour of the material. The relationship established is known as Wohler equation and is shown by S-N Curve or Wohler curve (Oh, 1986). The use of S-N curve or Wohler curve is the most basic method of

representing the fatigue behaviour of concrete specimen. The S-N curve is an important parameter in the analysis of fatigue data, where ‘S’ denotes the stress amplitude and ‘N’ denotes the number of cycles to complete failure. This S-N curve enables one to predict the mean fatigue life of concrete under given stress level or amplitude of cyclic stress (Roylance 2001).

## 6.2 PROBABILISTIC ANALYSIS OF FATIGUE DATA

As the fatigue test data of concrete shows a considerable scatter and is random in nature, a probabilistic approach can be introduced for analyzing the fatigue data and evaluating the probability of unfavorable performance (Oh 1986). The ASTM guidelines for fatigue testing and the statistical analysis of fatigue data (ASTM 1963) suggest that the fatigue life may be assumed to be normally distributed and thus a lognormal distribution is extensively used (Mohammadi and Kaushik 2005). Later experimental studies on the basis of physical valid assumptions have shown that the distribution of fatigue life of concrete under given stress level follows the Weibull distribution and is most commonly employed in assessing reliability of composite structures (Sakin and Ay 2008). A Weibull distribution is characterized by three parameters:

- 1) Shape parameter ( $\alpha$ ) which describes the shape of the distribution;
- 2) Characteristic life or scale parameter ( $\mu$ ); and
- 3) Location parameter ( $n_0$ ).

The hazard function (Mohammadi and Kaushik, 2005) can be obtained from

$$h_N(n) = \alpha \left( \frac{n-n_0}{\mu-n_0} \right)^{\alpha-1}; n \geq n_0 \quad (6.1)$$

The hazard function or failure rate function of Weibull distribution increases with time or with an increase in the number of cycles for  $\alpha \geq 1$  only, which is compatible with the expected fatigue behaviour of engineering material (Singh and Kaushik 2000). When the location parameter is set to zero ( $n_0=0$ ), it is reduced to two parameter Weibull distribution.



There are several methods of estimating external parameters namely: 1) Graphical method; 2) Method of maximum likelihood; and 3) Method of moments, etc.

### 6.2.1 Graphical Method

The survival function of Weibull distribution can be expressed as follows:

$$L_N(n) = \exp \left[ - \left( \frac{n}{\mu} \right)^\alpha \right] \quad (6.2)$$

'n' represents specific value of random variable, ' $\alpha$ ' represents shape parameter or Weibull slope at stress level 'S' and  $\mu$  characteristic life at stress level 'S'.

Taking twice the logarithm of both sides of Eq. 6.2.

$$\left[ \ln \left[ \ln \left( \frac{1}{L_N(n)} \right) \right] \right] = \alpha \ln(n) - \alpha \ln(\mu) \quad (6.3)$$

Eq. 6.3 may be written in the following form:

$$Y = \alpha X - B \quad (6.4)$$

$$\text{Where; } Y = \left[ \ln \left[ \ln \left( \frac{1}{L_N(n)} \right) \right] \right],$$

$$X = \ln(n)$$

$$\text{And } B = \alpha \ln(\mu).$$

The distribution parameters ' $\alpha$ ' and ' $\mu$ ' can be obtained from the straight line, if fatigue life data follow Weibull distribution, which is possible if the relationship between X and Y in Eq.6.4 is linear. Hence, linear regression analysis for fatigue life data needs to be performed to get the relation for each stress level 'S' as in Eq.6.4.

In order to obtain a graphic form of Eq.6.4, the fatigue life data at a given stress level are arranged in ascending order of cycles to failure. The empirical survivorship

function  $L_N(n)$  for each fatigue life data ranked in the order of number of cycles to failure at a given stress level is calculated using mean rank.

The empirical survivorship function  $L_N(n)$  for each fatigue life data at a given stress level is calculated using the following Eq.6.5 (Mohammadi and Kaushik, 2005).

$$L_N(n) = 1 - \frac{i}{k+1} \quad (6.5)$$

Where 'i' represent failure order number and 'k' represents sample size under consideration at a particular stress level.

By plotting a graph between  $[\ln[\ln(\frac{1}{L_N(n)})]]$  and  $\ln(n)$ , the parameters ' $\alpha$ ' and ' $\mu$ ' of Weibull distribution can be directly obtained; where the slope of the line provides shape factor ' $\alpha$ ', while the characteristic life ' $\mu$ ' can be calculated from the equation,  $B = \alpha \ln(\mu)$ . The graph between  $[\ln[\ln(\frac{1}{L_N(n)})]]$  and  $\ln(n)$  is plotted for all the stress levels and for all concrete mixes and the Weibull distribution parameters are calculated.

### 6.3 FATIGUE LIFE OF CONCRETE MIXES

The fatigue life (N) i.e. the number of cycles up to failure for OPCC, AASC and AASFC mixes with/without steel slag aggregates are tabulated in Tables 6.1 to 6.4. The S-N curves obtained by plotting the stress ratio (SR) v/s number of cycles (N) up to failure for OPCC and AASC (100:0) mixes with partial or complete replacement of natural coarse aggregates with steel slag are presented in Fig.6.1. Similarly S-N curves for AASFC mixes (B, C and D) with different replacement levels of steel slag are plotted and are presented in the Appendix III. The equations obtained from the S-N curves can be utilized for estimation of fatigue cycles at any stress level. The equations generated from S-N curves for different concrete mixes are tabulated in Table 6.5.

Table 6.1 Fatigue life of OPCC and AASC (100:0) concrete mixes

Mix ID	Specimen No	Stress Ratio			
		0.85	0.80	0.75	0.70
No of cycles to failure (Fatigue Life), N					
OPCC	1	76	498	8978	28475
	2	118	788	24758	39763
	3	140	901	30866	59247
	4	220	1578	48145	79868
	5	317	1986	57835	97587
4-A-0	1	91	578	12014	30254
	2	111	876	30758	47369
	3	163	970	32677	63471
	4	326	1842	46339	100000*
	5	364	2124	61214	100000*
4-A-50	1	69	602	8325	12614
	2	132	645	16768	24786
	3	157	889	37896	69753
	4	204	1309	40707	75649
	5	350	1698	49175	92475
4-A-100	1	76	236	6012	23485
	2	126	764	26981	42141
	3	189	1104	34859	54756
	4	223	1176	43111	67348
	5	291	1478	54014	85412

Note:\* represents values after which the test was terminated

Table 6.2 Fatigue life of AASFC (75:25) concrete mixes

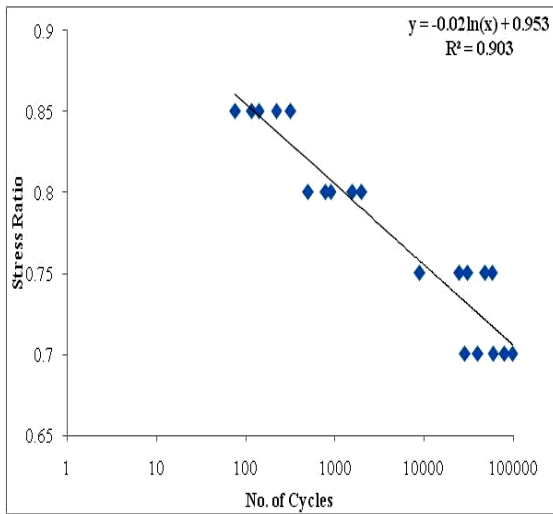
Mix ID	Specimen No	Stress Ratio			
		0.85	0.80	0.75	0.70
No of cycles to failure (Fatigue Life), N					
4-B-0	1	80	521	6412	33689
	2	121	723	16994	39475
	3	142	1022	33258	50782
	4	244	1766	55241	83695
	5	340	2018	59146	100000*
4-B-50	1	84	395	7697	20258
	2	112	488	20475	30475
	3	159	978	31789	46987
	4	173	1481	32547	79863
	5	321	1576	63545	82456
4-B-100	1	55	212	8475	14587
	2	69	612	30217	33477
	3	207	1006	35961	41223
	4	254	1075	41578	59336
	5	346	1374	44696	89621

Table 6.3 Fatigue life of AASFC (50:50) concrete mixes

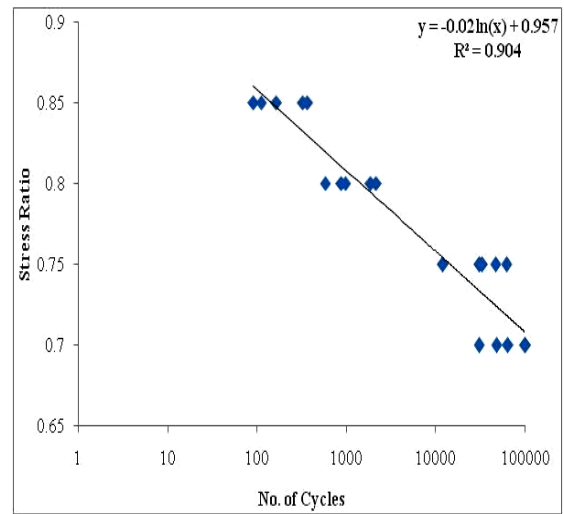
Mix ID	Specimen No	Stress Ratio			
		0.85	0.80	0.75	0.70
		No of cycles to failure (Fatigue Life), N			
4.5-C-0	1	64	601	7658	24758
	2	170	741	26335	43694
	3	188	893	32558	79866
	4	245	1691	49689	94758
	5	377	2344	64124	100000*
4.5-C-50	1	73	512	11245	20174
	2	98	683	15785	49687
	3	155	752	37863	56869
	4	201	1254	42012	67586
	5	349	1855	55974	94786
4.5-C-100	1	61	411	4755	17258
	2	110	824	18142	24758
	3	186	903	29874	46878
	4	140	1102	45332	72586
	5	287	1653	52369	85747

Table 6.4 Fatigue life of AASFC (25:75) concrete mixes

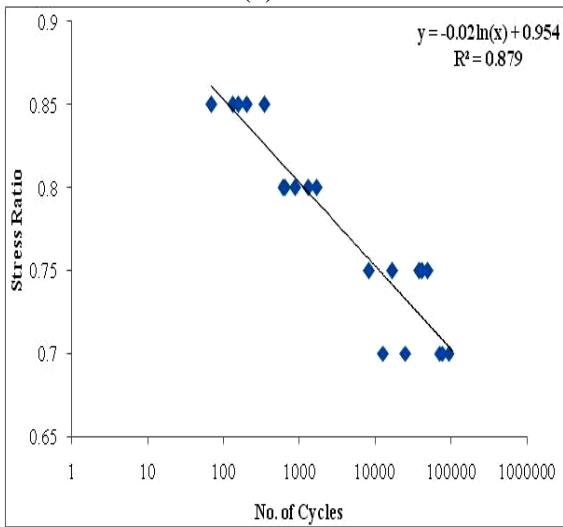
Mix ID	Specimen No	Stress Ratio			
		0.85	0.80	0.75	0.70
		No of cycles to failure (Fatigue Life), N			
5.5-D-0	1	54	758	11058	12087
	2	144	873	36985	45712
	3	293	1424	46123	68211
	4	310	1896	56778	90117
	5	422	2175	67963	100000*
5.5-D-50	1	61	312	4785	32401
	2	83	1025	16896	39888
	3	187	1259	28796	61201
	4	332	1674	50485	71356
	5	391	1910	54278	87633
5.5-D-100	1	79	357	2253	19324
	2	96	501	19312	45398
	3	212	1050	37801	50147
	4	241	1388	44777	61476
	5	306	1469	47213	81204



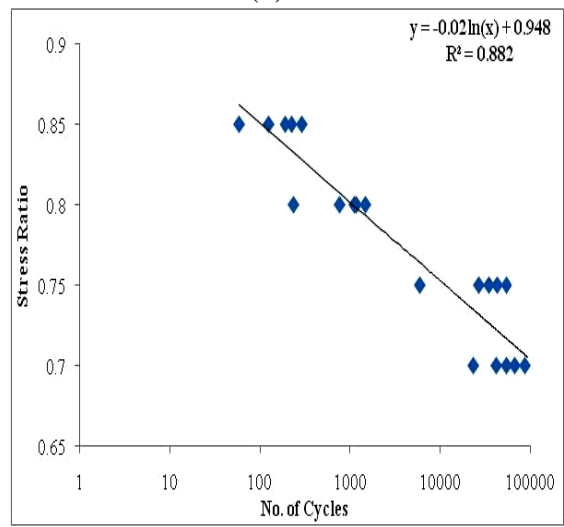
(a) OPCC



(b) 4-A-0



(c) 4-A-50



(d) 4-A-100

Fig.6.1 S-N curve for AASC (100:0) with/without steel slag aggregates

Table 6.5 Relationship between fatigue cycle (N) and stress level (SR)

Mix ID	Equations	R <sup>2</sup>
OPCC	$\ln(N)=0.953-SR/0.02$	0.903
4-A-0	$\ln(N)=0.957-SR/0.02$	0.904
4-A-50	$\ln(N)=0.954-SR/0.02$	0.879
4-A-100	$\ln(N)=0.948-SR/0.02$	0.882
4-B-0	$\ln(N) = 0.954-SR/0.02$	0.899
4-B-50	$\ln(N) = 0.952-SR/0.02$	0.888
4-B-100	$\ln(N) = 0.944-SR/0.02$	0.855
4.5-C-0	$\ln(N)=0.955-SR/0.02$	0.894
4.5-C-50	$\ln(N)=0.951-SR/0.02$	0.898
4.5-C-100	$\ln(N)=0.950-SR/0.02$	0.880
5.5-D-0	$\ln(N)=0.956-SR/0.02$	0.856
5.5-D-50	$\ln(N)=0.953-SR/0.02$	0.885
5.5-D-100	$\ln(N)=0.949-SR/0.02$	0.867

From the Table 6.1, it can be noticed that the AASC/AASFC mixes with 100% natural aggregates display higher resistance to fatigue failure as compared to OPCC, irrespective of the applied stress level. This may be due to the highly dense interfacial transition zone between the paste and the aggregate occurring in alkali activated binders as compared to that occurring in conventional cement (Bernal et al. 2012). The fatigue life of AASC mixes decreased with the inclusion of steel slag in AASC and AASFC mixes. This may due to the presence of weak aggregate-paste interface (due to presence of calcite coating) that may lead to higher and faster propagation of the crack leading to earlier failure. A similar trend was observed in AASFC mixes incorporating steel slag aggregates. The fatigue behaviour with higher contents of FA in AASFC mixes could not be clearly understood. It was observed that specimens exhibit lower fatigue life when subjected to higher stress ratios, while at lower stress ratios, specimens exhibited higher



fatigue lives. The fatigue lives of all the concrete mixes satisfied the minimum fatigue cycles as recommended by IRC 58:2002. The failures of the specimens were visually examined and were found to have failed within the middle one third spans. The statistical correlation coefficient values from the Table 6.5 for different concrete mixes at different stress levels were found to be in the range 0.85 to 0.91 indicating statistical significance.

#### **6.4 PROBABILISTIC ANALYSIS OF FATIGUE DATA OF CONCRETE MIXES**

The experimental fatigue data of concrete generally exhibit scatter and variability, even when tested under controlled conditions due to heterogeneity of materials and other reasons. Hence, in order to obtain satisfactory information on fatigue resistance and prediction of fatigue life of structures, it is desirable to make use of a probabilistic approach in the fatigue design of structures (Ramakrishnan et al. 1996). The fatigue data of concrete mixes were statistically analyzed at each stress level to obtain fatigue equation with survival probability. Due to its relative ease of use, well developed statistics and sound experimental verification, the two parameter Weibull distribution is the most widely accepted method for analyzing fatigue data of concrete structures (Oh 1991, Kumar et al. 2012). The Weibull distribution takes into account two major parameters; ‘ $\alpha$ ’ which defines the shape of the distribution and ‘ $\mu$ ’ which defines the characteristic life. The parameters  $\alpha$  and  $\mu$  can be estimated using different methods, however in this investigation, the graphical method is used due to its relative ease in use.

#### **6.5 ESTIMATION OF WEIBULL DISTRIBUTION PARAMETERS USING GRAPHICAL METHOD**

The graph between  $[\ln[\ln(\frac{1}{L_N(n)})]]$  and  $\ln(n)$  is plotted for all the stress levels and for all concrete mixes and the Weibull distribution parameters are determined. Fig. 6.2 presents the sample plot for mix A-100 at stress level of 0.70. Similar graphs are plotted for the fatigue data of all concrete mixes and the Weibull distribution parameters for OPCC and AASC/AASFC mixes at different stress levels are tabulated in Tables 6.6 to 6.9. From the Tables 6.6 to 6.9, it may be observed that correlation coefficients of

mixes at different stress levels are in the range 0.87 to 0.97, thus indicating that the fatigue life data for OPCC and AASC/AASFC mixes with/without steel slag follow Weibull distribution. The Weibull distribution parameters may be utilized for predicting the fatigue life cycles considering desired probability of failure.

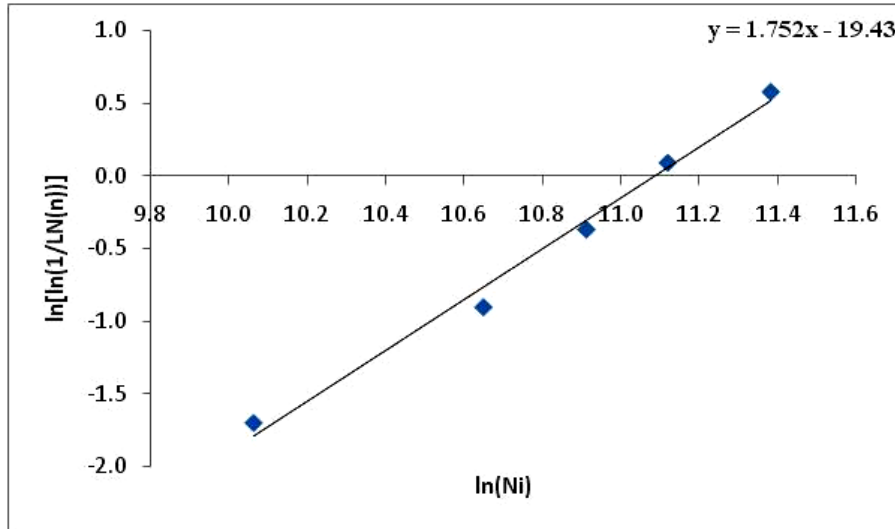


Fig. 6.2 Graphical analysis of fatigue data for 4-A-100 at stress ratio of 0.70

Table 6.6 Weibull parameters for AASC (100:0) mixes at different stress ratios

Mix ID	OPCC			4-A-0		
Stress Ratio	$\alpha$	$\mu$	$R^2$	$\alpha$	$\mu$	$R^2$
0.85	1.578	207	0.972	1.408	247	0.929
0.80	1.568	1366	0.963	1.584	1515	0.937
0.75	1.185	42184	0.955	1.339	46482	0.936
0.70	1.752	71790	0.988	1.761	79488	0.997
Mix ID	4-A-50			4-A-100		
Stress Ratio	$\alpha$	$\mu$	$R^2$	$\alpha$	$\mu$	$R^2$
0.85	1.468	217	0.971	1.404	215	0.969
0.80	1.888	1208	0.910	1.136	1216	0.875
0.75	1.143	38222	0.930	0.951	42721	0.869
0.70	0.992	68810	0.923	1.752	65524	0.988

Table 6.7 Weibull parameters for AASFC (75:25) mixes at different stress ratios

Mix ID	OPCC			4-B-0		
Stress Ratio	$\alpha$	$\mu$	$R^2$	$\alpha$	$\mu$	$R^2$
0.85	1.578	207	0.972	1.382	224	0.947
0.80	1.586	1374	0.976	1.508	1443	0.961
0.75	1.185	42184	0.955	0.936	42491	0.960
0.70	1.992	70946	0.950	1.777	73444	0.922
Mix ID	4-B-50			4-B-100		
Stress Ratio	$\alpha$	$\mu$	$R^2$	$\alpha$	$\mu$	$R^2$
0.85	1.689	201	0.928	1.035	230	0.917
0.80	1.347	1197	0.9547	1.138	1080	0.912
0.75	1.11	38506	0.952	1.165	41217	0.808
0.70	1.424	62715	0.959	1.29	57598	0.983

Table 6.8 Weibull parameters for AASFC (50:50) mixes at different stress levels

Mix ID	OPCC			4.5-C-0		
Stress Ratio	$\alpha$	$\mu$	$R^2$	$\alpha$	$\mu$	$R^2$
0.85	1.578	207	0.972	1.322	244	0.989
0.80	1.586	1374	0.976	1.462	1498	0.900
0.75	1.185	42184	0.955	1.002	48943	0.918
0.70	1.992	70946	0.950	1.416	84272	0.947
Mix ID	4.5-C-50			4.5-C-100		
Stress Ratio	$\alpha$	$\mu$	$R^2$	$\alpha$	$\mu$	$R^2$
0.85	1.419	209	0.961	1.41	239	0.983
0.80	1.646	1193	0.913	1.704	1164	0.964
0.75	1.246	39891	0.937	0.886	38467	0.937
0.70	1.452	73010	0.935	1.301	58915	0.971

Table 6.9 Weibull parameters for AASFC (25:75) mixes at different stress ratios

Mix ID	OPCC			5.5-D-0		
Stress Ratio	$\alpha$	$\mu$	$R^2$	$\alpha$	$\mu$	$R^2$
0.85	1.578	207	0.972	1.045	318	0.912
0.80	1.568	1366	0.963	1.851	1674	0.942
0.75	1.185	42184	0.955	1.165	55185	0.883
0.70	1.752	71790	0.988	0.977	80813	0.898
Mix ID	5.5-D-50			5.5-D-100		
Stress Ratio	$\alpha$	$\mu$	$R^2$	$\alpha$	$\mu$	$R^2$
0.85	1.087	258	0.964	1.296	224	0.896
0.80	1.161	1564	0.893	2.254	1293	0.934
0.75	0.867	38985	0.948	0.717	39900	0.850
0.70	2.119	68043	0.97	1.581	62545	0.928

## 6.6 GOODNESS-OF-FIT TEST FOR FATIGUE DATA

From the analysis, it is established that the fatigue life at various stress levels of OPCC, AASC and AASFC mixes with/without steel aggregates can be described using Weibull distribution. However, it would be convincing to carry out a goodness-of-fit test in order to confirm that it is a valid distribution model for statistical description of fatigue life of OPCC and AASC/AASFC mixes. Hence, the Kolmogorov-Smirnov test was carried out for this purpose (Mohammadi and Kaushik 2005).

The Kolmogorov–Smirnov test can be performed by using Eq.6.6.

$$D = \max_{i=1}^k [|F^+(X_i) - F_N(X_i)|] \quad (6.6)$$

where,  $F^+(X_i) = i/k$  = observed cumulative histogram.

$i$  = order number of the data point.

$k$  = total number of data points in the sample under consideration at a given stress level.

$F(X_i)$  = hypothesized cumulative distribution function given by Eq.6.7.

$$F_N(n) = 1 - \exp \left[ - \left( \frac{n-n_0}{\mu-n_0} \right)^\alpha \right]; n \geq n_0 \quad (6.7)$$

where  $n$  is the specific value of a random variable  $N$ ;  $\alpha$ =shape parameter or Weibull slope at stress level  $S$ ;  $\mu$ =scale parameter or characteristic life at given stress level  $S$ ; and  $n_0$ =location parameter or minimum life at stress level  $S$ .

Table 6.10 shows the results calculated by Kolmogorov–Smirnov test of fatigue life for 4-A-100 at stress level  $SR=0.70$ .

Table 6.10 Kolmogorov–Smirnov test of fatigue life for 4-A-100 at  $S=0.70$

Stress Level	$i$	$X_i$	$F^+(X_i) = i/k$	$F(X_i)$	$ F^+(X_i) - F(X_i) $
A-0	1	23485	0.2	0.1527	0.0473
	2	42141	0.4	0.3696	0.0304
	3	54756	0.6	0.5181	0.0819
	4	67348	0.8	0.6498	0.1502
	5	87548	1	0.8101	0.1899

Note:  $k=5$ ,  $X_i$ = number of cycles to failure

From the Table 6.10, it can be observed that the maximum difference is 0.1899 (for  $i=5$ ) for this case. The critical value  $D_c$  for  $n=5$  and 5% significance level is found to be 0.563 from Kolmogorov–Smirnov Table. Since  $D_t < D_c$  ( $0.1899 < 0.563$ ), the present two parameter Weibull distribution model for fatigue life at stress ratio  $SR=0.70$  is acceptable at the 5% significance level. The goodness-of-fit test is performed for the fatigue life data for OPCC and AASC/AASFC at different stress levels and the model was found to be acceptable at 5% level of significance in all cases.

## 6.7 SURVIVAL PROBABILITY AND S–N RELATIONSHIP

The fatigue life for different probability of failure (Chandrashekar 2013) can be expressed as follows:

$$n = \exp \left[ \frac{\ln \left\{ \ln \left( \frac{1}{1-P_f} \right) \right\} + \alpha \ln(\mu)}{\alpha} \right] \quad (6.8)$$

Where  $P_f$  is probability of failure

Since the fatigue life data of concrete mixes follow Weibull distribution, it can be used for the calculation of fatigue lives corresponding to different survival probabilities. The Eq.6.8 gives the fatigue life ( $n$ ) for different failure probabilities. Using the values of Weibull distribution parameters ( $\alpha$  and  $\mu$ ) obtained earlier for the fatigue life data of concrete mixes, the Eq.6.8 can be used to calculate the fatigue lives corresponding to different failure probabilities ( $P_f$ ). The Fig.6.3 presents the predicted flexural fatigue life of OPCC and AASC mixes with/without steel slag aggregates calculated at different survival probabilities (0.05, 0.5 and 0.95) using Eq.6.8. Similarly, prediction curves for AASFC mixes (B, C and D) with with/without steel slag aggregates are plotted and are presented in the Appendix III. From the Fig.6.3, it can be noticed that for a particular stress level, the number of expected cycles which a concrete mix can sustain decreases with the increasing probability of failure. The expected number of cycles is greater at lower probability of failure, i.e. at 0.95 (failure probability=5%). The graphs presented in Fig.6.4 can be used to predict the number of cycles, which the OPCC and AASC/AASFC (with/without steel slag aggregates) mixes can sustain at any desired stress level at a particular probability of failure.

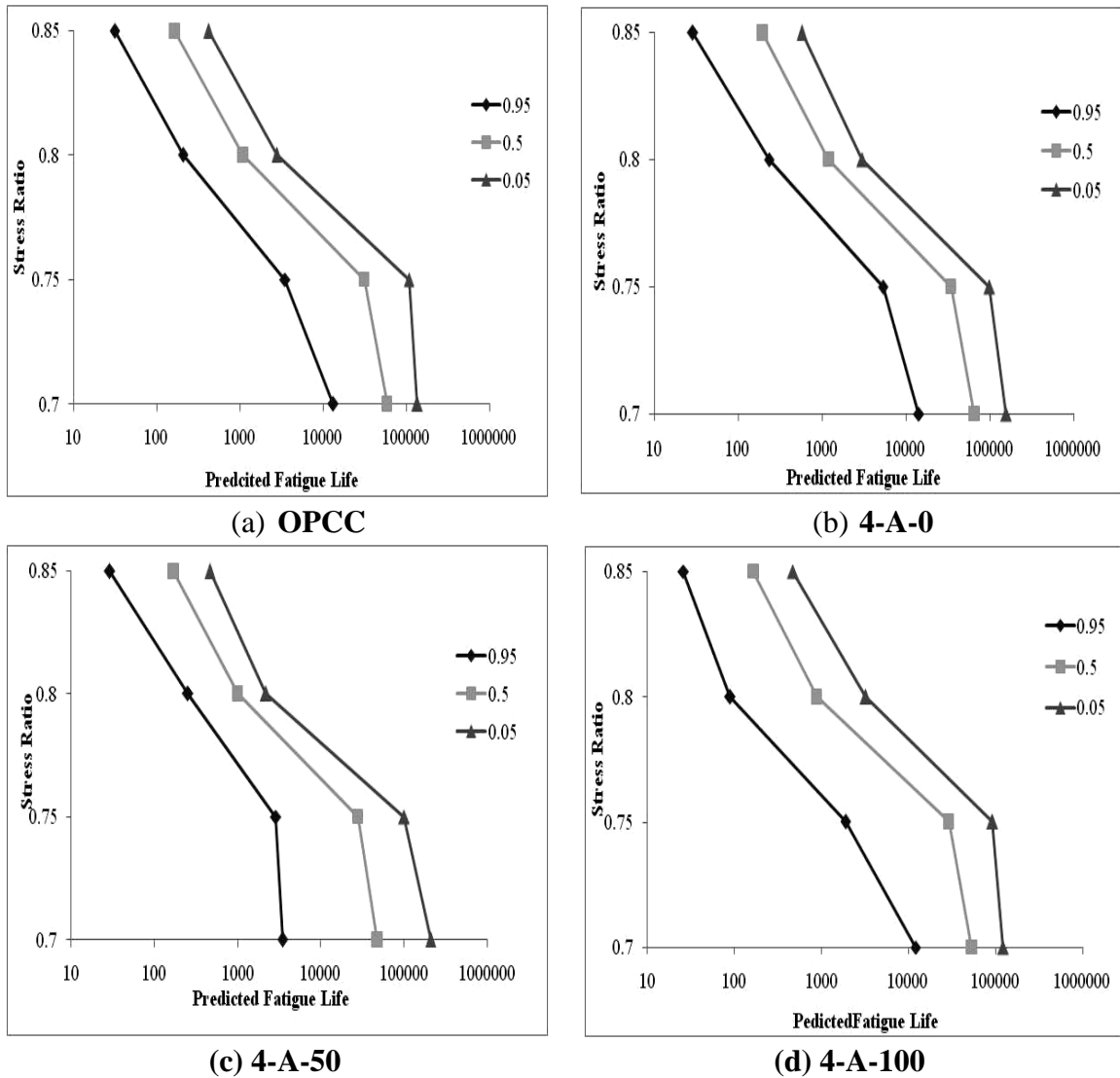


Fig.6.3 Predicted fatigue lives corresponding to different survival probabilities for various concrete mixes

## 6.8 SUMMARY

The present chapter summarizes the results of the fatigue experiments carried out on concrete mixes. The flexural fatigue performance of AASC and AASFC mixes incorporating 0%, 50% and 100% (by volume) steel slag coarse aggregate have been investigated. The specimens were subjected to different stress ratios (0.70, 0.75, 0.80 and

0.85) and the number of cycles for failure of the specimen was determined. The fatigue data were represented using S-N curves. A probabilistic analysis of the obtained fatigue test data was carried out to ascertain the fatigue life of the material using two parameter Weibull distributions. Graphical method was adopted to determine the Weibull parameters. The tests for goodness-of-fit are carried out to verify the statistical significance of the obtained data. The outcomes of the Weibull distribution are analyzed to predict the fatigue life of concrete mixes with the desired probability of failure. The AASC/AASFC mixes with normal coarse aggregates display higher resistance to fatigue failure as compared to OPCC irrespective of the applied stress level. This may be due to the highly dense interfacial transition zone between the paste and the aggregate occurring in alkali activated binders as compared to that occurring in conventional cement. The fatigue life of AASC mixes decreased with the inclusion of steel slag aggregates in AASC and AASFC mixes which may be due to the presence of weak bond between the aggregate and the paste which may lead to higher and faster propagation of the crack leading to earlier failure. A similar trend was observed in other AASFC mixes (B, C and D) incorporating steel slag. The fatigue behaviour with higher contents of FA in AASFC mixes could not be clearly understood. The fatigue data of concrete mixes were found to follow two parameter Weibull distribution with a statistical significance greater than 0.85. Probabilistic analysis of fatigue data was carried out and it was found that the Weibull distribution parameters can be used to predict the fatigue life of concrete mixes with the desired survival probability. The goodness-of-fit test is performed for the fatigue life data for OPCC and AASC/AASFC mixes at different stress levels and the model was found to be acceptable at 5% level of significance in all cases.



## **CHAPTER 7**

### **ANALYSIS AND DESIGN OF RIGID PAVEMENTS**

#### **7.0 INTRODUCTION**

The manufacture of cement involves various naturally occurring minerals such as calcium (60% by weight) mainly from limestone ( $\text{CaCO}_3$ ), silicon (20%), aluminum (10%), iron (10%) and small amounts of other ingredients which are heated in a kiln to about  $1500^\circ\text{C}$  to produce clinker. This process involves emission of huge amounts of  $\text{CO}_2$  mainly during the burning process of calcinations, where  $\text{CaCO}_3$  is broken down to calcium oxide. The  $\text{CO}_2$  emission also occurs during other processes such as operation of mining equipment to extract the raw materials and transportation of the raw materials to the cement plant (NRMCA, 2008). The Embodied Energy (EE) is the energy consumed, while Embodied Carbon Dioxide Emission ( $\text{ECO}_{2e}$ ) is the total  $\text{CO}_2$  released during the entire duration of the product life, starting from raw material extraction, transportation, manufacture, assembly, installation, disassembly and deconstruction for the concrete system (Yang et al. 2013). The global  $\text{CO}_2$  emissions from cement production account for about 3.8% of global  $\text{CO}_2$  releases (Marland, 2007). Concrete uses about 7% to 15% cement by weight, in which about 100 to 300 kg of  $\text{CO}_2$  is embodied, that amounts to 5% to 13% of the weight of concrete (Marceau, 2007). The ecological and economical analysis of various concrete mixes was examined by considering the EE,  $\text{ECO}_{2e}$  and cost of various ingredients of concrete mixes. Also the influence of mechanical properties of alkali activated concrete mixes (AASC and AASFC) on the pavement design is discussed here.

#### **7.1 ECOLOGICAL AND ECONOMICAL ANALYSIS OF CONCRETE MIXES**

An attempt has been made here in to compute the EE,  $\text{ECO}_{2e}$  and cost of the alkali activated concrete mixes to examine their ecological and economic effects. The data base for computation of EE and  $\text{ECO}_{2e}$  for the ingredients and the concretes are

taken from the literature (Rajamane 2013, Mithun and Narasimhan 2015). Costs of various ingredients (without considering transport charges) for concrete mixes were also calculated based on industry or market data (SOR 2015). The EE, ECO<sub>2e</sub> and cost of the concrete mixes were evaluated considering one kilometre divided highway stretch with a pavement thickness of 0.30 m and total width of 14 m. The details of the calculations are indicated in Table 7.1.

Table 7.1 Input data for calculation of EE, ECO<sub>2e</sub> and Cost

		Data for each material		
		(per kg)		
Ingredients		EE (MJ)	ECO <sub>2e</sub> (kgCO <sub>2e</sub> )	Cost (Rs)
Binder	GGBFS	1.6	0.083	4
	FA	0.1	0.01	0.125
	OPC	4.8	0.93	8
Activator Solution	NaOH	20.5	3.2	45
	LSS	10.2	2	14
	Water	0.2	0.0008	0.05
Admixture	Super plasticizer	11.5	0.6	175
Aggregates	Sand	0.081	0.0051	1
	Steel slag	-	-	0.05
	Granite Aggregate	0.083	0.0048	1.3
Processing		0.15	0.0038	0.52

## 7.2 PAVEMENT ANALYSIS AND DESIGN

The procedure suggested by IRC 58-2002 is adopted for the design. The analysis is carried out considering wheel load of 80 kN. The values of modulus of subgrade reaction are varied from 0.06 N/mm<sup>3</sup> to 0.45 N/mm<sup>3</sup>. Firstly, the total stresses (load stresses + temperature stresses) are evaluated for a fixed pavement thickness of 200 mm. Later, the safe thickness requirements for various concrete mixes for different conditions

(varying values of modulus of subgrade reaction from 0.06 N/mm<sup>3</sup> to 0.45 N/mm<sup>3</sup>) are evaluated.

The properties of OPCC, AASC (with 100% natural aggregates), AASC-SS (with 100% steel slag aggregates) and AASFC (with 100% natural aggregates) are adopted in the analysis. The strength properties of concrete mixes for analysis are slightly modified, i.e. 25% reduction on 90-day flexural strengths is adopted, in order to suit the field conditions. For AASFC mixes, the average of 90-day flexural strengths of AASFC mixes (75:25; 50:50 and 25:75 with natural aggregates) are considered, since the flexural strengths are in a similar range. The flexural strength of OPCC, AASC, AASC-SS and AASFC mixes considered are 4.80 MPa, 5.5 MPa, 4.6 MPa and 5.1 MPa respectively. Table 7.2 shows the other important parameters considered for the analysis. A sample design is provided in appendix V.

Table 7.2 Parameters considered for the analysis

SI No	Property	Value
1	Modulus of Elasticity 'E'	30000 MPa
2	Tyre pressure 'p'	0.80 N/mm <sup>2</sup>
3	Poisson's ratio 'μ'	0.15
4	Coefficient of Thermal Expansion, 'e'	10x10 <sup>-6</sup> °C
5	Wheel load 'P'	80 kN
6	Contraction joint spacing 'Lx'	4.5 m

## 7.3 RESULTS AND DISCUSSIONS

### 7.3.1 Ecological and Economical Analysis of Concrete Mixes

The total EE, ECO<sub>2e</sub> and cost considering different concrete mixes for one kilometre divided highway stretch is calculated and the results are summarized in Table 7.3. The detailed calculation of EE, ECO<sub>2e</sub> and cost for each mix is presented in Appendix IV.

Table 7.3 EE, ECO<sub>2e</sub> and Cost of concrete mixes per kilometre

Mix ID	EE (MJ/km)	ECO <sub>2e</sub>	Cost (lakh Rs/km)
		(kgCO <sub>2e</sub> /km)	
OPCC	11988528	1746970	303.62
4-A-0	8779088	899711.8	271.66
4-A-50	8574808	887898.1	241.19
4-A-100	8370529	876084.3	210.73
4-B-0	8100574	866573.4	252.85
4-B-50	7899780	854961.2	222.91
4-B-100	7698986	843349.1	192.96
4.5-C-0	7830039	913068.7	240.22
4.5-C-50	7633777	901718.6	210.95
4.5-C-100	7437167	890348.3	181.63
5.5-D-0	8525521	1156423	239.41
5.5-D-50	8330305	1145134	210.30
5.5-D-100	8134741	1133824	181.14

From the Table 7.3, it may be noticed that the EE, ECO<sub>2e</sub> and cost for OPCC are 11988528 MJ/km, 1746970 kgCO<sub>2e</sub>/km and 303.62 lakhRs/km respectively. The mixes 4-A-0, 4-B-0, 4.5-C-0 and 5.5-D-0 displayed a reduction in EE by around 27%, 32%, 35% and 29%, respectively, while the reduction of ECO<sub>2e</sub> was 48%, 50%, 48% and 34% respectively and the cost reduction of 11%, 17%, 20% and 21% respectively as compared to OPCC. The incorporation of steel slag aggregates in alkali activated concrete mixes led to further reduction in the EE, ECO<sub>2e</sub> and cost as compared to OPCC. The incorporation of steel slag aggregates up to 100% in alkali activated concrete mixes displayed a total average reduction in the EE by 33%, ECO<sub>2e</sub> by 46% and cost by 36% as compared to OPCC, while reductions in EE by 3%, ECO<sub>2e</sub> by 1.5% and cost by 24% as compared to alkali activated concrete mixes with 100% natural coarse aggregates. From the analyses, it may be noted that the alkali activated concrete mixes display lower energy requirement along with lower carbon dioxide emissions and lower cost as compared to OPCC, which may be of huge ecological and economical benefit to the construction industry. The replacement of natural aggregates with steel slag may lead to additional ecological and

economical benefits; however, this may require slight compromise with the strength and durability of alkali activated concrete mixes. Since, alkali activated concrete mixes are air-cured, there is no need of water for curing, and hence such a type of concrete may be of utmost advantage in places facing acute shortage of water resources. The utilization of industrial waste materials such as FA, GGBFS, steel slag, etc., in alkali activated concrete mixes will lead to reduced environmental problems associated with the disposal of such industrial wastes; along with reduced production of OPCC, which will further lead to lower greenhouse gas emissions emerging from the production of OPC. The effective recycling of such industrial wastes will also reduce the disposal costs of such wastes, along with conservation of natural resources for future concrete.

### **7.3.2 Pavement analysis and design**

Figure 7.1 presents the variation of total stress for different values of modulus of subgrade reaction for different temperature zones (temperature zone as IRC: 58:2002). Fig.7.2 presents the variation of total stress for different values of pavement thickness and modulus of subgrade reaction calculated considering temperature zone1 (temperature zone as per IRC: 58:2002).

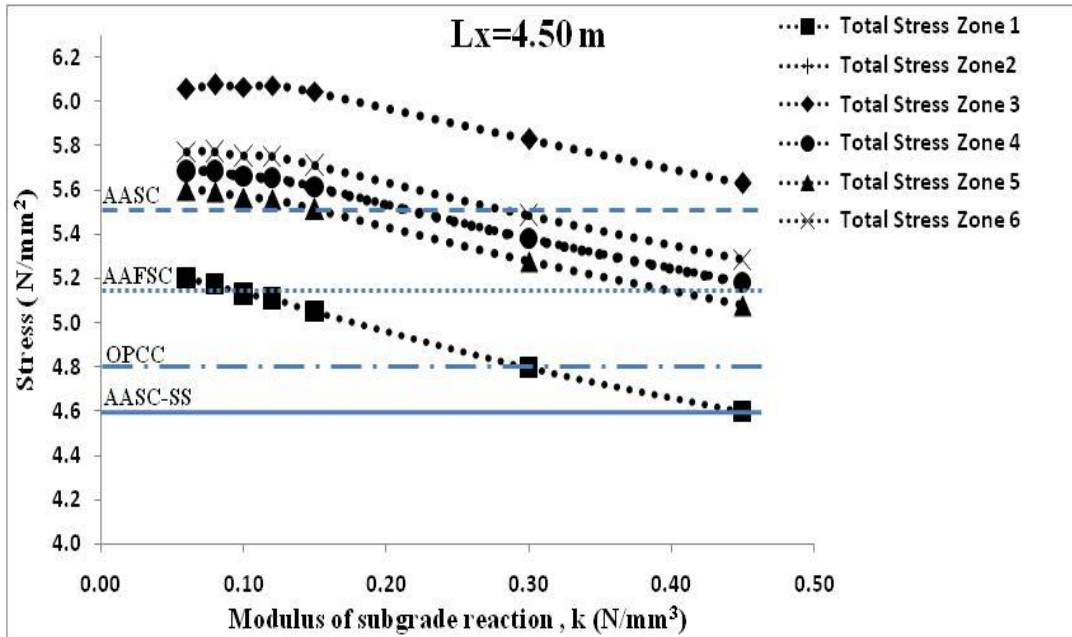


Fig.7.1 Stress Vs Modulus of Subgrade Reaction for pavement thickness of 200 mm for contraction joint spacing of 4.5 m.

Note: AASC represents mix 4-A-0, AASC-SS represents mix 4-A-100 and AAFSC represents average values of mixes 4-B-0, 4.5-C-0 and 5.5-D-0.

Since alkali activated concrete achieved quite higher flexural strength as compared to conventional cement concrete; it may be beneficial in reducing the pavement thickness to some extent. Although, there was a reduction in the flexural strength in AASC/AAFSC mixes with the incorporation of steel slag aggregates, all the AAFSC mixes (including 100% steel slag aggregates) achieved the minimum strength requirements of 4.5MPa as suggested by the Indian standard code for rigid pavement design (IRC:58:2011). From Fig 7.1, it may be noticed that the mixes with higher flexural strength can withstand higher flexural stresses occurring in the pavement structures. The AASC mix with highest flexural strength amongst the other mixes can withstand higher stress as compared to other mixes. The AASC-SS mix with least flexural strength cannot withstand higher stress and would require a higher thickness to provide a safe design. AASC and AAFSC mixes with higher flexural strength can lead to slight reduction in the pavement thickness.

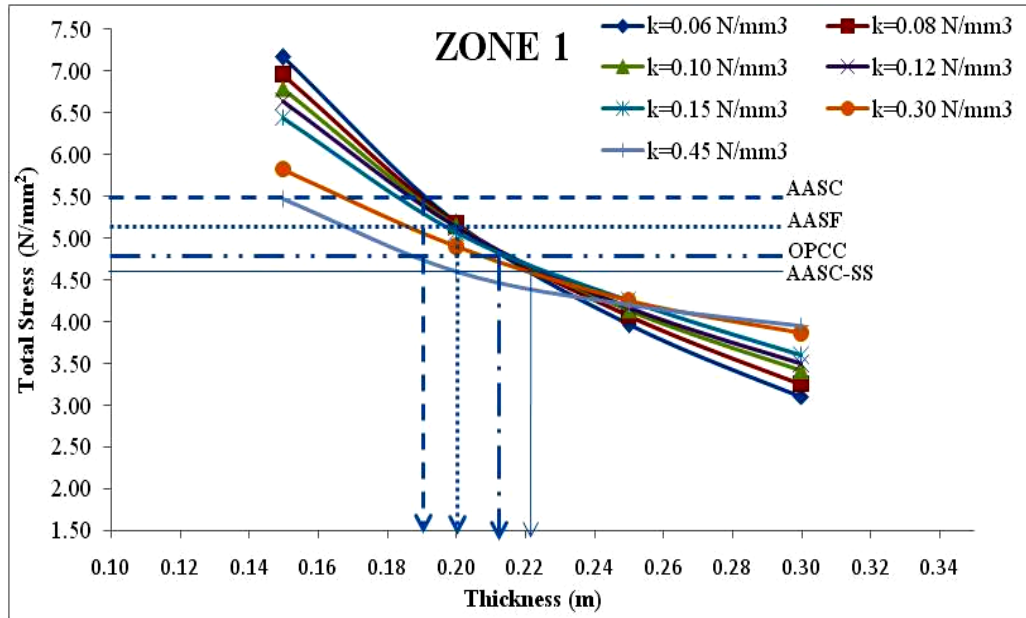


Fig. 7.2 Variation of total stress for different pavement thickness for zone 1

Note: AASC represents mix 4-A-0, AASC-SS represents mix 4-A-100 and AASFC represents average values of mixes 4-B-0, 4.5-C-0 and 5.5-D-0.

The effect of high flexural strength of concrete mixes is presented in Fig.7.2. From the Fig.7.2, it may be noticed that for a constant modulus of subgrade reaction, the AASC mix with high flexural stress can withstand higher total stress and hence the thickness required for safe design is lower than that compared to OPCC. For a constant  $k=0.45 \text{ N/mm}^3$ , the AASC would require a thickness of 0.15m for a safe design against thickness of 0.19 m for OPCC. The AASC-SS would require a thickness of 0.20m for a safe design at  $k=0.45 \text{ N/mm}^3$ . The thicknesses required for a safe design for various concrete mixes and at different modulus of subgrade reaction are presented in Table 7.4. The safe design thickness obtained from Table 7.4 cannot be directly considered for field design until the thickness is checked for fatigue stability. The higher flexural strength of AASC/AASFC mixes also has a beneficial effect on the fatigue design aspects, as it tends to decrease the stress ratio for a constant axle load group and constant thickness, thus improving the fatigue life. The decrease in the stress ratio tends to increase the number of cyclic repetitions (fatigue life) before undergoing fatigue failure. For pavements

constructed with AASC/AASFC mixes, an appropriate reduction in the pavement thickness may be done in order to match the stress behaviour (to bring the total stress closer to OPCC) occurring in those with pavements with OPCC mixes.

Table 7.4 Thickness requirement for safe design for various concrete mixes for zone 1

Mix ID	Modulus of subgrade reaction (N/mm <sup>3</sup> )						
	0.06	0.08	0.10	0.12	0.15	0.30	0.45
	Thickness (m)						
OPC	0.22	0.22	0.22	0.22	0.22	0.21	0.19
AASC	0.19	0.19	0.19	0.19	0.19	0.17	0.15
AASFC	0.20	0.20	0.20	0.20	0.20	0.19	0.17
AAS-SS	0.23	0.23	0.23	0.23	0.23	0.22	0.20

## 7.4 SUMMARY

The ecological and economical analysis of various concrete mixes is examined by considering the embodied energy, embodied carbon dioxide emission and cost of various ingredients of concrete mixes. An attempt has been made here in to compute the EE, ECO<sub>2e</sub> and cost of the alkali activated concrete mixes to examine their ecological and economic effects. The data base for computation of EE and ECO<sub>2e</sub> for the ingredients and the concretes are taken from the literature. Costs of various concrete mixes were also calculated based on industry or market data. The EE, ECO<sub>2e</sub> and cost of the concrete mixes were evaluated considering one kilometre divided highway stretch with a pavement thickness of 0.30 m and total width of 14 m. The EE, ECO<sub>2e</sub> and cost of alkali activated concrete mixes with natural aggregates are found to be quite lower as compared to OPCC. The reduction in EE for mixes 4-A-0, 4-B-0, 4.5-C-0 and 5.5-D-0 is found to be 27%, 32%, 35% and 29% respectively, while the reduction of ECO<sub>2e</sub> of 4-A-0, 4-B-0, 4.5-C-0 and 5.5-D-0 is 48%, 50%, 48% and 34% respectively, and the cost reduction of 4-A-0, 4-B-0, 4.5-C-0 and 5.5-D-0 is 11%, 17%, 20% and 21% respectively as compared to OPCC. The incorporation of steel slag aggregates in alkali activated concrete mixes led to further reduction in the EE, ECO<sub>2e</sub> and cost as compared to OPCC. The incorporation



of steel slag aggregates up to 100% in alkali activated concrete mixes displayed a total average reduction in the EE by 33%,  $\text{ECO}_2\text{e}$  by 46% and cost by 36% as compared to OPCC, while reductions in EE by 3%,  $\text{ECO}_2\text{e}$  by 1.5% and cost by 24% as compared to alkali activated concrete mixes with 100% natural coarse aggregates. From the analyses, it may be noted that the alkali activated concrete mixes display lower energy requirement along with lower carbon dioxide emissions and lower cost as compared to OPCC which may be of huge ecological and economical benefit to the construction industry. The replacement of natural aggregates with steel slag aggregates may lead to additional ecological and economical benefits. The influence of mechanical properties of alkali activated concrete mixes (AASC and AASFC) on the pavement design is evaluated and found that alkali activated concrete mixes with higher flexural strength can withstand a higher total stress in concrete pavements, and can lead to slight reduction in the pavement thickness.



## CHAPTER 8

### CONCLUSIONS

The development and understanding of AASC and AASFC mixes are of significant interest because these new materials can be cost-effective along with superior mechanical and durability performance, with lower carbon footprints as compared to OPC. The present thesis presents the investigations carried out on the suitability of GGBFS, FA, and steel slag to produce concrete. Characteristics of AASC and AASFC mixes with partial or complete replacement of natural coarse aggregates with steel slag were found to be satisfactory for highway applications.

The following conclusions are drawn based on the results on the mechanical and durability properties of AASC and AASFC mixes with steel slag as coarse aggregate.

#### A. Strength of AASC and AASFC mixes

1. The strength properties of AASC and AASFC mixes are influenced by the activator modulus ( $M_s$ ) and the sodium oxide ( $\text{Na}_2\text{O}$ ) dosage of the alkaline solution. The mixes 100:0, 75:25 and 50:50 mixes attained the highest compressive strength at an optimal activator modulus of 1.25 at both 4% and 5% sodium oxide dosages; however, for mix for the of 25:75, the optimal activator modulus was 1.50. The compressive strength of the AASFC mixes reduced with the incorporation of FA for a constant  $\text{Na}_2\text{O}$  dosage. This may be attributed to the lower reactivity to FA as compared to GGBFS. At a constant water/binder ratio of 0.40, the mixes containing FA displayed higher workability. The strength of the AASC and AASFC mixes depend on the sodium oxide dosage of the alkaline activator. Higher the sodium oxide dosage, the higher is the strength achieved.
2. The incorporation of steel slag in AASC and AASFC mixes slightly affected the workability and the unit weight of the concrete mixes. The AASC and

AASFC mixes with steel slag showed reduced workability; while the unit weight of the mixes increased with higher contents of steel slag, as compared to those concrete mixes with natural aggregates.

3. The AASC and AASFC mixes exhibit higher early and ultimate strength as compared to OPCC. All AASC and AASFC mixes with partial or complete replacement of natural coarse aggregates with steel slag attained 28-day compressive strength in the range of  $55\pm 5$  MPa and flexural strengths greater than 5.5 MPa after 28 days of curing. The incorporation of steel slag as coarse aggregate slightly lowered the mechanical properties in both AASC and AASFC mixes, which is mainly due to the weak aggregate-paste interface on account of the presence of a coating of calcite (formed due to weathering) on the surface of steel slag aggregates.
4. AASC/AASFC mixes with 100% natural aggregates display higher tensile (flexural and split tensile) strength as compared to OPCC. This may be due to the existence of distinct microstructure and a dense interfacial transition zone between the paste and aggregates in alkali activated concrete mixes as compared to OPCC. The incorporation of steel slag aggregates led to decrease in the tensile properties of the AASC and AASFC mixes. The inclusion of high content of FA in the AASFC mixes slightly resulted in a decrease in tensile properties and modulus of elasticity for similar compressive strength as compared to AASC mix.
5. The static modulus of elasticity of OPCC mixes was higher than that of AASC and AASFC mixes with/without steel slag. For a similar grade of concrete, modulus of elasticity of AASFC mixes exhibit lower values with replacement of GGBFS with FA, which is due to the differences in the microstructure and binder chemistry. The modulus of elasticity of AASC and AASFC mixes decrease with the replacement of natural aggregates with steel slag, due to the

weak aggregate-paste interface formed, in the presence of calcite coating on the steel slag aggregate surface.

### B. Durability of Concrete Mixes

6. AASC and AASFC (75:25) mixes with normal aggregates having same binder content and water-binder ratio as that of OPCC, show reduced water absorption and VPV values as compared to OPCC at 28 days of curing. This may be due to the presence of very refined closed pore structure in the AASC samples that restrict the water to penetrate into the structure. The water absorption and VPV values increased with FA replacement in the AASFC mixes. The water absorption and subsequent VPV increase with the replacement of steel slag in both AASC and AASFC mixes, due to the higher water absorption of steel slag.
7. Alkali activated concrete mixes with 100% natural aggregates exhibited better resistance to sulphuric acid as compared to OPCC, which is due to the properties/structure of the binders. The inclusion of higher FA in AASFC mixes improved the resistance to acid attack, due to decrease in calcium content in the binder with the addition of FA content, that tends to make the binder further resistant to acid attack. The acid resistance of alkali activated mixes decreased with the replacement of natural coarse aggregates with steel slag. The strength loss with steel slag may be due to the softening and deterioration of the steel slag. The deterioration of the steel slag was due to leaching out of calcium present in the aggregates.
8. OPCC samples exhibit lower magnesium sulphate resistance as compared to alkali activated concrete mixes with 100% natural aggregates. The higher reduction in compressive strength in OPCC may be attributed to the presence of  $\text{Ca(OH)}_2$  in OPCC. The incorporation of steel slag in the alkali activated concrete resulted in the higher reduction in the strength after immersion in

magnesium sulphate solution. The higher strength loss with steel slag may be due to the weakening of interfacial transition zone between the aggregates and the paste, occurring due to volumetric expansion. The volumetric expansion occurs due to the reaction of calcium carbonate present on steel slag surface with magnesium sulphate solution to form gypsum.

### C. Flexural Fatigue performance of concrete mixes

9. The AASC/AASFC mixes with 100% natural aggregates exhibit better fatigue life as compared to OPCC, due to the dense interfacial transition zone between the paste and aggregates in alkali activated binders. The AASC/AASFC mixes with steel slag display lower fatigue life as compared to AASC/AASFC mixes with natural coarse aggregates.
10. The probability distribution of fatigue data of OPCC, AASC and AASFC mixes with/without steel slag can be approximately modelled using two parameter Weibull distribution.
11. The goodness-of-fit test was performed for the fatigue life data of OPCC and AASC/AASFC mixes at different stress levels and the model was found to be acceptable at 5% level of significance. Prediction of fatigue life cycles of OPCC and AASC/AASFC mixes at different survival probabilities can be done by utilizing the Weibull distribution parameters. Higher probability of failure, the shorter is the fatigue life of the specimen at the same stress ratio.

### D. Ecological and economical analysis of concrete mixes

12. The EE,  $ECO_2e$  and cost of alkali activated concrete mixes with 100% natural aggregates are found to be quite lower as compared to OPCC. The incorporation of steel slag aggregates upto 100% in alkali activated concrete mixes displayed additional reduction in the EE  $ECO_2e$  and cost as compared to alkali activated concrete mixes with 100% natural aggregates.

13. The AASC and AASFC mixes with higher flexural strength can withstand higher stresses and therefore lead to the reduction of thickness when used in pavements.

The test results on various strength and durability properties have revealed that, the use of steel slag based AASC/AASFC mixes have been at par or marginally lower than the conventional OPCC. It can be stated that AASC and AASFC mixes with steel slag as coarse aggregate can have several advantages over OPCC namely,

- Usage of industrial waste (Steel slag, GGBFS, FA).
- Consumption of natural aggregates can be reduced, which in-turn reduces the environmental and ecological problems associated with mining.
- Reduction in steel slag stockpiles would solve environmental problems.
- Due to air curing, water can be saved.
- High early strength development can be effectively used for early strip-off of formwork, thus helping faster construction and early use of pavements.
- Less energy consumption.
- Emission of CO<sub>2</sub> is reduced and it is economical.

The AASC and AASFC mixes with steel slag have shown satisfactory results for their use in highway applications. The utilization of AASC and AASFC mixes lead to minimized consumption and production of OPC, which in turn can contribute to lower CO<sub>2</sub> emissions. The utilization of steel slag in concrete leads to for the conservation of natural aggregates and solves the disposal related problem associated with steel slag. Efforts should be made with government to patronage and to popularize the use of these types of alternate binder systems in infrastructure projects.

## **8.1 RECOMMENDATIONS**

Although, steel slag provide satisfactory strength and durability performance in AASC and AASFC mixes, special attention needs to be paid for the proper weathering of the aggregates. Immediate implementation of steel slag aggregates in concrete pavements without studying the long-term properties is not advisable. When using steel slag in AASC and AASFC concrete mixes, it is important to optimize the mix design appropriately in order to guarantee the desired level of durability. The mixes containing steel slag aggregates may be aimed at higher compressive strength and lower water penetration as main characteristics. Systematic testing and monitoring has to be done to assure complete stabilization of steel slag during weathering to prevent any possible expansion. The steel slag must be tested to determine the free lime or magnesia content along with tests for volume expansion test. The steel slag aggregate must be carefully selected and used in concrete pavements, only if the slag has minimal volume expansion and low free lime or free magnesia content.

## **8.2 SCOPE FOR FUTURE STUDY**

The present investigation can be extended to:

- Extensive study of the micro-structural behavior of alkali activated concrete mixes with steel slag as coarse aggregates can be carried out.
- Evaluation of the temperature differential of alkali activated concrete slabs.
- Performance of steel slag subjected to different weathering process such as air aging, hot water aging and steam aging in concrete mixes may to be studied.



## REFERENCES

- Adam, A.A. (2009). "Strength and durability properties of alkali activated slag and fly ash-based geopolymer concrete." *Ph.D Thesis, School of Civil, Environmental and Chemical Engineering RMIT University Melbourne, Australia.*
- Alexander, M., Bertron, A. and De Belie, N. (2013). "Performance of cement-based materials in aggressive aqueous environments." *State-of-the-Art Reports 10, RILEM*, DOI 10.1007/978-94-007-5413-3\_1.
- Alexander, M.G., and Milne, T.I. (1995). "Influence of cement blend and aggregate type on stress– strain behavior and elastic modulus of concrete." *ACI Material Journal*, 92 (3), 227–234.
- Alexander, S.B. and Jeffery, R.R. (2014). "Concrete with steel furnace slag and fractionated reclaimed asphalt pavement." *Research Report No. ICT-14-015*, Illinois Center for Transportation.
- Alizadeh, R., Chini M., Ghods P., Hoseini M., Montazer Sh., Shekarchi M. (1996). "Utilization of electric arc furnace slag as aggregates in concrete – environmental issue." *Tehran: CMI Report.*
- Allahverdi, A. and František, Š. (2000). "Acidic corrosion of hydrated cement based materials Part 1. - mechanism of the phenomenon." *Ceramic – Silikaty*, 44(3), 114-120.
- Altan, E. and Erdog̃an, S.T. (2012). "Alkali activation of a slag at ambient and elevated temperatures." *Cement and Concrete Composites*, 34, 131–139.
- Ameri, M., Shahabishahmiri, H. and Kazemzadehazad, S. (2012). "Evaluation of the use of steel slag in concrete." *In: Proceedings of 25<sup>th</sup> ARRB Conference*, Perth, Australia, p.9.
- Armaghani, J.M., Larsen, T.J. and Smith, L.L. (1988). "Design-Related distress in concrete pavements." *Concrete International*, 10, 43-49.
- ASTM C618-15, (2015). "Standard specification for coal fly ash and raw or calcined natural pozzolan for use in concrete." *ASTM International*, West Conshohocken, PA, 015, [www.astm.org](http://www.astm.org)
- ASTM C642-06. "Standard test method for density, absorption, and voids in hardened concrete." *ASTM International*, West Conshohocken, PA, 015, [www.astm.org](http://www.astm.org).
- ASTM –STP- 91 (1963). "A guide for fatigue testing and the statistical analysis of fatigue data." *ASTM Special Technical Publication*, No. 91-A (Second Edition) American Society for Testing and Materials, 1916 Race Street, Philadelphia 3, Pa.

Australasian Slag Association. (2002). "A guide to the use of iron and steel slag in roads." ISBN 0 957705158, Revision 2, Wollongong: Australasian Slag Association Inc.

Aydın, S. and Baradan, B. (2012). "Mechanical and microstructural properties of heat cured alkali-activated slag mortars." *Materials and Design*, 35, 374–383.

Bakharev, T. (2005). "Durability of geopolymer materials in sodium and magnesium sulfate solutions." *Cement and Concrete Research*, 35(6), 1233–1246.

Bakharev, T. (2005). "Geopolymeric materials prepared using class f fly ash and elevated temperature curing, *Cement and Concrete Research*, 35 (6), 1224-1232

Bakharev, T., Sanjayan, J. G. and Cheng, Y. B. (1999). "Alkali activation of australian slag cements." *Cement and Concrete Research*, 29 (1), 113- 120.

Bakharev, T., Sanjayan, J.G. and Cheng, Y. B. (2000). "Effect of admixtures on properties of alkali-activated slag concrete." *Cement and Concrete Research*, 30 (9), 1367- 1374.

Bakharev, T., Sanjayan, J.G. and Cheng, Y. B. (2002). "Sulfate attack on alkali-activated slag concrete." *Cement and Concrete Research*, 32(2), 211–216.

Bakharev, T., Sanjayan, J.G., and Chen, Y.B. (2003). "Resistance of alkali activated slag concrete to acid attack." *Cement and Concrete Research*, 33(10), 1607–1611.

Bernal, S.A., Gutierrez R.D., Delvasto, S., and Rodriguez, E.D. (2010). "Performance of an alkali-activated slag concrete reinforced with steel fibers." *Construction and Building Materials*, 24 (2), 208–214

Bernal, S.A., Mejía de Gutiérrez, R., and Provis, J.L. (2012). "Engineering and durability properties of concretes based on alkali-activated granulated blast furnace slag/metakaolin blends." *Construction and Building Materials*, 33, 99-108.

Bernal, S.A., Provis, J.L., Rose, V., and Gutierrez, R.M. (2011) a. "Evolution of binder structure in sodium silicate-activated slag-metakaolin blends." *Cement and Concrete Composites*, 33(1), 46–54.

Bernal, S.A., Gutiérrez, R.D., Alba, L. P., Provis, J.L., Rodriguez, E.D. and Delvasto, S. (2011) b. "Effect of binder content on the performance of alkali-activated slag concretes." *Cement and Concrete Research*, 41(1), 1–8.

Bernard, E. and Dipayan, J. (2003). "Forces of hydration that can cause havoc in concrete." *ACI Journal*, 25, 51-57.

Bhattacharya. (2005). "Scope of concrete roads in India." Keynote address at National Workshop on Sustainability of Road Infrastructure-Scope of concrete roads, jointly organized by CMA India and ICI, Kolkata.

Bilim, C., Karahan, O., Ati, C.D. and lkentapar, S. (2015). "Effects of chemical admixtures and curing conditions on some properties of alkali-activated cementless slag mixtures." *KSCE Journal of Civil Engineering*, 19(3), 733-741.

Bonen, D. (1992). "Composition and appearance of magnesium silicate hydrate and its relation to deterioration of cement based materials." *Journal of American Ceramic Society*, 75(10), 2904– 2906.

Bonen, D., and Cohen, M.D. (1992). "Magnesium sulphate attack on Portland cement paste – I. Microstructural analysis." *Cement and Concrete Research*, 22, 169–180.

Carlo, P., Paolo, C., Flora, F., and Katya, B. (2013). "Properties of concretes with black/oxidizing electric arc furnace slag aggregate." *Cement and Concrete Composites*, 37, 232–240.

Cengiz, D., Atis, C.B., Zlem, O., Elik, C. and Okan, K. (2009). "Influence of activator on the strength and drying shrinkage of alkali-activated slag mortar." *Construction and Building Materials*, 23(1), 548–555.

Chandra, S. (2002). "Waste materials used in concrete manufacturing." Standard Publishers Distributors, New Delhi, India.

Chandrashekar, A. (2013). "Studies on potential usage of fly ash in steel fiber reinforced concrete for rigid pavements." *Ph.D Thesis*, NITK Surathkal, Karnataka, India.

Chandrashekar, A., Ravishankar, A.U., and Girish, M.G. (2010). "Fatigue behaviour of steel fibre reinforced concrete with fly ash," *Highway Research Journal*, 9-20.

Chang, J.J. (2003). "A study on the setting characteristics of sodium silicate activated slag pastes." *Cement and Concrete Research*, 33(7), 1005-1011.

Chassevent, L. (1937). 17. Cong. Chem. Ind. 147 (Paris).

Chen, W., Brouwers, H.J.H. (2007). "The hydration of slag. Part 1: Reaction models for alkali-activated slag." *Journal of Material Science*, 42, 428–443.

Chi, M. (2012). "Effects of dosage of alkali-activated solution and curing conditions on the properties and durability of alkali-activated slag concrete." *Construction and Building Materials*, 35, 240–245.

Chi, M., and Huang, R. (2013). "Binding mechanism and properties of alkali-activated fly ash/slag mortars." *Construction and Building Materials*, 40, 291–298.

Collins, F.G., and Sanjayan, J.G. (1999), “Workability and Mechanical Properties of Alkali Activated Slag Concrete”, *Cement and Concrete Research*, 29 (3), 455–458.

CPAM. (2012): <http://www.concreteisbetter.com/vs.html>, Concrete Paving Association of Minnesota, last accessed Sept 2012.

Davidovits, J.J. (1979). “Synthesis of new high temperature geo-polymers for reinforced plastics composites.” *SPE PACTEC 79 Society of Plastic Engineers, Brookfield Centre*, 151–154.

Davidovits, J. (1994). “Properties of geopolymer cements.” *In: Proceedings of 1<sup>st</sup> International Conference on Alkline Cement and Concrete, Kiev, Ukraine, SRIBM, Kiev State Technical University*, 131-149.

Davidovits, J. (1999). “Chemistry of geopolymeric systems, terminology.” *In Geopolymer*, 99, 9-40.

Davidovits, J.J. (2005). “Geopolymer chemistry and sustainable development. The poly (sialate) terminology: a very useful and simple model for the promotion and understanding of green-chemistry.” *Proceedings of the World Congress Geopolymer, Davidovits, J. (Ed.), Saint Quentin, France*, 9-15.

Diaz-Loya, E. I., Allouche, E. N., and Vaidya, S. (2011). “Mechanical properties of fly-ash-based geopolymer concrete.” *ACI Material Journal*, 108, 300–306.

Douglas, E., Brandstetr, J. (1990). “A preliminary study on the alkali activation of ground granulated blast-furnace slag.” *Cement and Concrete Research*, 20,746–756.

Datta, D. and Ghosh, S. (2014). “Durability study of geopolymer paste blended with blast furnace slag.” *IOSR Journal of Mechanical and Civil Engineering*, 11 (2), 73-79.

Datta, D. and Ghosh, S. (2014). “Effect of curing profile on fly ash geopolymer with slag as supplementary.” *International Journal of Engineering Sciences and Research Technology*, 3(12), 143-148.

Duxson, P., Fernandez-Jimenez, A., Provis, J. L., Lukey, G. C., Palomo, A. and Deventer, J. S. J. V. (2007). “Geopolymer Technology: the current state of the art.” *Journal of Material Science*, 42(9), 2917-2933.

Fernandez-Jimenez, A., Palomo, J. G. and Puertas, F. (1999). “Alkali-activated slag mortars: mechanical strength behavior.” *Cement and Concrete Research*, 29(8), 1313-1321.

Fernandez-Jimenez,A., and Puertas, F. (2001). “Setting of alkali-activated slag cement-influence of activator nature.” *Advanced Cement Research*, 13 (3), 115-121.

Fernández-Jiménez, A., and Palomo, A. (2003). "Characterization of fly ash: potential reactivity as alkaline cements." *Fuel*, 82(18), 2259-2265.

Fernandez-Jimenez, A., and Palomo, A. (2005). "Composition and microstructure of alkali activated fly ash binder: effect of the activator." *Cement and Concrete Research*, 35 (10), 1984-1992.

Fernandez-Jiménez, F.A., Palomo, A. and , Criado, M. (2005). " Microstructure development of alkali-activated fly ash cement: a descriptive model." *Cement and Concrete Research*, 35(6), 1204–1209.

Fernández-Jiménez, A., Garcia-Lodeiro, I. and Palomo, A. (2007). "Durability of alkali-activated fly ash cementitious materials." *Journal of materials science*, 42(9), 3055-3065.

FHWA, (2012). "User guidelines for byproducts and secondary use materials in pavement construction." Publication Number: FHWA-RD-97-148.

FICCI. (2014): <http://blog.ficci.com/steel-slag/5291>.

Forster, S.W. (2006). "Significance of tests and properties of concrete and concrete making materials, chapter 31 – soundness, deleterious substances and coatings" *ASTM STP 169D*, West Conshohocken, PA: ASTM. DOI: 10.1520/STP169D-EB.

Fruehan, R.J. (1985). "The making shaping and treating of steel." *Association of Iron and Steel Engineers*. ISBN: 0–930767–02–0.

Gambhir, M.L. (2004). "Concrete technology, theory and practice." 4<sup>th</sup> ed. New Delhi: *Tata McGraw-hill (Education) Private Limited*.

Ganesan, N., Bharati, R.J. and Shashikala, A.P. (2013). "Flexural fatigue behavior of self compacting rubberized concrete." *Construction and Building Materials*, 44, 7–14.

Garcia, E., Campos-Venegas, K., Gorokhovskiy, A. and Fernandez-Jimenez, A. (2006). "Cementitious composites of pulverized fuel ash and blast furnace slag activated by sodium silicate: effect of Na<sub>2</sub>O concentration and modulus." *Advanced Applied Ceramics*, 105 (4), 201–208.

Gary, W.H., McLaughlin, J.F., and Antrim, J.C. (1961). "Fatigue properties of lightweight aggregate concrete." *ACI Materials Journal*, 58 (8), 149-162.

Gebhardt, R.F. (1988). "Rapid methods for chemical analysis of hydraulic cement." STP-985 *ASTM International*, West Conshohocken, PA, 015, [www.astm.org](http://www.astm.org).

GEOPAVE. (1993). "Steel Slag Aggregates.", *Material Technology, Technical note 2*.

- Glukhovsky, V. D. (1959). "Soil Silicates." *Kiev, Ukraine: Gastroi Publishers.*
- Glukhovsky, V.D. (1994). "Alkaline cements and concretes." *1<sup>st</sup> International Conference , Kiev, Ukraine,1-8.*
- González-Ortega, M.A., Segura, I., Cavalaro, S.P.H., Toralles-Carbonari, B., Aguado, A. and Andrello, A.C. (2014). "Radiological protection and mechanical properties of concretes with EAF steel slags." *Construction and Building Materials*, 51, 432–438.
- Gourley, J. T. (2003). "Geopolymers; opportunities for environmentally friendly construction materials." In: *Proceedings of Materials Conference: Adaptive Materials for a Modern Society, Sydney, Institute of Materials Engineering Australia.*
- Guerrrieri, M., and Sanjayan, J. (2009). "Behaviour of combined fly ash/slag based geopolymers when exposed to high temperatures." *Fire and Materials*, 34 (4), 163-175.
- Hafa M.B., Saout, G.L., Winnefeld, F. and Lothenbach, B. (2011). "Influence of activator type on hydration kinetics, hydrate assemblage and micro structural development of alkali-activated blast-furnace slags." *Cement and Concrete Research*, 41, 301–310.
- Heeralal, M., Rathish Kumar, P., and Rao, Y.V. (2009). "Flexural fatigue charecteristics of steel fiber reinforced recycled aggregate concrete." *Architecture and Civil Engineering*, 7(1), 19 – 33.
- Hsu, T. C. C.(1981). "Fatigue of plain concrete." *ACI Materials Journal*, 78 (4), 292-305
- Hui, L., Mao-hua, Z., and Jin-ping, O. (2006). "Flexural fatigue performance of concrete containing nano-particles for pavement." *International Journal of Fatigue*, 29 (2), 1292–1301.
- Idawati, I., Bernal, A. S., Provis, J.L., Rackel, S. N., David, G.B., Adam, R. K., Sinin, H., and van Deventer, J.S.J. (2013). "Influence of fly ash on the water and chloride permeability of alkali-activated slag mortars and concretes." *Construction and Building Materials*, 48, 1187–1201.
- IRC : 21-2000. "Standard specifications and code of practice for road bridges section: III cement concrete (Plain and Reinforced)." Third Revision, *Indian Roads Congress*, New Delhi, India.
- IRC: 58-2002. "Guidelines for the design of plain jointed rigid pavements for highways." *Indian Roads Congress*, New Delhi, India.
- IRC: 58-2011. "Guidelines for the design of plain jointed rigid pavements for highways." *Indian Roads Congress*, Third Revision, New Delhi, India.

IRC: SP:62-2004. "Guidelines for the design and construction of cement concrete pavements for rural roads." *Indian Road Congress*, New Delhi.

IS -14212-1995 (1995). "Sodium and potassium silicates- Methods of test." *Bureau of Indian Standards*, Manak Bhavan, 9 Bahadur Shah Zafar Marg, New Delhi- 110002.

IS: 1199-1959. "Method for sampling and analysis of concrete." *Bureau of Indian Standards*, New Delhi, India.

IS: 12089 - 1987. "Indian standard specification for granulated slag for the manufacture of Portland slag cement." *Bureau of Indian Standards*, New Delhi, India.

IS: 2386-1963. "Methods of test for aggregates for concrete." *Bureau of Indian Standards*, New Delhi, India.

IS: 383-1970. "Indian standard specification for coarse and fine aggregates from natural sources for concrete (second revision)." *Bureau of Indian Standards*, New Delhi, India.

IS: 516-1959. "Methods of tests for strength of concrete." *Bureau of Indian Standards*, New Delhi, India.

IS: 5816-1999. "Splitting Tensile Strength of Concrete - Method of Test." *Bureau of Indian Standards*, New Delhi, India.

IS: 8112-2013. "Ordinary Portland cement, 43 grade- specification (second revision)." *Bureau of Indian Standards*, New Delhi, India.

IS:10262-2009. "Indian standard concrete mix proportioning (First Revision)." *Bureau of Indian Standards*, New Delhi, India.

IS-3812-2-(2003). "Specification for pulverized fuel ash, *part 2*: for use as admixture in cement mortar and concrete." *Bureau of Indian Standards*, Manak Bhavan, 9 Bahadur Shah Zafar Marg New Delhi -110002.

Ivanka, N., Dubravka, B., Goran, V. (2011). "Utilisation of steel slag as an aggregate in concrete." *Materials and Structures*, 44, 1565–1575.

Jiang, W. (1997). "Alkali Activated Cementitious Materials: Mechanism, Microstructure and Properties." *Ph.D. Thesis, The Pennsylvania State University, Pennsylvania*.

Kalyoncu, R.S. (2001). "Slag iron and Steel." US Geological Survey Minerals Yearbook.

Kandhal, P.S., and Hoffman, G.L. (1997). "Evaluation of steel slag fine aggregate in hot-mix asphalt mixtures." *Transportation Resource and Recycling*, 1583, 28-36.

- Kawamura, M., ki Torii, K., Hasaba, S., Nicho, N. Oda, K. (1983). “Applicability of basic oxygen furnace slag as a concrete aggregate.” *ACI Materials Journal*, 79, 1123–1142.
- Klaiber, F.W., Thomas, T.L. and Lee, D.Y. (1979). “Fatigue behavior of air-entrained concrete: phase II.” Report, Ames, Iowa, Engineering Research Institute, Iowa State University.
- Kovtun, M. N., Kearsley, E. P. and Shekhovtsova, J. A. (2013). “Producing alkali-activated slag concrete in South Africa, *UKIERI Concrete Congress, Innovations in Concrete Construction*, 919-928.
- Krivenko, P. D. (1994). “Alkaline cements.” *In: Proceedings of 1<sup>st</sup> International Conference on Alkline Cement and Concrete, Kiev, Ukraine*, SRIBM, Kiev State Technical University, 11-14.
- Krizan, D. and Zivanovic, B. (2002). “effects of dosage and modulus of water glass on early hydration of alkali-slag cements.” *Cement and Concrete Research*, 32(8), 1181-1188.
- Kühl, H. (1930). “Zementchemie.” *Verlag Technik*, Berlin, Germany, Band III; 1958.
- Kumar, A.D. (2011). “Performance of geopolymer concrete mixes under fatigue and elevated temperature.” *M.Tech Thesis, Department of Civil Engineering, National Institute of Technology Karnataka, Surathkal*.
- Kumar, S.K., Kamalakara, G.K., Kamble, S. and Amaranth, M.S. (2012). “Fatigue analysis of high performance cement concrete for pavements using probabilistic approach.” *International Journal of Emerging Technology and Advanced Engineering*, 2(11), 640-644.
- Law, D.W, Adam, A.A., Molyneaux, T.K. and Patnaikuni, I. (2012). “Durability assessment of alkali activated slag (AAS) concrete.” *Materials and Structures*, 45, 1425–1437.
- Lee, M. K. and Barr, B.I.G. (2004). “An overview of the fatigue behaviour of plain and fiber reinforced concrete.” *Cement and Concrete Composites*, 26, 299-305.
- Lee, W.K.W., van Deventer, J.S.J. (2002). “The effect of ionic contaminants on the early-age properties of alkali-activated fly ash-based cements.” *Cement and Concrete Research*, 32, 577–584
- Li, Z., and Liu, S. (2007). “Influence of slag as additive on compressive strength of fly ash-based geopolymer.” *Journal of Materials in Civil Engineering*, 19(6), 470–474.



Li-Ping, G., Carpintre, A., Spagnoli, A., and Son, W. (2010). "Experimental and numerical investigation of fatigue damage propagation and life prediction of high performance concrete containing reactive mineral admixtures." *International Journal of Fatigue*, 32(2), 227-237.

Lu, C. (1992). "The research and the reactive products and mineral phase for FKJ cementitious material." In: *Proceedings of 9<sup>th</sup> International Congress on Chemical of Cement*, New Delhi, India, 319–24.

Malhotra, V. M. and Mehta, P. K. (1996). "Pozzolanic and Cementitious Materials." *Taylor & Francis ISBN 10: 2884492119 / 2-88449-211-9*.

Manjunath, G.S., Radhakrishna., Giridhar, C., and Jadhav, M. (2011). "Compressive strength development in ambient cured geo-polymer mortar." *International Journal of Earth Sciences and Engineering*, 4 (6), 830-834.

Manso, J. M., Polanco, J. A., Losan˜ez, M., and Gonzal˜ez, J.J. (2006). "Durability of concrete made with EAF slag as aggregate." *Cement and Concrete Composites*, 28, 528–534.

Marland, G., Boden, T.A., and Andres R. J., (2007). "Global, Regional, and National CO<sub>2</sub> Emissions." In *Trends: A Compendium of Data on Global Change*, Carbon Dioxide Information Analysis Center, Oak Ridge National Laboratory, U.S. Department of Energy, Oak Ridge, Tenn., U.S.A, 233-239.

Maslehuddin, M., Alfarabi, M., Sharif, M., Shameem, M., Ibrahim, M.S., and Barry. (2003). "Comparison of properties of steel slag and crushed limestone aggregate concretes." *Construction and Building Materials*, 17, 105–112.

Mathur, S., Soni, S.K., and Murty, M. (1999). "Utilization of industrial wastes in low-volume roads." *Transportation Resource and Recycling*, 1652, 246-256.

McGannon, H. (1971). "The making, shaping and treating of steel." *United States Steel Corporation, 9<sup>th</sup> Edition*.

Mehta, P. K. and Gjørv, O. E. (1974). "A new test for sulfate resistance of cements." *Journal of Testing and Evaluation, JTEVA*, 2(6), 510-514.

MII. (2015): <http://www.makeinindia.com/sector/roads-highways>.

Mindess, S., Young, J.F., and Darwin, D. (2003). "Concrete." *Second Edition, Prentice-Hall, Upper Saddle River, New Jersey*.

Mithun, B.M. and Narasimhan, M.C. (2015). "Performance of alkali activated slag concrete mixes incorporating copper slag as fine aggregates." *Journal of Cleaner Production*, 1–8. <http://dx.doi.org/10.1016/j.jclepro.2015.06.026>.

Mohammadi, Y., and Kaushik, S.K. (2005). "Flexural fatigue life distributions of plain and fibrous concrete at various stress levels." *Journal of Materials in Civil Engineering*, ASCE, 17, 650-658.

Morsy, M.S., Rashad, A.M., Shebl, S.S. (2008). "Effect of elevated temperature on compressive strength of blended cement mortar." *Building Research Journal*, 56(2–3), 173–185.

MORTH (2012) a: [www.morth.nic.in/annual report2011-12](http://www.morth.nic.in/annual%20report2011-12) last accessed Sept 2012.

MORTH (2012) b: [www.morth.nic.in/writereaddata/mainlinkFile/Passenger and freight Trafficdata.pdf](http://www.morth.nic.in/writereaddata/mainlinkFile/Passenger%20and%20freight%20Trafficdata.pdf)., last accessed Sept 2012.

MORTH (2012) c: [www.morth.nic.in/writereaddata/mainlinkFile/File420.pdf](http://www.morth.nic.in/writereaddata/mainlinkFile/File420.pdf)., last accessed Sept 2012.

MORTH (2014): <http://www.pppinindia.com/sector-highways.php>.

Motz, H., and Geiseler, J. (2001). "Products of steel slags: an opportunity to save natural resources." *Waste Management*, 21, 285–293.

Naik, T. R., Singh, S. and Congli, Ye. (1993). "Fatigue behavior of plain concrete made with or without fly ash." *A Progress Report Submitted to EPRI*.

Naik, T.R. (2008). "Sustainability of concrete" *Construction Practice Period on Structural Design and Construction*, ASCE, 98-103.

Naik, T.R., Singh, S. S., and Congli, Y. (1993). "Fatigue behavior of plain concrete made with or without fly ash." Center for By-Products Utilization University of Wisconsin-Milwaukee Department of Civil Engineering & Mechanics 3200 North Cramer Street Milwaukee, WI 53211.

Narasimhan, M.C., Nayak, G., Ajith, B.T. and Rao, M.K. (2011). "Development of alternative binders to portland cement concrete using fly ash and blast furnace slag: some experiences." In: *Proceedings of International UKIERI Concrete Congress, New Delhi, India*, 43-60.

Nath, P. and Sarker, P. K. (2012). "Geopolymer concrete for ambient curing condition." In: *Proceedings of Australasian Structural Engineering Conference: The past, present and future of Structural Engineering*. Barton, A.C.T.: Engineers Australia, 225-232.

National Slag Association. (2003) "Iron and Steel making Slag Environmentally Responsible Construction Aggregates." *NSA Technical Bulletin*. <http://www.nationalslag.org/steelslag.html>.

NRMCA. (2008). "Concrete CO<sub>2</sub> Fact Sheet, June 2008." *National Ready Mixed Concrete Association*, 13-32.

Oh, B.H., (1986). "Fatigue analysis of plain concrete in flexure", *Journal of Structural Engineering, ASCE*, 112 (2), 273-288.

Oh, B.H., (1991). "Cumulative damage theory of concrete under variable-amplitude fatigue loadings." *ACI Materials Journal*, 88(1), 41-48.

Pacheco-Torgal, F., Castro-Gomes, J. and Jalali, S. (2007). "Tungsten mine waste geopolymeric binder versus ordinary portland cement based concrete. abrasion and acid resistance", *International Conference on Alkaline Activated Materials – Research, Production and Utilization, Prague*, 693-702.

Pacheco-Torgal, F., Castro-Gomes, J., and Jalali, S. (2008), "Alkali-activated binders: A review: Part 1. Historical background, terminology, reaction mechanisms and hydration products", *Construction and Building Materials*, 22(7), 1305- 1314.

Pacheco-Torgal, F., Abdollahnejad, Z., Camões, A. F., Jamshidi, M. and Ding, Y. (2012). "Durability of alkali-activated binders: a clear advantage over Portland cement or an unproven issue?." *Construction and Building Materials*, 30, 400-405.

Palacios, M., and Puertas, Y.F. (2005). "Effect of superplasticizer and shrinkage-reducing admixtures on alkali-activated slag pastes and mortars." *Cement and Concrete Research*, 35, 1358–1367.

Palomo, A., Grutzeck, M.W. and Blanco, M.T. (1999). "Alkali-activated Fly Ashes: A cement for the future." *Cement and Concrete Research*, 29(8), 1323-1329.

Papayianni, I. and Anastasiou, E. (2010). "Utilization of electric arc furnace steel slags in concrete products." *In: Proceedings of 6<sup>th</sup> Euro Slag Conference*, Spain, Euroslag Publication, 5, 319-334.

Papayianni, I., Anastasiou, E. and Papachristoforou, M. (2010). "High performance concrete for pavements with steel slag aggregate." *In: Proceedings of 2<sup>nd</sup> International Conference on Sustainable Construction Materials and Technology*, Università Politecnica delle Marche, Ancona, Italy.

Patel, J.P. (2008). "Broader use of steel slag aggregates in concrete." *M.Tech.thesis*, Cleveland State University.

Pavlik, V. (1994). "Corrosion of hardened cement paste by acetic and nitric acids. Part I: Calculation of corrosion depth." *Cement and Concrete Research*, 24, 551–562.

Phull, Y.R. and Rao. J.P. (2007). "Assuring adequacy of concrete pavements: some essential needs." *Indian Highways*, 3, 9-19.

Popovics, S. (1992). "Concrete materials - properties, specifications and testing." *Publication SP-75, S.P. Shah, 2<sup>nd</sup> Ed., Detroit*.

PPPII. (2015): <http://www.pppinindia.com/sector-highways.php>.

Provis, J.L., Myers, R.J., White, C.E/, Rose, V., and van Deventer, J.S.J. (2012). "X-ray microtomography shows pore structure and tortuosity in alkali-activated binders." *Cement and Concrete Research*, 42(6), 855–864.

Provis, J.L. (2013). "Alkali-activated binders and concretes: The path to standardization geopolymer binder systems." *ASTM*, STP 1566, DOI: 10.1520/STP156620120078, 185-195.

Puertas, F. (1995). "Cementos de escoria activados alcalinamente: situación actual y perspectivas de futuro." *Materiales De Construcción*, 45 (239), 53-64.

Puertas, F., Martinez-Ramirez, S., Alonso, S. and Vazquez, T. (2000). "Alkali activated fly ash/slag cements: strength behaviour and hydration products." *Cement and Concrete Research*, 30(10), 1625-1632.

Purdon, A. (1940). "The action of alkalis on blast furnace slag." *Journal of the Society of Chemical Industry*. 59, 191–202.

Qureshi, M. N. and Ghosh, S. (2013). "Effect of curing conditions on the compressive strength and microstructure of alkali-activated ggbs paste." *International Journal of Engineering Science Invention*, 2(2), 24-31.

Rajamane, N.P. (2013). "Studies on development of ambient temperature cured fly ash and GGBS based geopolymer concretes." *PhD thesis*, VTU, Belgaum, India.

Ramakrishnan, V., Meyer, C., Naaman, A.E., Zhao, G., and Fang, L. (1996). "Cyclic behaviour, fatigue strength, endurance limit and models for fatigue behaviour of FRC." *In: Spon E, Spon FN, editors. High performance fibers reinforced cement composites*, 2, 101–148.

Rashad, A.M. and Zeedan S. R. (2011). "The effect of activator concentration on the residual strength of alkali-activated fly ash pastes subjected to thermal load." *Construction and Building Materials*, 25, 3098-3107.

- Rashad, A., M, Zeedan, S. R., Hassan, H. A. (2012). “ A preliminary study of autoclaved alkali-activated slag blended with quartz powder.” *Construction and Building Materials*, 33,70–77.
- Rashad, A. M. a (2013). “Utilizing of alkali activation fly ash concrete blended with slag.” *Iranian Journal of Material Science and Engineering*, 10(1), 57–64.
- Rashad, M.A. (2013) b. “A comprehensive overview about the influence of different additives on the properties of alkali-activated slag – a guide for civil engineer.” *Construction and Building Materials*, 47, 29–55.
- Rodriguez, E., Bernal, S., Guterrez M.R., and Puertas, Y.F. (2008). “Alternative concrete based on alkali-activated slag.” *Materiales De Construcción*, 58 (291), 53–67.
- Roy, D.M. and Silsbee, M.R. (1992). “Alkali activated materials – an overview.” *Proceedings of Materials Research Society Symposium*, 245, 153–164.
- Roy, D.M. (1999). “Alkali-activated cements opportunities and challenges.” *Cement and Concrete Research*, 29(2), 249–254.
- Roylance, D. (2001). “Fatigue.” <http://ocw.mit.edu/courses/materials-science-and-engineering/3-11-mechanics-of-materials-fall-1999/modules/fatigue.pdf>.
- Sakin, R. and Ay, I. (2008). “Statistical analysis of bending fatigue life data using Weibull distribution in gala-fiber reinforced polyester composites.” *Materials and Design*, 29, 1170-1181.
- Sakulich, A. R., Anderson, E., Schauer,C. and Barsoum, M.W. (2009). “Mechanical and microstructural characterization of an alkali-activated slag/limestone fine aggregate concrete.” *Construction and Building Materials*, 23(8), 2951–2957.
- Sharma, B.M., Sitaramanjanyalu, K., and Kanchan, P.K. (1995). “Effect of vehicle axle loads on pavement performance.” Road Transport Technology-4, University of Michigan Transportation Research Institute. Ann Arbor, 263-272.
- Shekarchi, M., Alizadeh, R., Chini, M., Ghods, P., Hoseini, M., and Montazer, S. (2003). “ Study on electric arc furnace slag properties to be used as aggregates in concrete.” *In: Proceedings of 6<sup>th</sup> CANMET/ACI International Conference on Recent Advances in Concrete Technology*, Bucharest, Romania, 451-464.
- Shekhovtsova, J., Kearsley, E. P. and Kovtun, M. (2014). “Effect of activator dosage, water-to-binder-solids ratio, temperature and duration of elevated temperature curing on the compressive strength of alkali activated fly ash cement pastes.” *Journal of the South African Institution of Civil Engineering*, 56 (3), 44–52.

- Shi, C., and Li, Y. (1989). "Investigation on some factors affecting the characteristics of alkali-phosphorus slag cement." *Cement and Concrete Research*, 19(4), 527-533.
- Shi, C. (1996). "Strength, pore structure and permeability of alkali-activated slag mortars." *Cement and Concrete Research*, 26 (12), 1789–1799.
- Shi, C. (2004). "Steel slag- its production, processing, characteristics and cementitious properties." *Journal of Materials in Civil Engineering, ASCE*, 16(3), 230-236.
- Shi, C., Krivenko, P.V. and Roy, D. (2006). "Alkali-Activated Cements and Concretes." *Taylor&Francis*, ISBN 0-415-70004-3.
- Silva, A.C.R. Silva, F.J. and Thaumaturgo, C. (2004). "Fatigue behavior of geopolymer cement concrete."
- Singh, S.P. and Kaushik, S.K. (2001). "Flexural fatigue analysis of steel fibre reinforced concrete." *ACI Materials Journal*, 98 (4), 306-312.
- Sofi, M., van Deventer, J. S. J., Mendis, P. A., and Lukey, G. C. (2007). "Engineering properties of inorganic polymer concretes (IPCs)," *Cement and Concrete Research*, 37, 251–257.
- SOR. (2015): Schedule of Rates (SOR) 2014-2015, Mangalore Circle, Public Works Department, and Karnataka. ISO 9001-2008 certified.
- Sravanthi, P., and Paramita, M. (2013). "Role of slag in microstructural development and hardening of fly ash-slag geopolymer." *Cement and Concrete Research*, 43, 70–80.
- Taha, R., Al-Nuaimi, N., Kilayli, A. and Salem, A.B. (2014). "Use of local discarded materials in concrete." *International Journal of Sustainable Built Environment*, 3, 35–46.
- Thokchom, S., Ghosh, P. and Ghosh, S. (2011). "Durability of fly ash geopolymer mortars in nitric acid–effect of alkali (Na<sub>2</sub>O) content, *Journal of Civil Engineering and Management*, 17(3), 393-399.
- Tripathy, P.S. and Mukherjee, S.N. (1997). "Perspectives on bulk use of fly ash." *Allied Publishers Limited, New Delhi*.
- van Der Laan S.R., van Hoek C.J.G., van Zomeren., Comans R.N.J., Kobesen J.B.A., Broersen P.G.J. (2008). "Chemical reduction of CO<sub>2</sub> to carbon at ambient conditions during artificial weathering of converter steel slag while improving environmental properties." *Proceedings of 2<sup>nd</sup> International Conference on Accelerated Carbonation for Environmental and Material Engineering, Rome, Italy*, 229–238.

- Varaprasad, G. (2006). "Eco-friendly geopolymer concrete – A preliminary study." *M.Tech Thesis, Department of Civil Engineering, National Institute of Technology Karnataka, Surathkal.*
- Wallah, S. E., and Rangan, B. V. (2006). "Low-calcium fly ash-based geopolymer concrete: long-term properties." *Research Report-GC2*, Curtin University, Australia. 76-80.
- Wang, S.D, Scrivener, K.L. and Pratt, P.L. (1994). "Factors affecting the strength of alkali-activated slag." *Cement and Concrete Research*, 24(6), 1033–1043.
- Wang, S.D. and Scrivener, K.L. (1995). "Hydration products of alkali activated slag cement." *Cement and Concrete Research*, 25, 561–571.
- Wang, A., Zhang, C. and Sun, W. (2003). "Fly ash effects: I. the morphological effect of fly ash." *Cement and Concrete Research*, 33(12), 2023–2029.
- Wardhono, A., Law, D.W and Molyneaux, T.K. (2015). "Long Term Performance of Alkali Activated Slag Concrete." *Journal of Advanced Concrete Technology*, 13, 187-192.
- Yang, K.H., Song, J.K., Song, K. (2013). "Assessment of CO<sub>2</sub> reduction of alkali-activated concrete." *Journal of Cleaner Production*, 39, 265-272.
- Yang Yang, K., Song, J., Lee, E. and Ashrou, A. F. (2008). "Properties of cementless mortars activated by sodium silicate." *Construction and Building Materials*, 22, 1981–1989.

## APPENDIX - I

### Mix Design method for OPC Concrete

For the concrete mix, OPC 43 grade cement was used. Sand conforming to Zone - II was used. Locally available crushed stone granite aggregates of 20 mm down size was used. For the design IS code method was followed (IS 10262 – 2009, IS 456-2009).

#### **Input parameters**

Derived characteristics strength of concrete $f_{ck}$	=	40 MPa
Grade of cement	=	43
Specific gravity of cement	=	3.14
Specific gravity of sand	=	2.64
Specific gravity of coarse aggregate	=	2.69
Maximum size of aggregate	=	20mm
Slump in mm	=	25-50

#### **Estimation of ingredients for M<sub>40</sub> grade concrete**

##### **(1) Target mean strength of concrete (TMS)**

$$\text{TMS} = f_{ck} + 1.65 * \text{S.D} = 40 + 1.65 * 5 = 48.25 \text{ N/mm}^2$$

(S.D =Standard Deviation, taken from Table 1 of IS: 10262:2009)

##### **(2) Selection of water cement ratio**

For Extreme exposure condition, the water cement ratio = 0.40 (From Table 5, IS: 456 -2009)

##### **(3) Selection of Water content**

From Table 2 of IS 10262 – 2009, Max water content for 20mm aggregate = 186 litre (for 25 to 50mm slump range)

Based on trials, with 0.4% super plasticizer, water content reduced to = 170 litre

Therefore, Water content (w) = 170 kg/m<sup>3</sup>



#### **(4) Calculation for cement content**

Water-cement ratio = 0.40

Cement content =  $170/0.4 = 425 \text{ kg/m}^3$

#### **(5) Proportion of volume of coarse aggregate and fine aggregate content**

Coarse aggregate content as percent of aggregate by absolute volume = 62% (0.62) (From Table 3, IS 10262 – 2009, for zone II sand and for water/binder ratio of 0.50)

For change in water cement ratio following adjustment is required for water/binder ratio of 0.40.

##### **Volume adjustment required for coarse aggregates**

For decrease in water cement ratio by 0.1 (0.5-0.4), the coarse aggregate volume content may be increased +.02. in total volume aggregates (From section 4.4, IS 10262 - 2009)

Therefore, required Coarse aggregate content as percentage of total aggregate by absolute volume, =  $0.62+0.02 = 0.64$ .

#### **(6) Mix Calculations**

(a) Volume of concrete =  $1 \text{ m}^3$

(b) Volume of cement = (Mass of cement/specific gravity of cement)\*1/1000  
=  $(425/3.140)/1000$   
=  $0.135 \text{ m}^3$

(c) Volume of super plasticizer (0.4% by mass of cement)  
= (Mass of chemical admixture/specific gravity of chemical admixture)\*1/1000  
=  $(1.7/1.20)$   
=  $0.00141 \text{ m}^3$

Water to be added = 170 – water present in super plasticizer  
=  $170 - (1.7*0.6) = 169 \text{ litres}$

(d) Volume of water = (Mass of water/sp gravity of water)\*1/1000  
=  $169/1000 = 0.169 \text{ m}^3$

(e) Volume of all in aggregate =  $[a-(b + c+ d)]$   
=  $1-(0.135+0.0014+0.169)$

$$= 0.694 \text{ m}^3$$

(f) Mass of coarse aggregate

$$= e * \text{volume of coarse aggregate} * \text{specific gravity of coarse aggregate} * 1000$$

$$= 0.694 * 0.64 * 2.69 * 1000$$

$$= 1195.6 \text{ kg/m}^3$$

(g) Mass of fine aggregate

$$= e * \text{volume of fine aggregate} * \text{specific gravity of fine aggregate} * 1000$$

$$= 0.694 * 0.36 * 2.64 * 1000$$

$$= 659.5 \text{ kg/m}^3$$

**(7) Mix proportions**

Ingredients of mix	Cement (kg/m <sup>3</sup> )	Fine aggregate (kg/m <sup>3</sup> )	Coarse aggregate (kg/m <sup>3</sup> )	Water (kg/m <sup>3</sup> )	Super Plastisizer (kg/m <sup>3</sup> )
	425	660	1196	169	1.7

## APPENDIX - II

### Sample Mix Design for Alkali Activated Slag Concrete

For AASC mix 100% GGBFS by weight is replaced by weight of OPC and alkali solution is used instead of only water.

#### Input parameters

Derived characteristics strength of concrete $f_{ck}$	=	40 MPa
Specific gravity of GGBS,	=	2.9
Specific gravity of sand	=	2.64
Specific gravity of coarse aggregate	=	2.69
Specific gravity of alkali solution (4%Na <sub>2</sub> O, Ms 1.25)	=	1.22
Maximum size of aggregate	=	20mm
Slump in mm	=	25-50 mm

#### Estimation of ingredients for AASC

##### (1) Target mean strength of concrete (TMS)

$$\text{TMS} = f_{ck} + 1.65 * S = 40 + 1.65 * 5 = 48.25 \text{ N / mm}^2$$

##### (2) Based on trials, Na<sub>2</sub>O Dosage required: 4%

$$\text{Activator Modulus (Ms)} : 1.25$$

##### (3) Calculations for alkali solution

Composition of Sodium silicate solution

$$\text{Na}_2\text{O} = 14.7\%,$$

$$\text{SiO}_2 = 32.8\%,$$

$$\text{Water} = 52.5\% \text{ by weight}$$

Hence, 1 kg of sodium silicate contains

$$\text{Na}_2\text{O} = 0.147 \text{ kg},$$

$$\text{SiO}_2 = 0.328 \text{ kg}$$

$$\text{Water} = 0.525 \text{ kg}.$$

Ms of sodium silicate as obtained =  $\text{SiO}_2/\text{Na}_2\text{O} = 32.8/14.7 = 2.23$

The molecular weight of NaOH is 40 and atomic weight of Na=23, O=16, H=1.

$$\begin{aligned}\text{NaOH flakes having Na}_2\text{O fraction} &= (2*\text{Na} + \text{O})/2*(\text{Na} + \text{O} + \text{H}) \\ &= (2*23 + 16)/2*(23 + 16 + 1) \\ &= 62/80 = \mathbf{0.775}\end{aligned}$$

Therefore, 1kg of NaOH contains 0.775 kg of  $\text{Na}_2\text{O}$

$\text{Na}_2\text{O}$  required by weight for 425 kg of GGBFS at 4% =  $425*0.04 = \mathbf{17 \text{ kgs}}$

$\text{SiO}_2$  required by weight for 425 kg of GGBFS to maintain Ms of 1.25 =  $\text{SiO}_2/\text{Na}_2\text{O}$   
= 1.25

$$\begin{aligned}\text{Therefore SiO}_2 \text{ required} &= 1.25*\text{Na}_2\text{O} \\ &= 1.25*17\end{aligned}$$

Therefore  $\text{SiO}_2$  required = **21.25 kgs**

Amount of Sodium silicate solution required for 21.25kg for  $\text{SiO}_2$

$$\begin{aligned}&= \text{SiO}_2 \text{ required} / \text{SiO}_2 \text{ present in sodium silicate solution} \\ &= 21.25/0.328 = \mathbf{64.78 \text{ kgs}}\end{aligned}$$

$\text{Na}_2\text{O}$  present in 64.78 kg sodium silicate solution =  $64.78*0.148 = 9.58 \text{ kg}$

Hence  $\text{Na}_2\text{O}$  required from NaOH =  $17 - 9.58 = 7.41 \text{ kg}$

NaOH flakes required =  $7.41/0.775 = \mathbf{9.60 \text{ kgs}}$

Extra water required to make w/b ratio of 0.4 =  $170 - \text{water present in sodium silicate}$

$$= 170 - (64.7*0.525)$$

= **136 kgs**

Alkali activator solution =  $64.78 + 9.60 + 136 = \mathbf{210.4 \text{ kgs}}$

#### (4) Mix Calculations

(a) Volume of concrete =  $1 \text{ m}^3$

(b) Volume of GGBS =  $(\text{Mass of GGBS} / \text{specific gravity of GGBS}) * 1/1000$   
=  $(425/2.9)/1000$   
=  $0.146 \text{ m}^3$

(c) Volume of Alkali Solution

$$\begin{aligned}
&= (\text{Mass of Alkali Solution}/\text{specific gravity of Alkali Solution}) * 1/1000 \\
&= (210.4/1.22)/1000 \\
&= 0.172 \text{ m}^3
\end{aligned}$$

(d) Volume of all in aggregate = [a-(b+c)]

$$\begin{aligned}
&= 1-(0.146+0.172) \\
&= 0.682 \text{ m}^3
\end{aligned}$$

(e) Mass of coarse aggregate

$$\begin{aligned}
&= d * \text{volume of coarse aggregate} * \text{specific gravity of coarse aggregate} * 1000 \\
&= 0.682 * 0.64 * 2.69 * 1000 \\
&= 1172.1 \text{ kg/m}^3
\end{aligned}$$

(f) Mass of fine aggregate (sand)

$$\begin{aligned}
&= d * \text{volume of fine aggregate} * \text{specific gravity of fine aggregate} * 1000 \\
&= 0.682 * 0.36 * 2.64 * 1000 \\
&= 647 \text{ kg/m}^3
\end{aligned}$$

(g) Mass of coarse aggregates ( 75% natural aggregates +25% steel slag)

Volume of total aggregates \* volume of coarse aggregates \* 0.75 \* specific gravity of natural coarse aggregates aggregate\* 1000

Mass of natural coarse aggregates =  $0.682 * 0.64 * 0.75 * 2.64 * 1000 = 879 \text{ kg/m}^3$

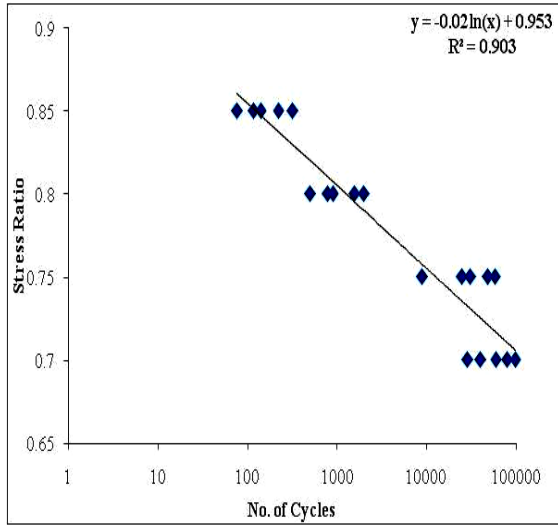
Mass of steel slag =  $0.682 * 0.64 * 0.25 * 3.35 * 1000 = 365 \text{ kg/m}^3$

Total mass of fine aggregate =  $1244 \text{ kg/m}^3$

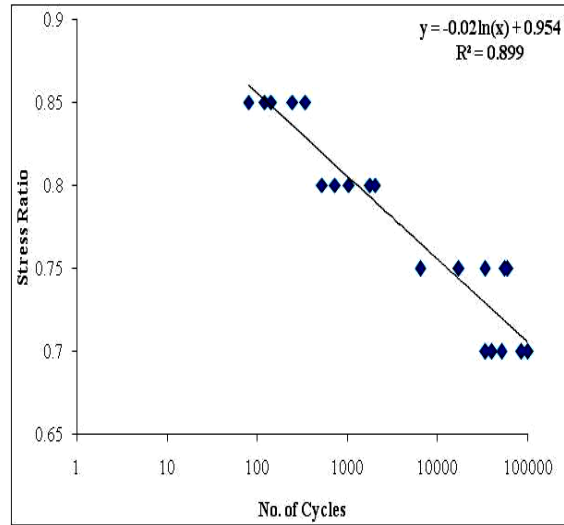
**(5) Mix proportions (all quantities in kg/m<sup>3</sup>)**

Ingredients of mix	GGBS	Sand	Coarse aggregate	Water	Sodium Silicate	NaOH
	425	647	1172	136	64.78	9.6

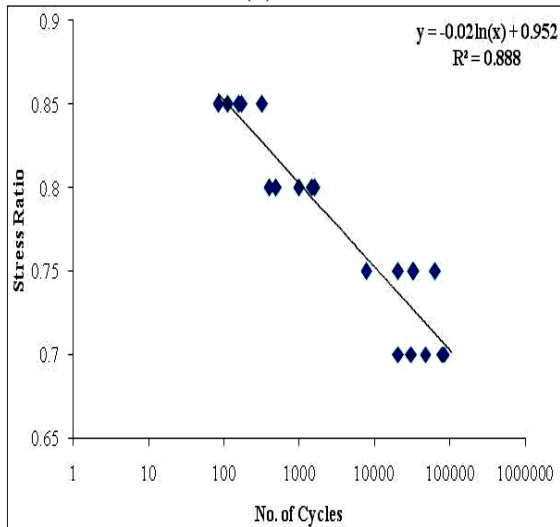
### APPENDIX III



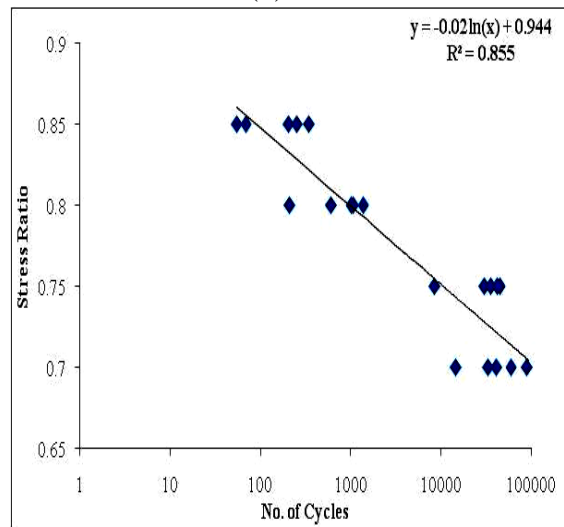
(a) OPCC



(b) 4-B-0

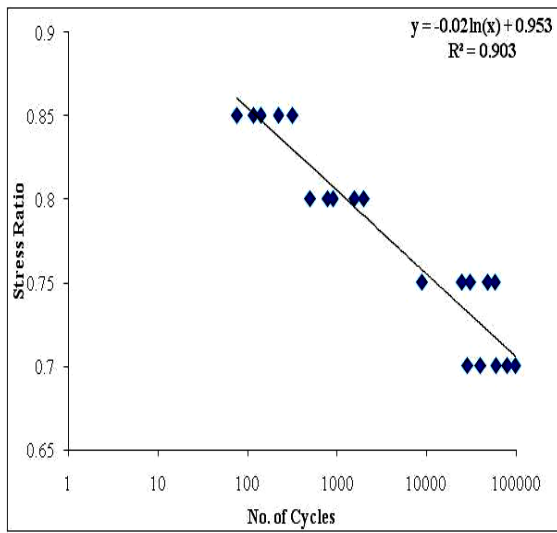


(c) 4-B-50

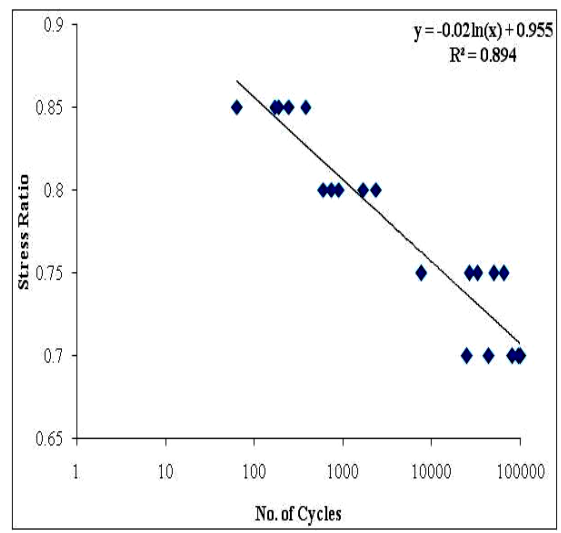


(d) 4-B-100

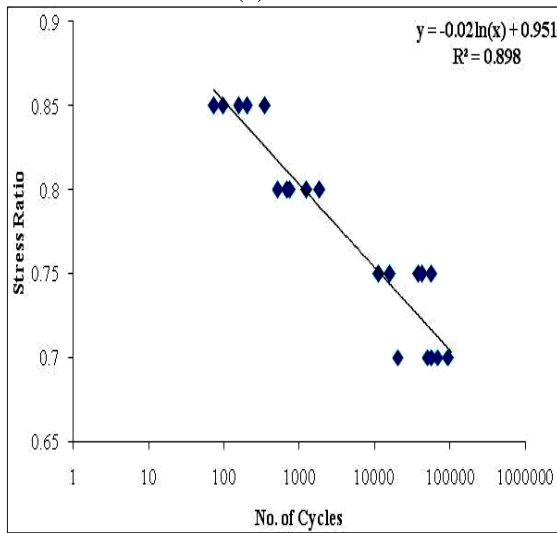
Fig.A.3.1 S-N curve for AASFC (75:25) mix with/without steel slag aggregates



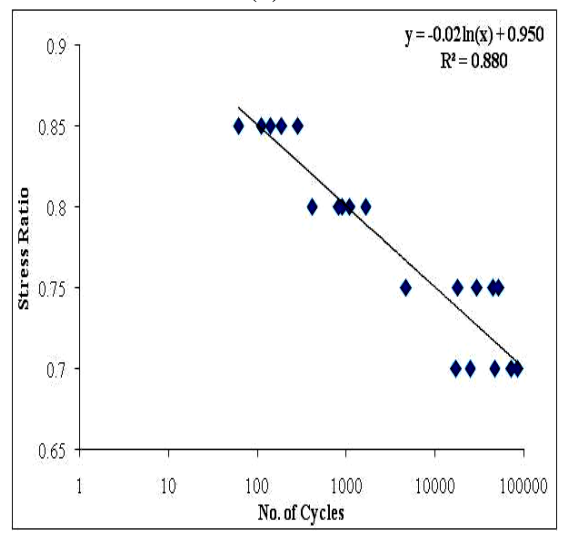
(a) OPCC



(b) 4.5-C-0

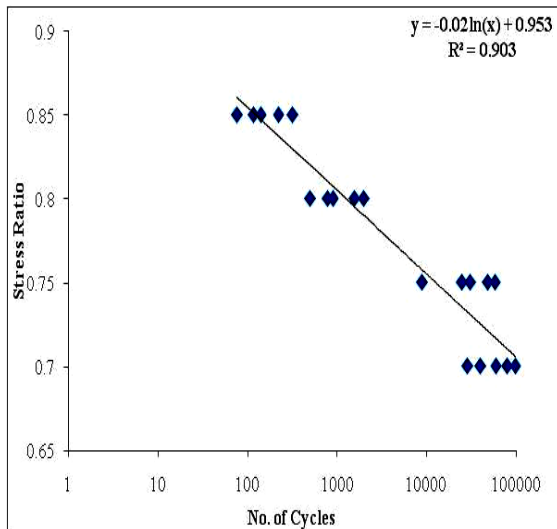


(c) 4.5-C-50

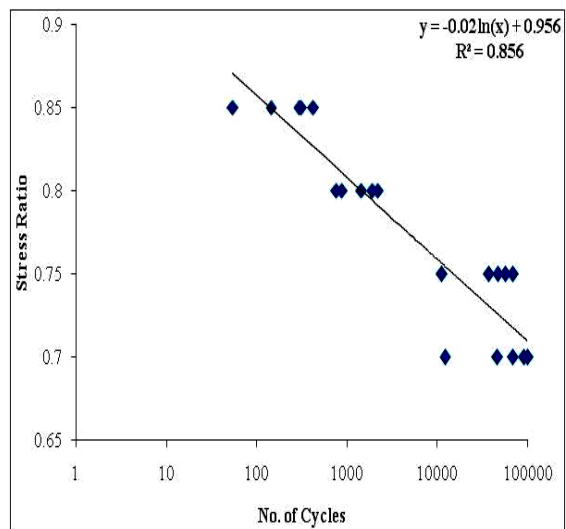


(d) 4.5-C-100

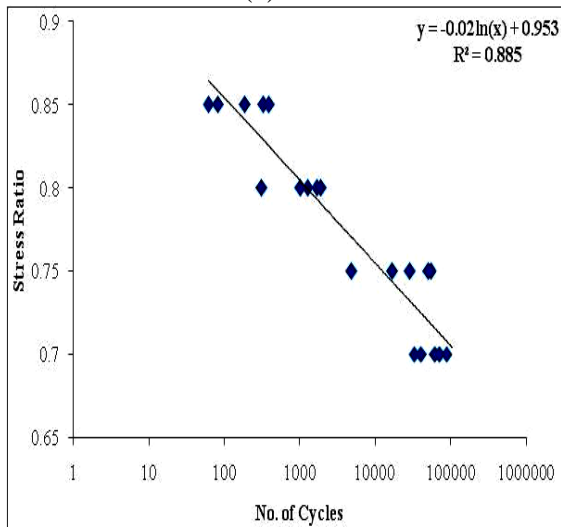
Fig.A.3.2 S-N curve for AASFC (50:50) mix with/without steel slag aggregates



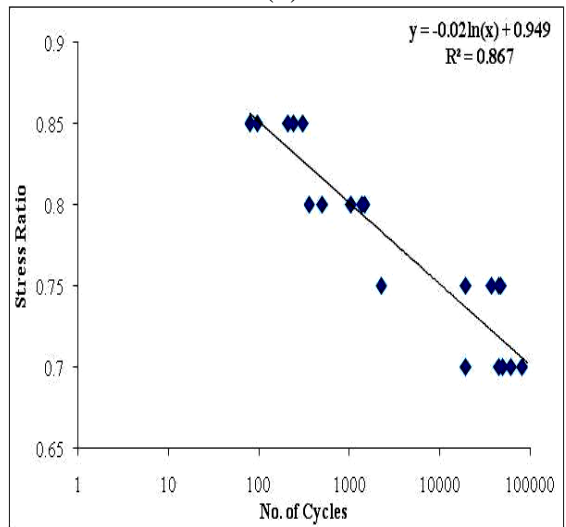
(a)OPCC



(b)5.5-D-0



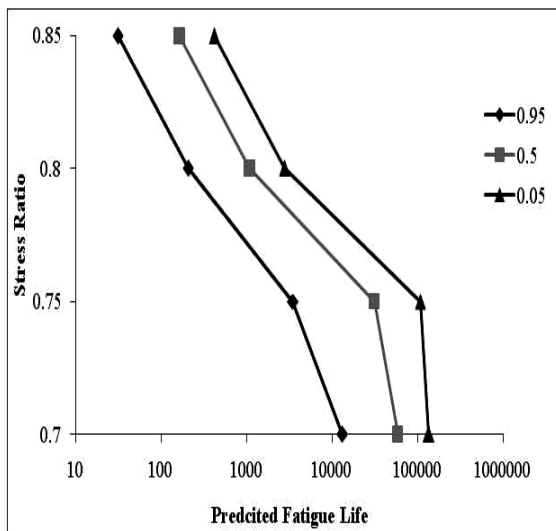
(c) 5.5-D-50



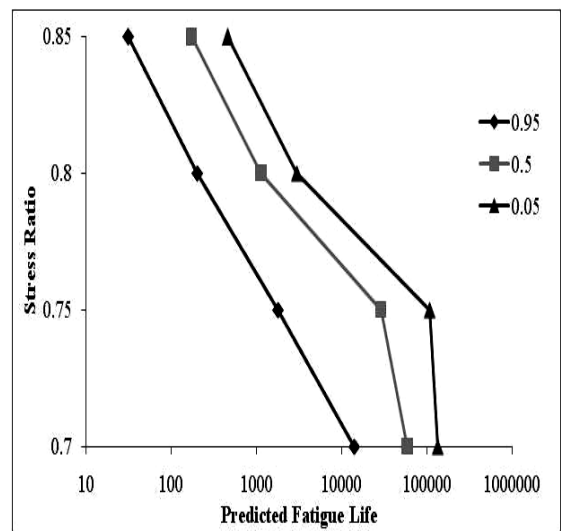
(d) 5.5-D-100

Fig.A.3.3 S-N curve for AASFC (25:75) mix with/without steel slag aggregates

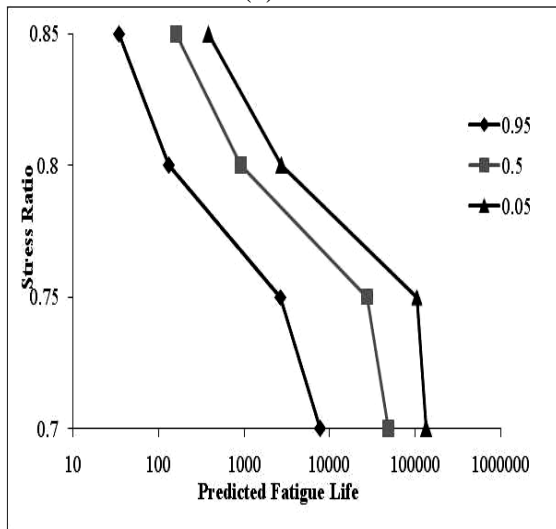




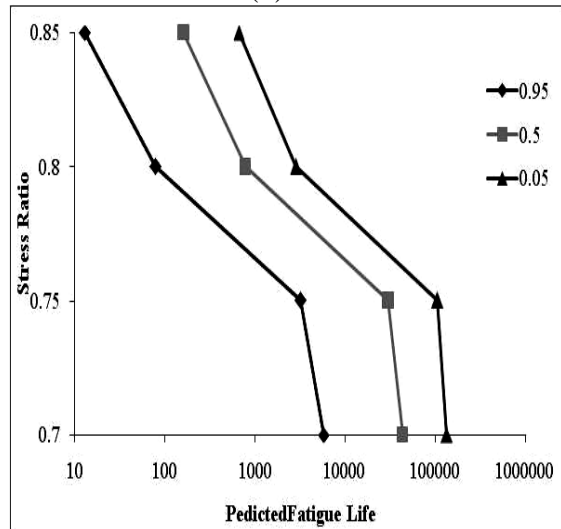
(a) OPCC



(b) 4-B-0

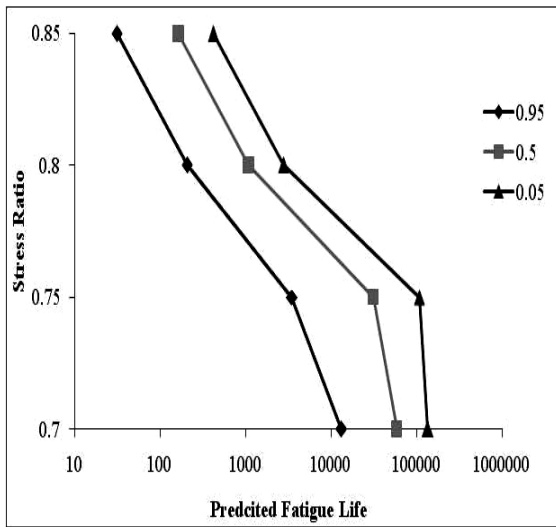


(c) 4-B-50

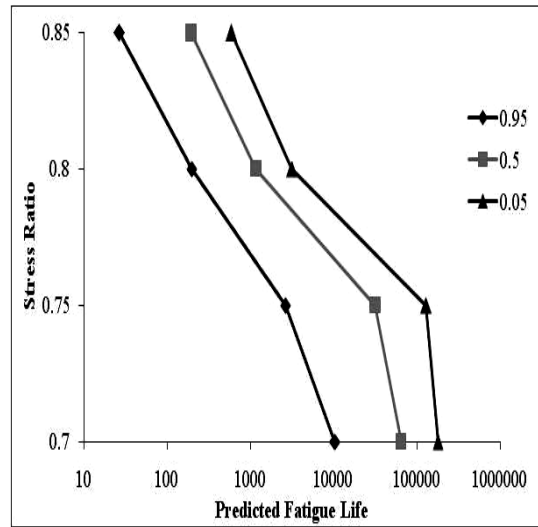


(d) 4-B-100

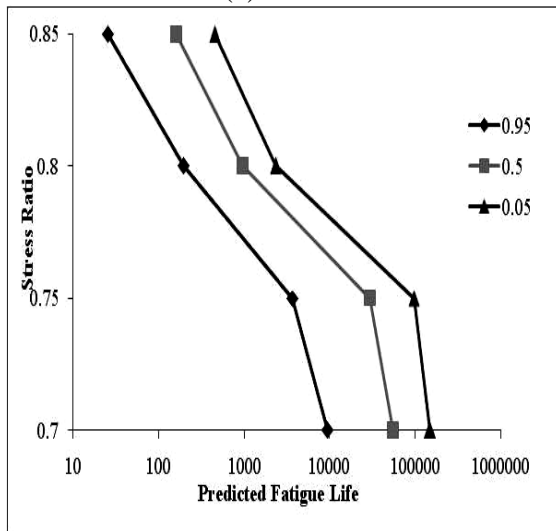
Fig.A.3.4 Predicted fatigue lives at different survival probabilities for AASFC (75:25) mix



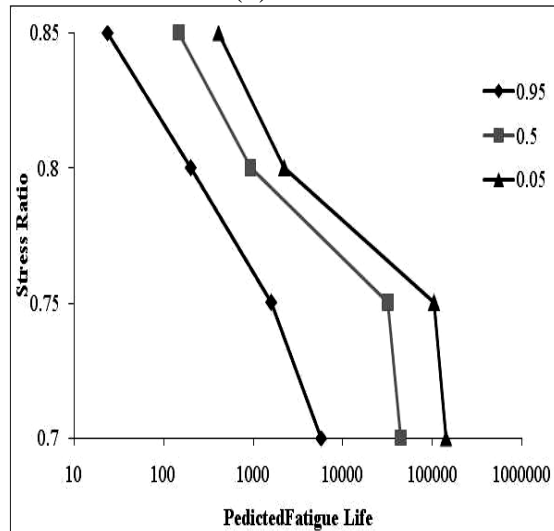
(a) OPCC



(b) 4.5-C-0



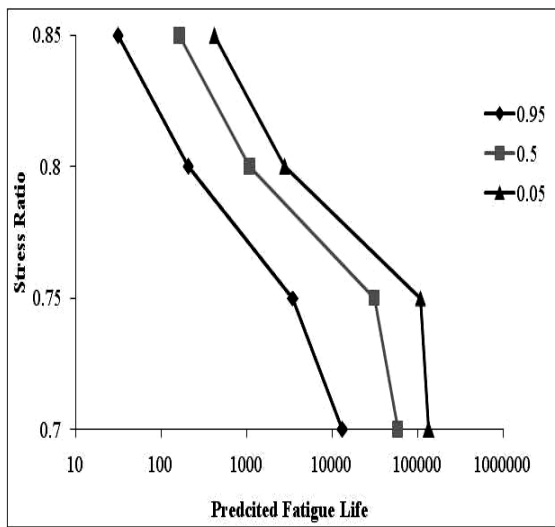
(c) 4.5-C-50



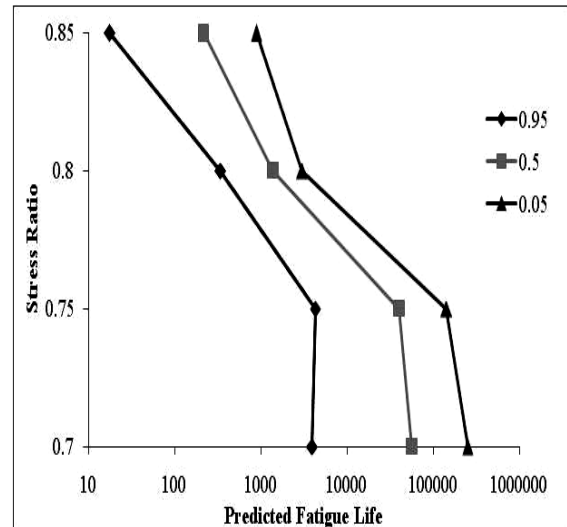
(d) 4.5-C-100

Fig.A.3.5 Predicted fatigue lives at different survival probabilities for AASFC (50:50)

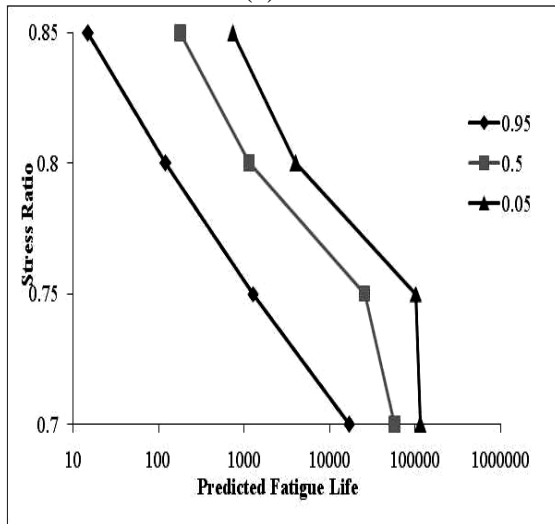
mix



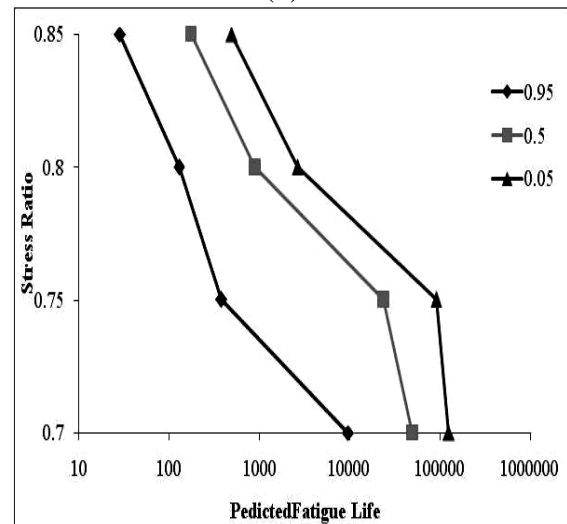
(a) OPCC



(b) 5.5-D-0



(c) 5.5-D-50



(d) 5.5-D-100

Fig.A.3.6 Predicted fatigue lives at different survival probabilities for AASFC (25:75)

mix

## APPENDIX IV

Table A 4-1 Detailed calculation for total EE per kilometer of highway

Ingredients	EE (MJ)	OPCC	4-A-0	4-A-50	4-A-100	4-B-0	4-B-50	4-B-100	4.5-C-0	4.5-C-50	4.5-C-100	5.5-D-0	5.5-D-50	5.5-D-100
GGBFS	1.6	0	680	680	680	510.4	510.4	510.4	340	340	340	169.6	169.6	169.6
FA	0.1	0	0	0	0	10.6	10.6	10.6	21.25	21.25	21.25	31.9	31.9	31.9
OPC	4.8	2040	0	0	0	0	0	0	0	0	0	0	0	0
NaOH	20.5	0	197.6	197.6	197.6	197.6	197.6	197.6	215.7	215.7	215.7	202.5	202.5	202.5
LSS	10.2	0	660.8	660.8	660.8	660.8	660.8	660.8	743.4	743.4	743.4	1090.4	1090.4	1090.4
Water	0.2	33.8	27.2	27.2	27.2	27.2	27.2	27.2	24.6	24.6	24.6	20.2	20.2	20.2
plasticizer	11.5	19.55	0	0	0	0	0	0	0	0	0	0	0	0
Sand	0.081	53.5	52.4	52.4	52.4	51.5	51.5	51.5	50.9	50.9	50.9	47.2	47.2	47.2
Steel slag	0	0	0	0	0	0	0	0	0	0	0	0	0	0
Coarse Aggregate	0.083	99.3	97.3	48.6	0.0	95.6	47.8	0.0	93.5	46.8	0.0	93.0	46.6	0.0
EE /m <sup>3</sup>		2246.1	1715.3	1666.6	1618.0	1553.7	1505.9	1458.1	1489.3	1442.6	1395.8	1654.9	1608.4	1561.8
Total quantity of concrete per km =4200 kg/m <sup>3</sup>														
EE /m <sup>3</sup> x 4200 kg/m <sup>3</sup>		9433527.6	7204088	6999808	6795529	6525574	6324780	6123986	6255039	6058777	5862167	6950521	6755305	6559741
Processing	375	1575000	1575000	1575000	1575000	1575000	1575000	1575000	1575000	1575000	1575000	1575000	1575000	1575000
Curing water for OPC	0.2	980000												
<b>Total EE per km</b>		<b>11988527</b>	<b>8779088</b>	<b>8574808</b>	<b>8370529</b>	<b>8100574</b>	<b>7899780</b>	<b>7698986</b>	<b>7830039</b>	<b>7633777</b>	<b>7437167</b>	<b>8525521</b>	<b>8330305</b>	<b>8134741</b>

*Note: water for curing is calculated by considering 5cm flooding of water*

Table A 4-2 Detailed calculation for total ECO<sub>2e</sub> per kilometer of highway

Ingredient	ECO <sub>2e</sub> (kgCO <sub>2e</sub> )	OPCC	4-A-0	4-A-50	4-A-100	4-B-0	4-B-50	4-B-100	4.5-C-0	4.5-C-50	4.5-C-100	5.5-D-0	5.5-D-50	5.5-D-100
GGBFS	0.083	0.0	35.3	35.3	35.3	26.5	26.5	26.5	17.6	17.6	17.6	8.8	8.8	8.8
FA	0.01	0.0	0.0	0.0	0.0	1.1	1.1	1.1	2.1	2.1	2.1	3.2	3.2	3.2
OPC	0.93	395.3	0.0	0.0	0.0	0.0	0.0	0.0	0.0	0.0	0.0	0.0	0.0	0.0
NaOH	3.2	0.0	30.8	30.8	30.8	30.8	30.8	30.8	33.7	33.7	33.7	31.6	31.6	31.6
LSS	2	0.0	129.6	129.6	129.6	129.6	129.6	129.6	145.8	145.8	145.8	213.8	213.8	213.8
Water	0.0008	0.1	0.1	0.1	0.1	0.1	0.1	0.1	0.1	0.1	0.1	0.1	0.1	0.1
plasticizer	0.6	1.02	0	0	0	0	0	0	0	0	0	0	0	0
Sand	0.0051	3.4	3.3	3.3	3.3	3.2	3.2	3.2	3.2	3.2	3.2	3.0	2.9733	2.9
Steel slag	0	0.0	0.0	0.0	0.0	0.0	0.0	0.0	0.0	0.0	0.0	0.0	0	0
Coarse Aggregate	0.0048	5.7	5.6	2.8	0.0	5.5	2.8	0.0	5.4	2.7	0.0	5.4	2.6	0
ECO <sub>2e</sub> /m <sup>3</sup>		405.5	204.7	201.9	199.1	196.8	194.1	191.3	207.9	205.2	202.5	265.8	263.1	260.4
Total quantity of concrete per km =4200 kg/m <sup>3</sup>														
ECO <sub>2e</sub> /m <sup>3</sup> x 4200 kg/m <sup>3</sup>		1703150. 4	859811. 8	847998. 1	836184. 3	826673. 4	815061. 2	803449. 1	873168. 7	861818. 6	850448.3	1116523. 4	1105233. 8	1093924
Processing	9.5	39900.0	39900.0	39900.0	39900.0	39900.0	39900.0	39900.0	39900.0	39900.0	39900.0	39900.0	39900	39900
Curing water for OPC	0.0008	3920.0												
<b>Total ECO<sub>2e</sub> per km</b>		<b>1746970</b>	<b>899711</b>	<b>887898</b>	<b>876084</b>	<b>866573</b>	<b>854961</b>	<b>843349</b>	<b>913068</b>	<b>901718</b>	<b>890348</b>	<b>1156423</b>	<b>1145133</b>	<b>1133824</b>

Note: \* water for curing is calculated by considering 5cm flooding of water

Table A 4-3 Detailed calculation for total cost per kilometer of highway

Ingredient	Cost (Rs)	OPCC	4-A-0	4-A-50	4-A-100	4-B-0	4-B-50	4-B-100	4.5-C-0	4.5-C-50	4.5-C-100	5.5-D-0	5.5-D-50	5.5-D-100
GGBFS	4	0	1700	1700	1700	1276	1276	1276	850	850	850	424	424	424
FA	0.125	0	0	0	0	13.25	13.25	13.25	26.5625	26.5625	26.5625	39.875	39.875	39.875
OPC	8	3400	0	0	0	0	0	0	0	0	0	0	0	0
NaOH	45	0	433.8	433.8	433.8	433.8	433.8	433.8	473.4	473.4	473.4	444.6	444.6	444.6
LSS	14	0	906.92	906.92	906.92	906.92	906.92	906.92	1020.32	1020.32	1020.32	1496.6	1496.6	1496.6
Water	0.05	8.45	6.8	6.8	6.8	6.8	6.8	6.8	6.15	6.15	6.15	5.05	5.05	5.05
plasticizer	175	297.5	0	0	0	0	0	0	0	0	0	0	0	0
Sand	1	660	647	647	647	636	636	636	628	628	628	583	583	583
Steel slag	0.05	0	0	36.5	73	0	35.85	71.7	0	35.1	70.2	0	34.9	69.8
Coarse Aggregate	1.3	1554.8	1523.6	761.8	0	1497.6	748.8	0	1465.1	733.2	0	1457.3	729.3	0
Cost /m <sup>3</sup>		5920.7	5218.1	4492.8	3767.5	4770.3	4057.42	3344.4	4469.5	3772.7	3074.6	4450.4	3757.3	3062.9
Total quantity of concrete per km =4200 kg/m <sup>3</sup>														
Cost /m <sup>3</sup> x 4200 kg/m <sup>3</sup>		22617798	19485312	17146752	14808192	18019512	15720768	13422024	17096058	14849394	12598530	17480274	15245538	13006602
Processing	1250	5250000	5250000	5250000	5250000	5250000	5250000	5250000	5250000	5250000	5250000	5250000	5250000	5250000
Curing water for OPC*	49 L lit	245000												
<b>Total Cost per km</b>		<b>30362150</b>	<b>27166104</b>	<b>24119844</b>	<b>21073584</b>	<b>25285554</b>	<b>22291164</b>	<b>19296774</b>	<b>24022037</b>	<b>21095477</b>	<b>18163457</b>	<b>23941785</b>	<b>21030765</b>	<b>18114285</b>

Note: \* water for curing is calculated by considering 5cm flooding of water

## APPENDIX V

### Sample Pavement Design for AASC mix.

A cement concrete pavement is to be designed for a four-lane divided National Highway with two lanes in each direction in the state of Bihar. Design the pavement for a period of 30 years. Lane width = 3.5 m; transverse joint spacing = 4.5 m. It is expected that the road will carry, in the year of completion of construction, about 3000 commercial vehicles per day in each direction. Axle load survey of commercial vehicles indicated that the percentages of front single (steering) axle, rear single axle, rear tandem axle and rear tridem axle are 45 percent, 15 percent, 25 percent and 15 percent respectively. The percentage of commercial vehicles with spacing between the front axle and the first rear axle less than 4.5 m is 55 percent. Traffic count indicates that 60 percent of the commercial vehicles travel during night hours (6 PM to 6 AM). Details of axle load spectrum of rear single, tandem and tridem axles are given in Table 1. Front (steering) axles are not included. The average number of axles per commercial vehicle is 2.35 (due to the presence of multi-axle vehicles). Effective CBR of compacted subgrade = 8 percent.

Table A-5-1 Axle Load Spectrum

Axle Load Spectrum Data								
Rear Single Axle			Rear Tandem Axle			Rear Tridem Axle		
Load Group (kN)	Mid-Point of Load Group (kN)	Frequency (%)	Load Group (kN)	Mid-Point of Load Group (kN)	Frequency (%)	Load Group (kN)	Mid-Point of Load Group (kN)	Frequency (%)
185-195	190	18.15	380 - 400	390	14.5	530-560	545	5.23
175-185	180	17.43	360 - 380	370	10.5	500-530	515	4.85
165-175	170	18.27	340 - 360	350	3.63	470-500	485	3.44
155-165	160	12.98	320 - 340	330	2.5	440-470	455	7.12
145-155	150	2.98	300 - 320	310	2.69	410-440	425	10.11
135-145	140	1.62	280 - 300	290	1.26	380-410	395	12.01
125-135	130	2.62	260 - 280	270	3.9	350-380	365	15.57
115-125	120	2.65	240 - 260	250	5.19	320-350	335	13.28
105-115	110	2.65	220 - 240	230	6.3	290-320	305	4.55
95-105	100	3.25	200 - 220	210	6.4	260-290	275	3.16
85-95	90	3.25	180 - 200	190	8.9	230-260	245	3.1
< 85	80	14.15	< 180	170	34.23	< 230	215	17.58
		100			100			100

Design a concrete pavement with tied concrete shoulder with doweled transverse joints.



**Solution:**

Typical cross-section of a concrete pavement is shown in Fig.

PQC
DLC/ CEMENT TREATED SUBBASE
DRAINAGE LAYER
FILTER/SEPARATION LAYER
SUBGRADE

**(a) Selection of modulus of subgrade reaction:-**

- Effective CBR of compacted subgrade = 8 percent.

Hence, Modulus of subgrade reaction = 50.3 MPa/m (from Table 2 of IRC 58:2011)

- Provide **150 mm** thick granular subbase
- Provide a DLC subbase of thickness **150 mm** with a minimum 7 day compressive strength of 10 MPa
- Effective modulus of subgrade reaction of combined foundation of subgrade + granular subbase and DLC subbase (from Table 4 by interpolation) = **285 MPa/m**
- Provide a debonding layer of polythene sheet of 125 micron thickness between DLC and concrete slab.

**(b) Selection of Flexural Strength of Concrete**

- 90-day flexural strength of AASC mix (25% reduction to suit site conditions)  
= **5.5 MPa**

**(c) Selection of Design Traffic for Fatigue Analysis:**

- Design period =  $n = 30$  years
- Annual rate of growth of commercial traffic (expressed in decimal) =  $r = 0.075$
- Two-way commercial traffic volume per day =  $A = 6000$  commercial vehicles per day
- Percentage of traffic in predominant direction = 50% (3000 CVs in each direction)
- Total two-way commercial vehicles during design period,

$$C = 365 * A \{(1+r)^n - 1\} / r$$

$$C = 365 * 6000 \{(1+0.075)^{30} - 1\} / 0.075$$

$$C = 226,444,692 \text{ CVs}$$

- Average number of axles (steering/single/tandem/tridem) per commercial vehicle = **2.35**
- Total two-way axle load repetitions during the design period = 226,444,692 \* 2.35 = **532,145,025 axles**
- Number of axles in predominant direction = 532,145,025 \* 0.5 = **266,072,513**
- Design traffic after adjusting for lateral placement of axles (25 percent of predominant direction traffic for multi-lane highways) = 266,072,513. \* 0.25 = **66,518,128**
- Night time (12-hour) design axle repetitions = 66,518,128 \* 0.6 (60 percent traffic during night time) = **39,910,877**
- Day time (12-hour) design axle repetitions = 66,518,128 \* (1-0.6) = **26,607,251**
- Day-time Six-Hour axle load repetitions = 26,607,251 / 2 = **13,303,626**
- Hence, design number of axle load repetitions for **bottom-up cracking analysis** = **13,303,626**
- Night-time Six-Hour axle load repetitions = 39,910,877 / 2 = **19,955,439**
- Percentage of commercial vehicles having the spacing between the front (steering) axle and the first axle of the rear axle unit = 55 percent
- Hence, the Six-hour night-time design axle load repetitions for **Top-down cracking analysis (wheel base < 4.5m)** = 19,955,439 \* 0.55 = **10,975,491**
- The axle load category-wise design axle load repetitions for bottom-up and top-down fatigue cracking analysis are given in the following Table A-5-2.

Table A-5-2 Axle load category-wise design axle load repetitions

Axle Category	Proportion of Axle Category	Category-wise axle repetitions for bottom-up cracking analysis	Category-wise axle repetitions for top-down cracking analysis
Front (steering) single	0.45	5986632	4938971
Rear single	0.15	1995544	1646324
Tandem	0.25	3325906	2743873
Tridem	0.15	1995544	1646324

**(d) Cumulative Fatigue Damage (CFD) analysis for Bottom-up Cracking (BUC) and Top-down Cracking (TDC) and Selection of Slab Thickness :-**

- Effective modulus of subgrade reaction of foundation,  $k = 285 \text{ MPa/m}$
- Elastic Modulus of concrete,  $E = 30,000 \text{ MPa}$
- Poisson's ratio of concrete,  $= 0.15$
- Unit weight of concrete,  $\gamma = 24 \text{ kN/m}^3$
- Design flexural strength of concrete =  $5.5 \text{ MPa}$
- Max. day-time Temperature Differential in slab (for bottom-up cracking) =  $16.8 \text{ }^\circ\text{C}$  (for Bihar)
- Night-time Temperature Differential in slab (for top-down cracking)  
 $= \text{day-time diff}/2 + 5 = 13.4 \text{ }^\circ\text{C}$

**Concrete pavement with tied concrete shoulder with dowel bars across transverse joints**

- Trial thickness of slab,  $h = 0.24 \text{ m}$
  - Radius of relative stiffness,  $l = [E h^3 / 12k \times (1 - \mu^2)]^{(0.25)}$   
 $= 0.78758 \text{ m}$
  - 'Beta' factor in the stress equations will be 0.66 for doweled transverse joints for carrying out TDC analysis.
  - The flexural stresses are calculated according to the IRC: 58:2011
- Computation of bottom-up and top-down cumulative fatigue damage is illustrated in **Tables A-5-3 and A-5-2-4.**

**Fatigue Damage analysis**

Table A-5-3 Bottom-up Cracking Fatigue Analysis

Bottom-up Cracking Fatigue Analysis for Day-time (6 hour) traffic and Positive Temperature Differential									
Rear Single Axles					Rear Tandem Axles				
Expected Repetition (ni)	Flex Stress MPa	Stress Ratio (SR)	Allowable Repetitions (Ni)	Fatigue Damage (ni/Ni)	Expected Repetitions (ni)	Flex Stress MPa	Stress Ratio (SR)	Allowable Repetitions (Ni)	Fatigue Damage (ni/Ni)
362191	3.053	0.505	612362	0.591	482256	2.626	0.434	infinite	0.000
347823	2.943	0.486	1580598	0.220	349220	2.527	0.418	infinite	0.000
364586	2.833	0.468	6044220	0.060	120730	2.428	0.401	infinite	0.000
259022	2.723	0.450	61161340	0.004	83148	2.329	0.385	infinite	0.000
59467	2.613	0.432	infinite	0.000	89467	2.23	0.369	infinite	0.000
32328	2.503	0.414	infinite	0.000	41906	2.131	0.352	infinite	0.000
52283	2.393	0.396	infinite	0.000	129710	2.031	0.336	infinite	0.000
52882	2.283	0.377	infinite	0.000	172615	1.932	0.319	infinite	0.000
52882	2.174	0.359	infinite	0.000	209532	1.833	0.303	infinite	0.000
64855	2.064	0.341	infinite	0.000	212858	1.734	0.287	infinite	0.000
64855	1.954	0.323	infinite	0.000	296006	1.635	0.270	infinite	0.000
282369	1.844	0.305	infinite	0.000	1138458	1.536	0.254	infinite	0.000
1995544	Fat Dam from Sing Axles =			0.876	3325906	Fat Dam from Tand Axles			0.000
Total Bottom-up Fatigue Damage due to single and tandem axle loads =					0.876	+	0.000	=	0.876
<b>DESIGN IS SAFE</b>									

**Note:** Expected Repetition= frequency (table A-5-1) \* Category-wise axle repetitions (table A-5-2), Flex stress calculated from IRC 58:2011 and Allowable Repetitions taken from IRC58:2011 for each stress ratio.

Table A-5-4 Top-Down Cracking Fatigue Analysis

Top-Down Cracking Fatigue Analysis for Night-time (6 hour) traffic and Negative Temperature Differential														
Rear Single Axles					Rear Tandem Axles (Stress computed for 50% of axle load)					Rear Tridem Axles (Stress computed for 33% of axle load)				
Expected Repetitions (ni)	Flex Stress MPa	Stress Ratio (SR)	Allowable Repetitions (Ni)	Fatigue Damage (ni/Ni)	Expected Repetitions (ni)	Flex Stress MPa	Stress Ratio (SR)	Allowable Repetitions (Ni)	Fatigue Damage (ni/Ni)	Expected Repetitions (ni)	Flex Stress MPa	Stress Ratio (SR)	Allowable Repetitions (Ni)	Fatigue Damage (ni/Ni)
298808	2.772	0.458	17878646	0.017	397862	2.81	0.464	8784961	0.045	86103	2.709	0.448	infinite	0.000
286954	2.697	0.446	infinite	0.000	288107	2.734	0.452	44383810	0.006	79847	2.634	0.435	infinite	0.000
300783	2.621	0.433	infinite	0.000	99603	2.659	0.439	Infinite	0.000	56634	2.558	0.423	infinite	0.000
213693	2.546	0.421	infinite	0.000	68597	2.583	0.427	Infinite	0.000	117218	2.483	0.410	infinite	0.000
49060	2.470	0.408	infinite	0.000	73810	2.508	0.415	Infinite	0.000	166443	2.407	0.398	infinite	0.000
26670	2.394	0.396	infinite	0.000	34573	2.432	0.402	Infinite	0.000	197723	2.331	0.385	infinite	0.000
43134	2.319	0.383	infinite	0.000	107011	2.357	0.390	Infinite	0.000	256333	2.256	0.373	infinite	0.000
43628	2.243	0.371	infinite	0.000	142407	2.281	0.377	Infinite	0.000	218632	2.18	0.360	infinite	0.000
43628	2.168	0.358	infinite	0.000	172864	2.206	0.365	Infinite	0.000	74908	2.105	0.348	infinite	0.000
53506	2.092	0.346	infinite	0.000	175608	2.13	0.352	Infinite	0.000	52024	2.029	0.335	infinite	0.000
53506	2.017	0.333	infinite	0.000	244205	2.055	0.340	Infinite	0.000	51036	1.954	0.323	infinite	0.000
232955	1.941	0.321	infinite	0.000	939228	1.979	0.327	Infinite	0.000	289424	1.878	0.310	infinite	0.000
1646324	Fat Dam from Sing. Axles =			0.017	2743873	Fat Dam from Tand Axles =			0.052	1646324	Fat Dam from Tridem Axles =			0.000
Total Top-Down Fatigue Damage =								0.017	+	0.052	+	0.000	=	0.068
<b>DESIGN IS SAFE</b>														

**Note:** Expected Repetition= frequency (table A-5-1) \* Category-wise axle repetitions (table A-5-2), Flex stress calculated from IRC 58:2011 and Allowable Repetitions taken from IRC58:2011 for each stress ratio.

From the calculations given in the table A-5-3 and 4, it can be observed that for the slab thickness of 0.24 m, the total fatigue damage for bottom-up cracking case is  $0.876 + 0 = 0.876 < 1$ .

Total fatigue damage for top-down cracking case=  $0.017 + 0.052 + 0.00 = 0.068 < 1$ .

**Hence, the trial thickness of 0.24 m is adequate.**

## **PUBLICATIONS BASED ON PRESENT RESEARCH**

### **International/National Journals**

Nitendra Palankar, A.U. Ravishankar and B.M. Mithun, (2014). “Experimental investigation on air-cured alkali activated GGBFS-fly ash concrete mixes.” *International Journal of Advanced Structures and Geotechnical Engineering*, 3 (4), 326-332.

Nitendra Palankar, A.U. Ravishankar and B.M. Mithun, (2015). “Studies on eco-friendly concrete incorporating industrial waste as aggregates.” *International Journal of Sustainable Built Environment*, Elsevier, 4, 378-390.

Nitendra Palankar, A.U. Ravishankar and B.M. Mithun, (2015). “Investigations on alkali activated slag/fly ash concrete with steel slag coarse aggregate for pavement structures.” *International Journal of Pavement Engineering*, Taylor and Francis, 1-13.

Nitendra Palankar, A.U. Ravishankar and B.M. Mithun, (2015). “Air-cured alkali activated binders for concrete pavements.” *International Journal of Pavement Research and Technology*, Chinese Society of Pavement Engineering, 8 (4), 289-294.

Nitendra Palankar, A.U. Ravishankar and B.M. Mithun, (2015). “Performance and fatigue behaviour of alkali activated slag concrete with steel slag as coarse aggregate for concrete pavement.” *Indian Roads Congress, Accepted for publication.*

Nitendra Palankar, A.U. Ravishankar and B.M. Mithun, “Durability of alkali activated slag/fly ash concrete with steel slag coarse aggregate.” *Journal of Cleaner Production*, Elsevier. (Under review- resubmitted after minor corrections).

### **International Conferences**

Nitendra Palankar and A.U. Ravishankar, (2014). “Alkali activated binders for white topping and the effect of modulus of subgrade reaction and panel size on white topping.” *International Conference on Sustainable Civil Infrastructures*, ASCE.

Nitendra Palankar, A.U. Ravishankar and B.M. Mithun, (2014). “Performance of air-cured alkali activated ggbfs-fly ash concrete mixes.” *3<sup>rd</sup> World Conference on Applied Sciences, Engineering and Technology (WCSET)*, Kathmandu, NEPAL, 27-29.

## BIO DATA

Name : Mr. Nitendra Palankar  
Date of Birth : 12 Mar 1988  
Permanent Address : 6<sup>th</sup> Cross, R.K. Marg,  
Hindwadi, Belgaum,  
590011, Karnataka,  
India.  
Contact Number : +91-9964545852  
Email : [nitendrapalankar@gmail.com](mailto:nitendrapalankar@gmail.com)

### ACADEMIC QUALIFICATION:

<b>Degree</b>	<b>Major</b>	<b>Institute</b>	<b>Duration</b>	<b>Percentage/ CGPA</b>
Ph.D	Performance of Alkali Activated Concrete Mixes With Steel Slag as Coarse Aggregate for Rigid Pavements	National Institute of Technology Karnataka, Surathkal	2012 – 2016	9.0/10
M Tech	Transportation Systems Engineering	National Institute of Technology Karnataka, Surathkal	2010 – 2012	7.91/10
B E	Civil Engineering	Gogte Institute of Technology Belgaum Karnataka	2006 – 2010	71.92%
Higher Secondary	Science	Govindram Seksaria Science College, Belgaum	2004 – 2006	65.5%
Class X		M.V.Herwadkar English Medium High School, Belgaum	2003 – 2004	83.03%

## **PROJECTS:**

**B.E:** “Geometric design of a Flyover at 1st Railway Gate Belgaum.”

**M.Tech:** “GRAVELS ROADS –Investigations on Blended Laterite Soils Using CBR Tests with Analysis and Design Using KENPAVE”

## **Undergone subjects in M.Tech**

1. Pavement Design
2. Traffic engineering and Management
3. Urban Transport Planning
4. Statistical Methods
5. Soil Mechanics
6. Pavement Materials and construction
7. Traffic flow Theory
8. Operational Research
9. Traffic Design and Studio lab
10. Transportation Engineering lab

## **SOFTWARE SKILLS:**

Programming : Basics in C

Softwares : KENPAVE, IITPAVE, Minitab 17.0, AutoCAD

## **PULICATIONS:**

### **Journals:**

1. Nitendra Palankar, A.U. Ravishankar and B.M. Mithun, (2015). “Studies on eco-friendly concrete incorporating industrial waste as aggregates.” *International Journal of Sustainable Built Environment*, Elsevier, 4, 378-390.
2. Nitendra Palankar, A.U. Ravishankar and B.M. Mithun, (2015). “Investigations on alkali activated slag/fly ash concrete with steel slag coarse aggregate for pavement structures.” *International Journal of Pavement Engineering*, Taylor and Francis, 1-13.



3. Nitendra Palankar, A.U. Ravishankar and B.M. Mithun, (2015). “Air-cured alkali activated binders for concrete pavements.” *International Journal of Pavement Research and Technology*, Chinese Society of Pavement Engineering, 8 (4), 289-294.
4. Nitendra Palankar, A.U. Ravishankar and B.M. Mithun, (2015). “Performance and fatigue behaviour of alkali activated slag concrete with steel slag as coarse aggregate for concrete pavement.” *Indian Roads Congress, Accepted for publication*.
5. Nitendra Palankar, A.U. Ravishankar and B.M. Mithun, “Durability of alkali activated slag/fly ash concrete with steel slag coarse aggregate.” *Journal of Cleaner Production*, Elsevier. (Under review- resubmitted after minor corrections).
6. Nitendra Palankar, A.U. Ravishankar and B.M. Mithun, (2014). “Experimental investigation on air-cured alkali activated GGBFS-fly ash concrete mixes.” *International Journal of Advanced Structures and Geotechnical Engineering*, 3 (4), 326-332.
7. Mithun, B.M., Narasimhan, M.C, Nitendra Palankar and Ravishankar, A.U. (2015) “Flexural Fatigue performance of Alkali Activated Slag Concrete mixes incorporating Copper Slag as Fine Aggregate.” *SSP - Journal of Civil Engineering, DE GRUYTER Publishers*, 10 (1), 7-18.
8. Mithun, B. M., Narasimhan, M. C. and Nitendra Palankar. (2015). “Strength Performance of Alkali Activated Slag Concrete with Copper Slag as Fine Aggregate Exposed To Elevated Temperatures.” *International Journal of Earth Sciences and Engineering*, 8 (2), 519-526.
9. Mithun. B. M., Narasimhan, M. C. and Nitendra Palankar. (2015). “Studies on Alkali Activated Slag Mortar with Copper Slag as Fine Aggregate.” *International Journal of Earth Sciences and Engineering*, 8 (2), 527-531.

10. Ravishankar, A.U. and Nitendra Palankar. (2014). “Effect of Modulus of Subgrade Reaction of the Design of Rigid Pavements”, *Journal of Indian Roads Congress, Indian Roads Congress*, 75 (2), 227-232.
11. Ravishankar, A.U. and Nitendra Palankar. (2014). “A Study on Porous Concrete Mixes for Rigid Pavements” *Indian Highways, Indian Roads Congress*, 43 (6), 37-41. (Abstract reprinted and indexed in TRB Library).
12. Nitendra Palankar, Ravishankar, A.U and Chandrashekar, A. (2015). “A Study on Elastic Deformation Behaviour of Steel Fibre Reinforced Concrete Slabs.” *Indian Roads Congress* (Under Review).

### **Conferences:**

1. Nitendra Palankar and A.U. Ravishankar, (2014). “Alkali activated binders for white topping and the effect of modulus of subgrade reaction and panel size on white topping.” *International Conference on Sustainable Civil Infrastructures*, ASCE.
2. Nitendra Palankar, A.U. Ravishankar and Mithun, B.M. (2014). “Performance of air-cured alkali activated ggbfs-fly ash concrete mixes.” *3<sup>rd</sup> World Conference on Applied Sciences, Engineering and Technology (WCSET)*, Kathmandu, NEPAL, 27-29.
3. Ravishankar, A.U and Nitendra Palankar (2014). “Effect of modulus of subgrade reaction of the design of rigid pavements”, *Guest Invitee, Proceedings of 75th Annual Meeting, Platinum Jubilee Session, Indian Roads Congress*.
4. Mithun B.M, Narasimhan M.C, Nitendra Palankar and Ravishankar A.U. (2015). “Experimental investigations on alkali activated slag concrete mixes incorporating copper slag as fine aggregate.” *UKIERI Concrete Congress-Concrete Research Driving Profit and Sustainability, NIT Jalandar, India*.